

2001

## **Kinetic and Mechanistic Studies of a Bimetallic Hydroformylation Catalyst.**

Novella Nicole Bridges  
*Louisiana State University and Agricultural & Mechanical College*

Follow this and additional works at: [https://digitalcommons.lsu.edu/gradschool\\_disstheses](https://digitalcommons.lsu.edu/gradschool_disstheses)

---

### **Recommended Citation**

Bridges, Novella Nicole, "Kinetic and Mechanistic Studies of a Bimetallic Hydroformylation Catalyst." (2001). *LSU Historical Dissertations and Theses*. 265.  
[https://digitalcommons.lsu.edu/gradschool\\_disstheses/265](https://digitalcommons.lsu.edu/gradschool_disstheses/265)

This Dissertation is brought to you for free and open access by the Graduate School at LSU Digital Commons. It has been accepted for inclusion in LSU Historical Dissertations and Theses by an authorized administrator of LSU Digital Commons. For more information, please contact [gradetd@lsu.edu](mailto:gradetd@lsu.edu).

## INFORMATION TO USERS

This manuscript has been reproduced from the microfilm master. UMI films the text directly from the original or copy submitted. Thus, some thesis and dissertation copies are in typewriter face, while others may be from any type of computer printer.

**The quality of this reproduction is dependent upon the quality of the copy submitted.** Broken or indistinct print, colored or poor quality illustrations and photographs, print bleedthrough, substandard margins, and improper alignment can adversely affect reproduction.

In the unlikely event that the author did not send UMI a complete manuscript and there are missing pages, these will be noted. Also, if unauthorized copyright material had to be removed, a note will indicate the deletion.

Oversize materials (e.g., maps, drawings, charts) are reproduced by sectioning the original, beginning at the upper left-hand corner and continuing from left to right in equal sections with small overlaps.

Photographs included in the original manuscript have been reproduced xerographically in this copy. Higher quality 6" x 9" black and white photographic prints are available for any photographs or illustrations appearing in this copy for an additional charge. Contact UMI directly to order.

ProQuest Information and Learning  
300 North Zeeb Road, Ann Arbor, MI 48106-1346 USA  
800-521-0600

UMI<sup>®</sup>



**KINETIC AND MECHANISTIC STUDIES  
OF A BIMETALLIC  
HYDROFORMYLATION CATALYST**

**A Dissertation**

**Submitted to the Graduate Faculty of the  
Louisiana State University and  
Agricultural and Mechanical College  
in partial fulfillment of the  
requirements for the degree of  
Doctor of Philosophy**

**in**

**The Department of Chemistry**

**by**

**Novella Nicole Bridges  
B.S., Jackson State University, 1994  
May, 2001**

UMI Number: 3016528



---

UMI Microform 3016528

Copyright 2001 by Bell & Howell Information and Learning Company.

All rights reserved. This microform edition is protected against  
unauthorized copying under Title 17, United States Code.

---

Bell & Howell Information and Learning Company  
300 North Zeeb Road  
P.O. Box 1346  
Ann Arbor, MI 48106-1346

**To my parents Willie and Carrie Bridges,  
you always encouraged me to reach for the stars,  
thank you for always being my backbone.  
To my four siblings, Lawrence, Katrina, Marilyn and William,  
You all are my entire the ultimate support system**

## **ACKNOWLEDGMENTS**

To my heavenly Father, without Him I would be nothing nor would I have made it this far. **THANK YOU JESUS!**

To Professor George Stanley, thank you for your patience and nurturing. Your guidance has proven to be invaluable. I would also like to thank my committee members for their support.

To my parents, Willie and Carrie Bridges, what can say but I LOVE YOU!

To my siblings, nieces and nephews, I LOVE YOU ALL!

To my adoptive families, Birdie and Ollie of Jackson, Mississippi; Ms. Stephens, Marcia, Mama, and Aunt Ro of Baton Rouge, Louisiana; Mr. and Mrs. Carter, Rhonda and Monty and the entire Jones family of Baton Rouge, Louisiana; Adonis, Ms. Barbia, Aeneas, Monique and Ms. Alice and the entire McClain family; I would like to thank you from the bottom of my heart. Thank you for allowing me to feel like I was part of your family.

To my church families, Greater New Guide Baptist Church, Refuge Church and Solomon's Temple, thank you for all your support and prayers. I don't know where I would have been without them.

# TABLE OF CONTENTS

<b>DEDICATION</b> .....	ii
<b>ACKNOWLEDGEMENTS</b> .....	iii
<b>LIST OF TABLES</b> .....	vi
<b>LIST OF FIGURES</b> .....	vii
<b>LIST OF ABBREVIATIONS</b> .....	xi
<b>ABSTRACT</b> .....	xii
<b>CHAPTER 1. INTRODUCTION</b> .....	1
1.1 Alkene Hydroformylation .....	1
1.2 Monometallic Hydroformylation Catalysts.....	2
1.3 Bimetallic Hydroformylation Catalysts .....	6
1.4 Hydroformylation Kinetic Studies.....	13
1.5 Polar Phase Hydroformylation to Hydrocarboxylation Catalysis.....	15
1.6 References .....	21
<b>CHAPTER 2. HYDROFORMYLATION KINETIC STUDIES</b> .....	23
2.1 Introduction.....	23
2.2 Initial Kinetic Studies and Problems Encountered .....	27
2.3 Kinetic Study of the Alkene Concentration .....	30
2.4 Kinetic Study of the Dinuclear Dicationic Catalyst .....	34
2.5 Bis-Acyl Species.....	38
2.6 Summary .....	39
2.7 References .....	40
<b>CHAPTER 3. HYDROCARBOXYLATION</b> .....	42
3.1 Introduction to Polar Phase Hydroformylation .....	42
3.2 Initial Polar Phase Hydroformylation Catalytic Runs .....	45
3.3 Background of Hydrocarboxylation Catalysis .....	50
3.4 Polar Phase Hydroformylation to Hydrocarboxylation	
-- New Studies .....	60
3.4.1 Original Hydrocarboxylation Experiment.....	61
3.4.2 Hydrogenation of Heptanoic Acid .....	63
3.4.3 Modified Hydrocarboxylation.....	65
3.5 Polar Phase Bimetallic Hydroformylation Mechanistic	
Consideration .....	71
3.6 Bimetallic Hydrocarboxylation Mechanism Discussion .....	77
3.7 References .....	85



<b>CHAPTER 4. CONCLUSION/ FUTURE STUDIES</b> .....	87
4.1 Hydroformylation Kinetic Studies.....	87
4.2 Aldehyde/Water Shift Reaction.....	87
<b>CHAPTER 5. EXPERIMENTAL</b> .....	91
5.1 General Synthesis .....	91
5.1.1 Synthesis of methylene bis(phenylphosphine) or bridge .....	91
5.1.2 Synthesis of diethylchlorophosphine (Et <sub>2</sub> PCl) .....	92
5.1.3 Synthesis of vinyl-diethylchlorophosphine .....	93
5.1.4 Synthesis of et,ph-P <sub>4</sub> ligand.....	94
5.1.5 Synthesis of Rh(nbd)acac .....	95
5.1.6 Synthesis of [Rh(nbd) <sub>2</sub> ]BF <sub>4</sub> .....	95
5.1.7 Nickel Separation of <i>meso</i> and <i>racemic</i> diastereomers of et,ph-P <sub>4</sub> .....	96
5.1.8 Synthesis of [ <i>rac</i> -Rh <sub>2</sub> (nbd) <sub>2</sub> (et,ph-P <sub>4</sub> )](BF <sub>4</sub> ) <sub>2</sub> .....	97
5.2 Hydroformylation and Hydrocarboxylation Experiments .....	98
5.3 Gas Chromatography Analysis.....	100
5.4 References .....	101
<b>APPENDIX A: GAS CHROMATOGRAMS</b> .....	102
<b>APPENDIX B: ALDEHYDE PRODUCTION CURVES</b> .....	105
<b>VITA</b> .....	109

## LIST OF TABLES

1.1	Hydroformylation results for 1-hexene at 90 °C, 90 psig .....	9
2.1	Previous studies on the hydroformylation of $\alpha$ -olefins by 1r showing the "false" odd olefin effect .....	26
2.2	Initial alkene concentration dependency hydroformylation results affected by alkene purity and autoclave leak problems .....	28
2.3	New alkene concentration dependency results (90 °C, 90 psig 1:1 H <sub>2</sub> /CO, 1M 1-hexene, acetone solvent) .....	32
2.4	Initial catalyst dependency results .....	35
2.5	New catalyst concentration dependency results (90 °C, 90 psig 1:1 H <sub>2</sub> /CO, 1M 1-hexene, acetone solvent) .....	36
3.1	Catalytic results from Pruchnik's [RhI(CO)(mpta <sup>+</sup> I <sup>-</sup> ) <sub>2</sub> ] precursor for the hydroformylation of 1-hexene at 60 atm 1:1 H <sub>2</sub> /CO and 80 °C .....	56
3.2	Date analysis form GC/MS of hydroformylation of 1-hexene systems using different % water in acetone .....	63
3.3	Results of H <sub>2</sub> /CO reaction time experiments for modified hydrocarboxylation .....	67
5.1	Order of retention times .....	100

## LIST OF FIGURES

1.1	The general reaction for hydroformylation.....	1
1.2	Heck's mechanism for $\text{HCo}(\text{CO})_4$ catalyzed hydroformylation .....	2
1.3	The Union Carbide $\text{Rh}-\text{Ph}_3$ hydroformylation mechanism .....	5
1.4	The et,ph-P4 ligand system.....	7
1.5	$[\text{rac-Rh}_2(\text{nbd})_2(\text{et,ph-P4})]^{+2}$ catalyst precursor, <b>1r</b> .....	8
1.6	Illustration of open and closed mode complexes .....	8
1.7	Example of intramolecular hydride transfer .....	10
1.8	Spaced bimetallic analogs.....	11
1.9	Proposed structure of $\text{rac-}[\text{Rh}_2\text{H}_2(\text{u-CO})_2(\text{CO})_2(\text{et,ph-P4})]^{2+}$ , <b>2r</b> .....	11
1.10	Proposed bimetallic dicationic hydroformylation mechanism.....	12
1.11	Proposed structure of bis-acyl species, <b>H</b> .....	13
1.12	Proposed formation of the bis-acyl bimetallic complex, <b>H</b> , and a bimolecular reductive elimination to produce the diketone product .....	14
1.13	<i>In situ</i> FT-IR spectra of catalyst precursor under hydroformylation conditions (90 psig 1:1 $\text{H}_2/\text{CO}$ and 90 °C in the following solvents:(a) $\text{CH}_2\text{Cl}_2$ , (b) 1:1 $\text{CH}_2\text{Cl}_2/\text{acetone}$ , and (c) acetone).....	16
1.14	Illustration of electrostatic effects for conversion of open to closed mode bimetallic structures .....	17
1.15	Hydrocarboxylation catalysis .....	20
2.1	Garland's precatalytic reaction sequence.....	24
2.2	General hydroformylation kinetic rate expression.....	27

2.3	Aldehyde production curve of run Rh560 showing only 68% conversion of alkene to aldehyde .....	29
2.4	Illustrations of the impurity distorted hydroformylation runs using the same alumina column to purify the 1-hexene substrate (top to bottom are three consecutive runs showing the detrimental effect on increased alkene impurities on the hydroformylation) .....	31
2.5	Alkene dependency kinetic order plot.....	32
2.6	Aldehyde production for run Rh638 .....	33
2.7	Hydroformylation run Rh548 showing only 50% conversion of alkene to aldehyde product .....	36
2.8	Catalyst concentration dependency kinetic order plot .....	38
2.9	Aldehyde production for run Rh650 .....	38
2.10	Bis-acyl species.....	39
3.1	The Shell higher olefin process (SHOP).....	42
3.2	Production curve for run Rh596 based on gas uptake .....	45
3.3	Production curve for run Rh595 based on gas uptake .....	45
3.4	Production curve for run Rh598 based on gas uptake .....	46
3.5	Representative GC/MS analysis of Rh595 (30%).....	47
3.6	Production and consumption plot for run Rh589e .....	48
3.7	GC/MS traces of run Rh594 (25% water) showing the loss of acid from the organic phase .....	50
3.8	Different types of hydrocarboxylation reactions.....	51
3.9	Heck's proposed mechanism for Ni-catalyzed hydrocarboxylation of alkenes .....	52

3.10	Proposed mechanism for Monsanto acetic acid process .....	53
3.11	Alternate Heck proposal for the activation of alkenes by HI to perform hydrocarboxylation catalysis .....	54
3.12	Monsanto mechanism for $[\text{RhI}_2(\text{CO})_2]^-$ catalyzed hydrocarboxylation .....	55
3.13	Structure of $\text{mtpa}^+\text{I}^-$ .....	56
3.14	Pd-catalyzed hydrocarboxylation catalysis .....	57
3.15	Proposed Pd-catalyzed hydrocarboxylation mechanism .....	58
3.16	Polarization of Pd-acyl and water and an alternate carbene mechanism .....	60
3.17	GC trace of run Rh618 .....	62
3.18	GC trace of run Rh632 (30% water) .....	63
3.19	Thermodynamics for hydrocarboxylation catalysis and reaction of aldehyde with water to produce carboxylic acid and $\text{H}_2$ .....	64
3.20	GC trace of run Rh687 where the hydrogenation of heptanoic acid to heptanal and $\text{H}_2\text{O}$ was attempted .....	65
3.21	GC final product analysis of catalytic Run Rh690 with 30% water and 10 min of $\text{H}_2/\text{CO}$ -then switching over to pure CO .....	67
3.22	Reactant loss and product production plot of run Rh696 from GC analysis of autoclave samples .....	69
3.23	GC analysis of run Rh701 with 20% water and 10 min $\text{H}_2/\text{CO}$ .....	71
3.24	GC analysis of run Rh700 with 40% water and 10 min $\text{H}_2/\text{CO}$ .....	71
3.25	Proposed fragmentation mechanism to produce catalytically inactive mono- and bimetallic rhodium complexes .....	73

3.26	Phosphine ligand dissociation equilibria for monometallic rhodium hydroformylation catalyst.....	75
3.27	Rotation of open-mode hydride catalyst complex to the closed-mode conformation.....	76
3.28	The two catalytic reactions occurring to transform alkene, water and CO into carboxylic acid.....	78
3.29	Possible catalyst for the aldehyde-water shift reaction .....	80
3.30	MO diagram proposed by Gray .....	81
3.31	Proposed mechanism for aldehyde-water shift catalysis .....	82
3.32	Proposed mechanism for Tyler's $[\text{Cp}'\text{Mo}(\text{OH})(\text{H}_2\text{O})]^+$ -catalyzed aldehyde-water shift reaction.....	83
5.1	Diagram of the autoclave setup.....	98

## LIST OF ABBREVIATIONS

acac	acetyl-acetate
DCM	dichloromethane
dd	doublet of doublets (NMR)
DMF	dimethylformamide
et,ph-P4	tetraphosphine ligand
FTIR	Fourier transform infrared spectroscopy
GC	Gas Chromatography
GC-MS	Gas Chromatography- Mass Spectrometry
Hz	Hertz, sec <sup>-1</sup>
IR	Infrared Spectroscopy
L/B	linear to branched
mL	milliliters
mM	millimolar
mol	moles
MS	Mass spectrometry
NMR	Nuclear magnetic resonance
Ph	phenyl
ppm	parts per million
psig	pounds per square inch, gauge
rac	racemic
tetraglyme	tetra(ethylene glycol) dimethyl ether
THF	tetrahydrofuran
TMS	tetramethylsilane

## ABSTRACT

Dicationic bimetallic rhodium complexes based on the novel binucleating tetraphosphine ligand system racemic-Et<sub>2</sub>PCH<sub>2</sub>CH<sub>2</sub>P(Ph)CH<sub>2</sub>P(Ph)CH<sub>2</sub>CH<sub>2</sub>PEt<sub>2</sub>, et,ph-P4, are highly active and selective hydroformylation catalysts that make use of bimetallic cooperativity to operate. *In situ* FT-IR and NMR studies indicate that the most active catalyst is the unique dinuclear dicationic hydrido-carbonyl Rh(+2) oxidation state complex, [racemic-Rh<sub>2</sub>H<sub>2</sub>(μ-CO)<sub>2</sub>(CO)<sub>2</sub>(et,ph-P4)<sup>2+</sup>]. A kinetic study was performed to determine the rate orders of the bimetallic catalyst, and the substrate (1-hexene). The rate orders were found to be one for both components. The study was also performed to test the hypothesis of a bis-acyl species, which was not observed.

The addition of 25-50% water to the acetone solvent caused a dramatic improvement in the hydroformylation catalysis with a 40% increase in the initial turnover frequency and a reduction in alkene isomerization and hydrogenation side reactions to less than 1%. The presence of water coupled with H<sub>2</sub> poor reaction conditions initiates a new catalytic reaction-an aldehyde-water shift process that takes aldehyde and water and produces carboxylic acid and H<sub>2</sub>. Too much H<sub>2</sub> strongly inhibits this aldehyde-water shift reaction, which is why it is not observed under normal hydroformylation catalysis conditions. The carboxylic acid products have very high linear/branched selectivities. These pieces of evidence continue to support our theory of bimetallic cooperativity.



## CHAPTER 1

### INTRODUCTION

#### 1.1. Alkene Hydroformylation

One of the most important applications of organometallic chemistry is the catalysis of organic reactions.<sup>1,2</sup> When the catalyst and substrate are in the same phase, the catalyst is said to function homogeneously. When the catalyst and substrate are in two separate phases, with the catalyst usually deposited onto a surface, it is said to be functioning heterogeneously.<sup>3</sup> In the late 1930's, Otto Roelen of Ruhrchemie discovered homogeneous hydroformylation, also known as the oxo process.

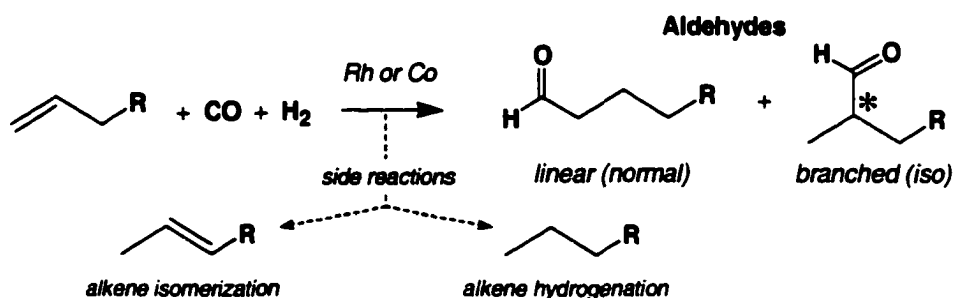


**Figure 1.1.** The general reaction for hydroformylation

Hydroformylation is the dominant homogeneous catalytic process for converting alkenes, carbon monoxide (CO) and hydrogen (H<sub>2</sub>) into aldehyde products. The aldehyde products can be either linear (normal) or branched (iso). Over 12 billion pounds of aldehydes are produced each year. Common commercial catalysts are based on cobalt or rhodium hydride carbonyl complexes often with added phosphine ligands to enhance the aldehyde linear to branched regioselectivity. These aldehydes are used to produce alcohols

and carboxylic acids, which are used in the production of fatty acids,<sup>4</sup> plasticizers, detergents, surfactants, lubricants and solvents.<sup>2</sup>

## 1.2. Monometallic Hydroformylation Catalysts

Heck and Breslow<sup>5</sup> proposed the generally accepted mechanism for  $\text{HCo}(\text{CO})_4$  in 1961 (Figure 1.2).

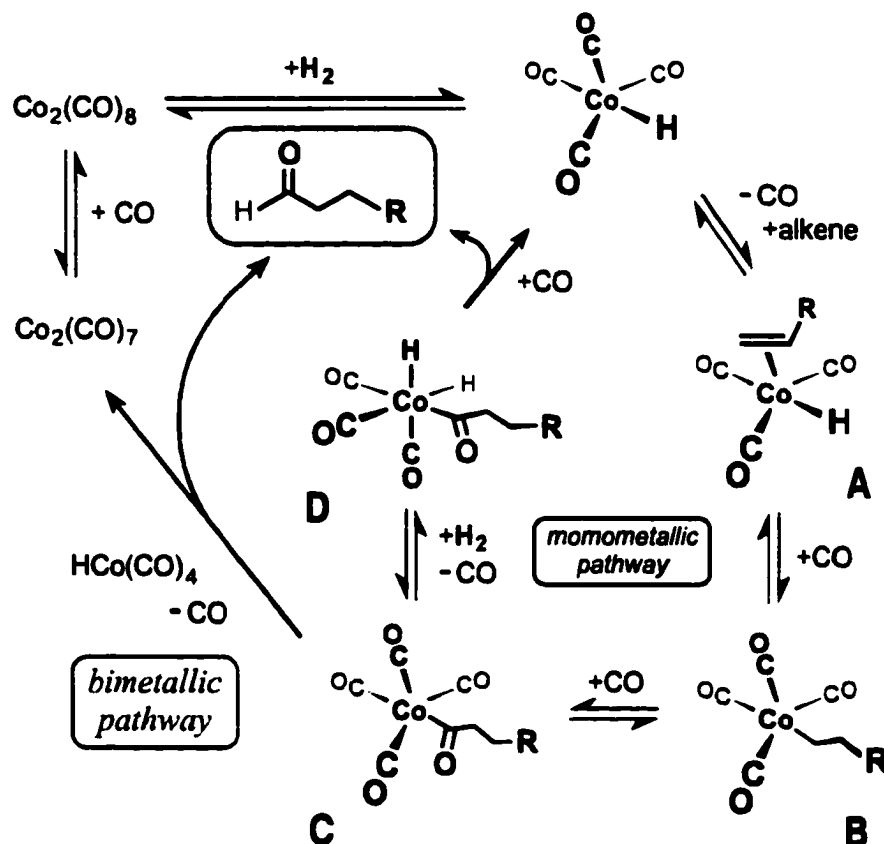


**Figure 1.2.** Heck's mechanism for  $\text{HCo}(\text{CO})_4$  catalyzed hydroformylation

The dissociation of a carbonyl from  $\text{HCo}(\text{CO})_4$  permits the addition of the alkene. An alkyl group is formed by a migratory insertion of the alkene into the metal-hydride bond (**A** → **B**). An acyl species is formed from the migratory insertion of CO with the alkyl (**B** → **C**). Oxidative addition of  $\text{H}_2$  occurs to

generate a Co(III) dihydride ( $C \rightarrow D$ ) and the aldehyde is then reductively eliminated followed by CO addition to regenerate the starting  $HCo(CO)_4$ .<sup>5</sup> Heck also proposed a bimetallic pathway in which  $HCo(CO)_4$  reacts with the acyl complex  $C$  through loss of CO and an intermolecular hydride transfer. This pathway was not favored by Heck due to the low concentration of the bimetallic catalyst species present to eliminate the aldehyde product. Stoichiometric model studies at high cobalt concentrations; however, have shown that this intermolecular hydride transfer pathway can occur. Spectroscopic studies under catalytic conditions strongly support the monometallic mechanism.<sup>5</sup>

Following Roelen's discovery there were several industrial plants built based on cobalt or rhodium metal catalysts. In 1947, Exxon built the world's first hydroformylation plant in Baton Rouge, Louisiana. They are currently the largest producer of aldehyde, which is hydrogenated to alcohols, via the  $HCo(CO)_4$  catalyst system, generating over 500,000 tons of product per year. Exxon hydroformylates olefins in the  $C_6$ - $C_{12}$  range using the cobalt carbonyl hydride catalyst system. They currently use Kuhlman's catalyst cycle recycling technology,<sup>6</sup> which allows the cobalt catalyst to be recycled without oxidizing Co(I) to Co(II). The recycling step involves two main components: 1) the recovery of  $Na[Co(CO)_4]$ , and 2) the regenerative conversion of  $Na[Co(CO)_4]$  to  $HCo(CO)_4$ . In contrast, the previous catalyst recycling used oxidation with air and acetic acid or thermal degradation. Kuhlman's process is considerably more efficient. The usual  $HCo(CO)_4$  hydroformylation conditions are 160-190°C,

and 200-300 bars (2940-4410 psig) of syn gas ( $\text{H}_2/\text{CO}$ ). Exxon typically observes around a 2:1 linear to branched production of aldehyde products.

Cobalt catalyst systems dominated hydroformylation until the 1970's. Shell Corporation has a hydroformylation in Geismar, Louisiana, and they use a phosphine-modified  $\text{HCo}(\text{CO})_4$  catalyst system. Shell is currently the 2<sup>nd</sup> largest world producer (400,000 tons annually) of oxo products via the cobalt technology. They use the phosphine modified classical cobalt carbonyl hydride discovered by Slaugh and Mullineux. Their normal conditions are 130-190°C, and 50-100 bars (735-1470 psig) of syn gas ( $\text{H}_2/\text{CO}$ ). Shell usually observes 88% conversion of the olefin to alcohol with an 8:1 linear to branched regioselectivity. The phosphine ligands also play a critical role in the regioselectivity of the catalyst system, i.e., if the phosphine ligand has a large enough cone angle it will favor the least sterically hindered product, (linear rather than branched). Shell also uses this system to hydrogenate most of the aldehyde product to alcohol.

In the late 1960's some corporations,<sup>7</sup> influenced by the work of Osborn, Young and Wilkinson, began using rhodium catalyst systems. They reported that  $\text{Rh}(\text{I})\text{-PPh}_3$  catalyst systems were highly selective and far more active than their cobalt counterparts, even under ambient conditions. Wilkinson proposed several mechanisms for these rhodium catalyst systems, all directly analogous to Heck's original mechanism. Union Carbide currently uses  $\text{HRh}(\text{CO})(\text{PPh}_3)_2$  as their catalyst system and has a hydroformylation plant in Taft, Louisiana that produces over 100,000 tons of aldehyde annually. Union Carbide uses a liquid

phase hydroformylation process that operates under mild conditions {85-130°C, 12-50 bar (176-735 psig)}. Union Carbide patented the key discovery that a large excess of  $\text{PPh}_3$  was required to produce a selective, active, and more stable catalyst.<sup>8</sup> The  $\text{PPh}_3$  must be kept at a constant concentration of 0.4 M or higher during the reaction. Excess  $\text{PPh}_3$  stabilizes the Rh complex minimizing the formation of  $14e^-$  Rh complexes that promote the fragmentation of  $\text{PPh}_3$  that ultimately leads to the formation of phosphide-bridged Rh dimers and clusters, which are not catalysts. The general mechanism for Rh/ $\text{PPh}_3$  catalyzed hydroformylation is shown in Figure 1.3.

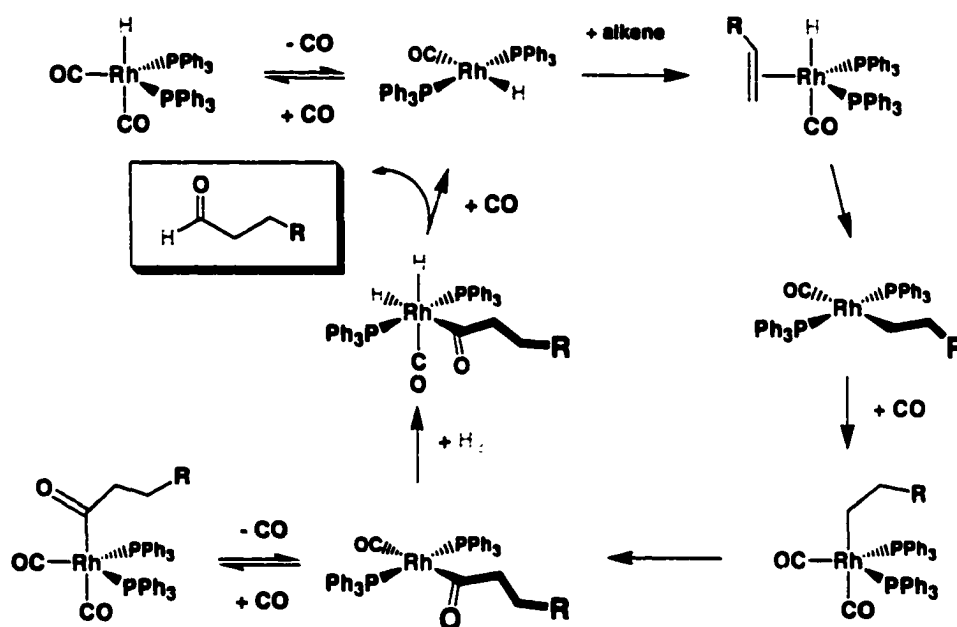


**Figure 1.3.** The Union Carbide Rh- $\text{PPh}_3$  hydroformylation mechanism

This remains the accepted mechanism for rhodium catalyst systems. The starting catalyst,  $\text{HRh}(\text{CO})(\text{PPh}_3)_2$ , is a derivative of Wilkinson's famous hydrogenation catalyst,  $\text{RhCl}(\text{PPh}_3)_3$ .

### 1.3. Bimetallic Hydroformylation Catalysts

The use of transition metal dimers and cluster species has attracted considerable interest in homogeneous catalysis. These multimetallic complexes have a number of potential advantages over their monometallic counterparts: 1) the ability to form multicenter metal-to-ligand bonds that may help activate difficult substrates, 2) the capacity to support multielectron transfers, 3) the potential to use metal-metal bonds as stabilizing and/or reactive sites, and 4) the ability to use mixed metal systems where two or more different metals can be used to selectively activate different substrates.<sup>9</sup>

In 1975, Muetterties proposed a cluster-surface analogy using multimetallic complexes for homogeneous catalysis.<sup>9</sup> Following this proposal, many transition metal dimer and cluster species were studied for catalysis but none had the key combination of high turnover frequency and high selectivity. Indeed, most of these systems were not even comparable to mediocre monometallic systems. It was also found that cluster systems often degrade and the monometallic fragments formed were, in many cases, the active catalyst not the polymetallic (or cluster) system itself.<sup>10</sup>

As previously discussed, Heck and Breslow proposed a bimetallic pathway for the  $\text{HCo(CO)}_4$  catalyzed hydroformylation, that involved an intermolecular hydride transfer between  $\text{HCo(CO)}_4$  and  $\text{Co(acyl)(CO)}_4$  in order to eliminate the aldehyde product. They did not favor this bimetallic pathway due to the low concentration of the  $\text{HCo(CO)}_4$  and  $\text{Co(acyl)(CO)}_4$  catalyst

species. Others have performed mechanistic studies in an attempt to show that stoichiometric (high concentration) intermolecular hydride transfers can occur between separate metal-hydride and metal-acyl species. Since 1975, a number of researchers have proposed the occurrence of this general mechanistic step in their specific polymetallic hydroformylation catalysts.<sup>11</sup>

The most dramatic example of bimetallic cooperativity in a homogenous (non-enzymatic) catalyst is that of Stanley and co-workers.<sup>12</sup> They use a binucleating tetraphosphine ligand,  $\text{Et}_2\text{PCH}_2\text{CH}_2\text{P}(\text{Ph})\text{CH}_2\text{P}(\text{Ph})\text{CH}_2\text{CH}_2\text{PEt}_2$  (et,ph-P4), which exists as the meso and racemic diastereomers (Figure 1.4) to chelate and bridge two metal centers. This system, unlike some of the other cluster or polymetallic systems, does not degrade to a catalytically active monometallic system that might mask the activity of the original bimetallic catalyst.

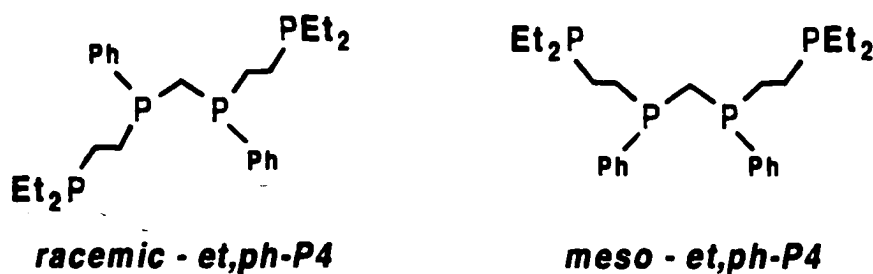


**Figure 1.4.** The et,ph-P4 ligand system

The *rac*-et,ph-P4 ligand reacts with 2 equivalents of  $[\text{Rh}(\text{nbd})_2](\text{BF}_4)$  (nbd = norbornadiene) to produce the bimetallic catalyst precursor  $[\text{rac-Rh}_2(\text{nbd})_2(\text{et,ph-P4})]^{2+}$ , **1r**, in high yields (Figure 1.5). The labeling system in

this dissertation uses numerals for species that have confirming spectroscopic data and letters for those that are proposed “unobserved” intermediates.

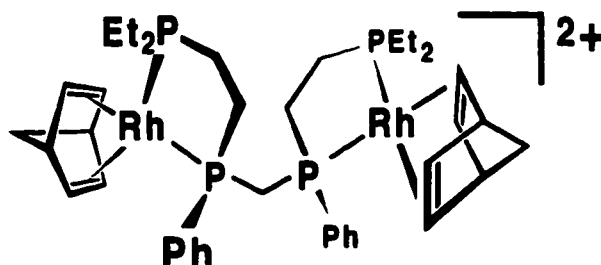


**Figure 1.5.**  $[rac-Rh_2(nbd)_2(et,ph-P4)]^{+2}$  catalyst precursor, **1r**

As seen in Figures 1.4 and 1.5, the design of the ligand is highly unusual because it can chelate and bridge two metal centers. Another interesting design element is the presence of only a single bridging functionality. This introduces a flexibility that allows the bimetallic complex to be in either an open- or closed-mode geometry. The open-mode occurs when the metals are rotated away from one another giving a  $M \cdots M$  separation of 5 to 7 Å. The closed-mode occurs when the metals are bonded or within 2.6 to 3 Å (Figure 1.6).<sup>13</sup>

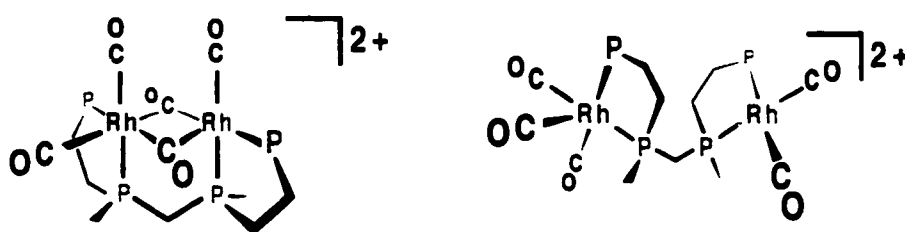


**Figure 1.6.** Illustration of open- and closed-mode complexes

The active hydrido-carbonyl catalyst is generated by reaction of the bimetallic catalyst precursor with synthesis gas (1:1 mixture of  $H_2/CO$ ) and then 1-hexene is added and hydroformylated. Currently, only the racemic form of



the ligand is used because it is 12 times more reactive than the meso diastereomer and is considerably more chemoselective (Table 1.1). It also reacts faster than the commercial Rh/PPh<sub>3</sub> catalyst under these mild conditions and has slightly higher aldehyde linear to branched (L/B) regioselectivity.

**Table 1.1.** Hydroformylation<sup>a</sup> results for 1-hexene at 90 °C, 90 psig<sup>14</sup>

Catalyst Precursor	Initial Turnovers (per hr) <sup>b</sup>	Aldehyde L/B ratio <sup>c</sup>	(%) Alkene isomerization	(%) Alkene hydrogenation
1r	640	28:1	8	4
Rh(CO) <sub>2</sub> (acac) + .82 M PPh <sub>3</sub>	540	17:1	3	3
1m	55	14:1	24	10

<sup>a</sup> At 90 psig, 1:1 H<sub>2</sub>/CO, 90°C, acetone solvent, 1 mM catalyst concentration, ~ 1.2 M 1-hexene

<sup>b</sup> (mol product/ mol catalyst); rate at the initial linear part of the uptake curve representing the highest catalytic rate

<sup>c</sup> linear: branched aldehyde product ratio based on GC and NMR analysis

Stanley's catalyst system is quite stable with respect to Rh-induced phosphine fragmentation reactions and it does not require any excess phosphine ligand as do virtually all other phosphine-modified hydroformylation catalysts. Earlier there was a brief discussion on Union Carbide use of excess PPh<sub>3</sub>. Union Carbide has reported Rh-induced PPh<sub>3</sub> cleavage reactions to produce the catalytically inactive dimer Rh<sub>2</sub>(μ-PPh<sub>2</sub>)<sub>2</sub>(CO)<sub>4</sub> and it is acknowledged that the excess PPh<sub>3</sub> adds extra stability by preventing the formation of 14e<sup>-</sup> unsaturated Rh complexes that promote this reaction. It should also be noted that the excess phosphine also strongly contributes to the formation of linear aldehyde. In marked contrast, excess et,ph-P4 ligand

deactivates Stanley's bimetallic catalyst because the *rac*-et,ph-P4 ligand coordinates and donates so strongly to the rhodium metal centers.

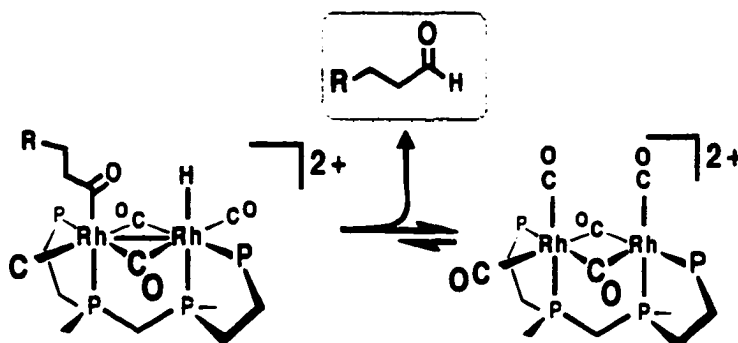


**Figure 1.7.** Example of intramolecular hydride transfer

It is thought that the catalyst employs bimetallic cooperativity via an intramolecular hydride transfer to assist in the elimination (Figure 1.7) of the final aldehyde product. The racemic bimetallic catalyst is very active and it hydroformylates selectively via bimetallic cooperativity.<sup>12</sup> Several persuasive points support this conclusion. The replacement of the methylene bridge with *p*-xylene or propyl "spacer" groups (Figure 1.8) showed that the rhodium metal centers were unable to cooperate effectively with each other due to the separation of the metal centers. These two "separated" bimetallic complexes were very poor hydroformylation catalysts (1-2 TO/hr, 3:1 linear to branched aldehyde selectivity, ~70% alkene isomerization and hydrogenation side reactions).<sup>12,14</sup>

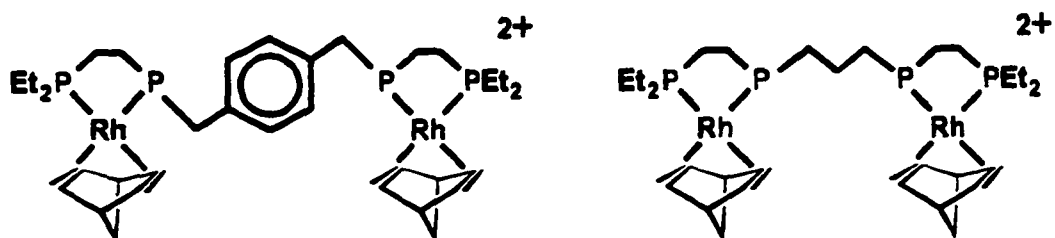


**Figure 1.8.** Spaced bimetallic analogs

Previously, it was stated that the racemic catalyst is 12 times faster than the meso catalyst (see Table 1.1). We believe this is due to the fact that the racemic catalyst has the ability to form a double bridged hydrido-carbonyl species,  $rac-[Rh_2H_2(\mu-CO)_2(CO)_2(et,ph-P4)]^{2+}$ , **2r** (Fig. 1.9), that favors the intramolecular hydride transfer.<sup>15</sup>

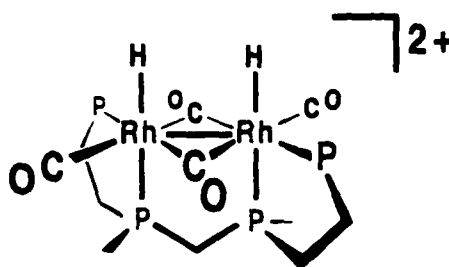


**Figure 1.9.** Proposed structure of  $rac-[Rh_2H_2(\mu-CO)_2(CO)_2(et,ph-P4)]^{2+}$ , **2r**

The racemic catalyst is more likely to form this species relative to the meso catalyst because of the stereochemical orientation of the phosphine chelate rings and the proximity of the ligands to the rhodium metal centers. FT-IR *in situ* spectroscopic studies have clearly indicated the importance of dicationic bimetallic complexes in the hydroformylation, with the activity of the catalyst directly related to the presence of bridging carbonyl bands in the IR. *In situ* high pressure NMR studies do not appear to directly show the active catalyst  $[rac-[Rh_2H_2(\mu-CO)_2(CO)_2(et,ph-P4)]^{2+}]$ , **2r**. The presence, however, of

the starting pentacarbonyl complex,  $[rac-Rh_2(CO)_5(et,ph-P4)]^{2+}$ , **3r**, and closed mode  $[rac-Rh_2(\mu-CO)_2(CO)_2(et,ph-P4)]^{2+}$ , **4r\***, both point to the presence of the proposed active hydride catalyst **2r**.

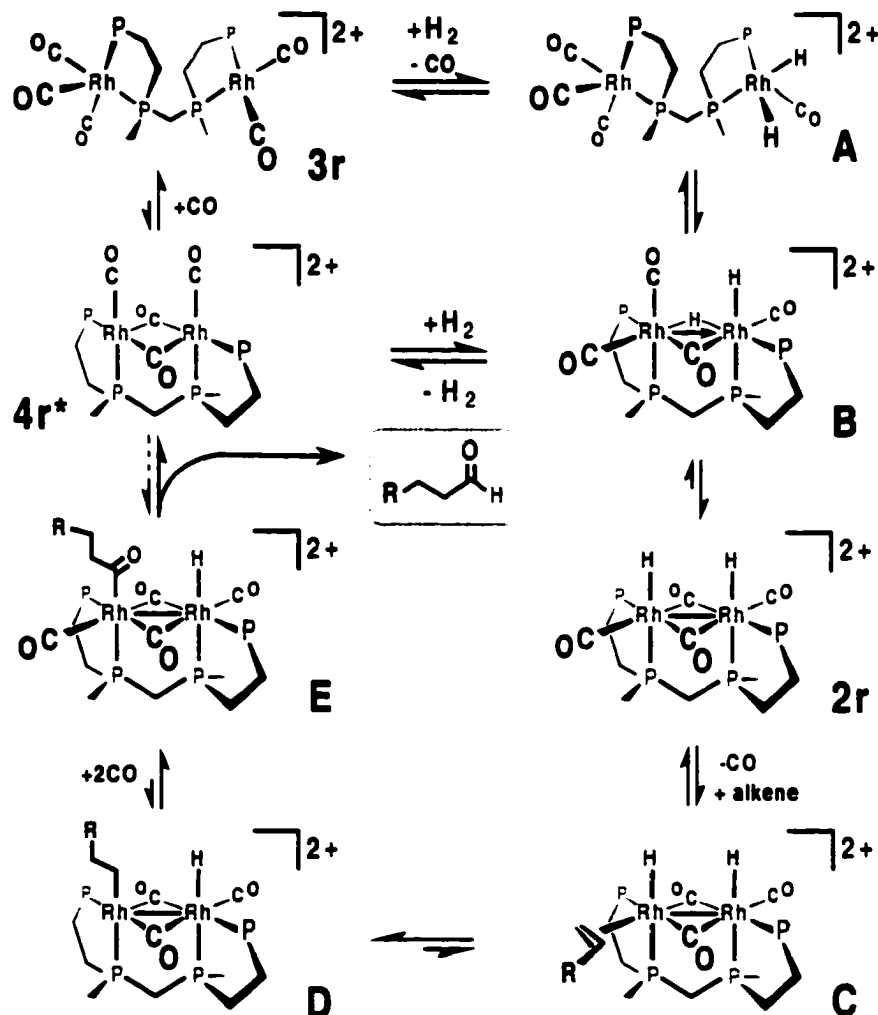


**Figure 1.10.** Proposed bimetallic dicationic hydroformylation mechanism

The mechanism (Figure 1.10) is proposed to begin with the pentacarbonyl complex,  $[rac-Rh_2(CO)_5(et,ph-P4)]^{2+}$ , **3r**. Oxidative addition of hydrogen produces a Rh(+1)/Rh(+3) mixed oxidation state complex,  $Rh_2H_2(CO)_4(et,ph-P4)]^{2+}$ , **A**. An intramolecular hydride transfer between the rhodium metal centers, via complex **B**, generates the active catalyst, **2r** (Figure 1.9).

The dissociation of one of the terminal carbonyls opens a coordination site for alkene (1-hexene) to coordinate, **C**. The alkene undergoes a migratory insertion into the rhodium-hydride bond giving an alkyl ligand, **D**. Carbonyl ligand coordination leads to migratory insertion into the metal-alkyl bond to produce the acyl ligand, **E**. Another intramolecular hydride transfer takes place between the metal centers to reductively eliminate the final aldehyde product producing **4r\***. This closed-mode bridging CO complex can either add a CO ligand and rotate to the open-mode complex, **3r**, or directly react with  $H_2$  to ultimately reform **2r**.

#### 1.4. Hydroformylation Kinetic Studies

One of the early puzzling features of this bimetallic catalyst was the apparent inhibition of the catalyst at high concentrations ( $> 2\text{-}3\text{ M}$ ) of 1-hexene. This observation, if correct, could represent an important piece of experimental data supporting the bimetallic cooperativity concept. Professor Stanley has proposed<sup>14</sup> that the inhibition could be caused by the formation of bis-acyl species, **H**, at high alkene concentrations (Fig. 1.11).

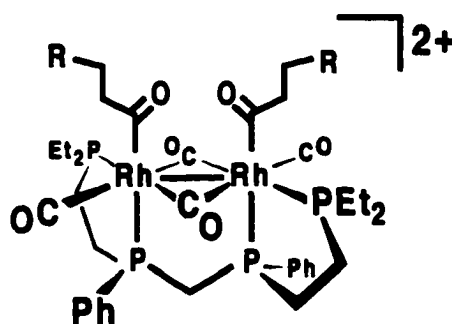


**Figure 1.11.** Proposed structure of bis-acyl species, **H**

This type of complex might inhibit the hydroformylation because there is no hydride present to perform the final intramolecular hydride transfer. There is a reaction that one can perform with this bis-acyl species: a bimolecular reductive elimination that leads to the formation of a diketone product (Figure 1.12). A partial proposed mechanism begins with the active catalyst, **2r**, that dissociates two carbonyls to open up coordination sites allowing the addition of excess alkene to produce the bis-alkene complex **F**. The alkenes undergo migratory insertion into the rhodium-hydride bonds to form two alkyl ligands producing **G**. Carbonyl coordination and migratory insertions produce the bis-acyl species, **H**. A bimolecular reductive elimination could then occur to form a diketone.

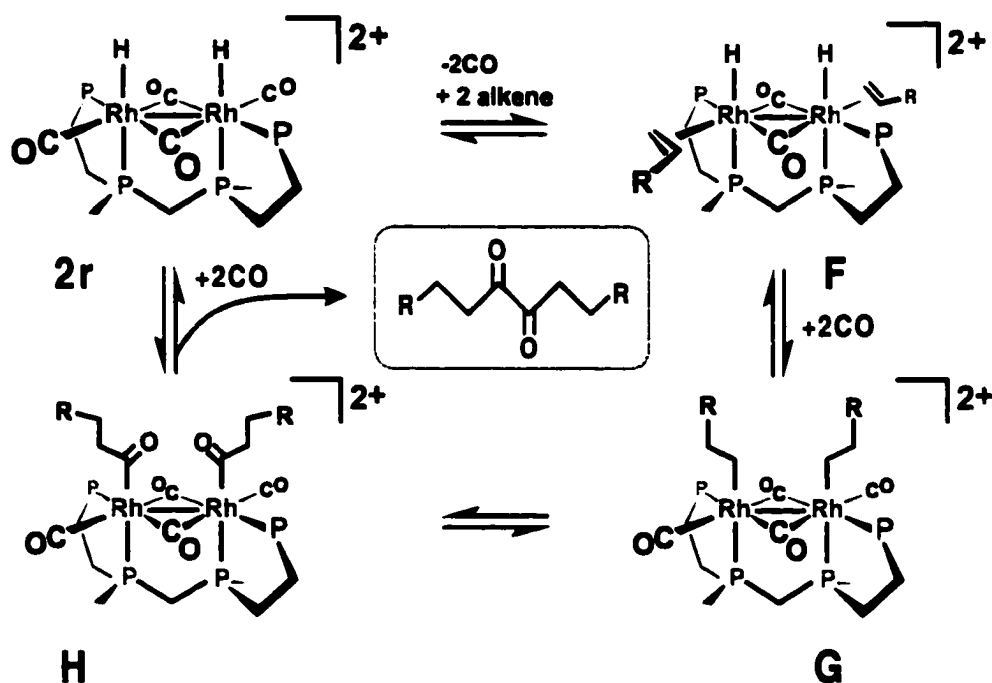


**Figure 1.12.** Proposed formation of the bis-acyl bimetallic complex, **H**, and a bimolecular reductive elimination to produce the diketone product

This, however, is a very unusual reaction and there is no precedence in the literature for a bimolecular reductive elimination forming a diketone. So we were quite skeptical that this could be occurring. We certainly did not have any experimental evidence for the formation of diketones in any of our reactions.

The interest in studying the effect of high alkene concentrations, therefore, fits quite nicely with our desire to collect some detailed kinetic data on the effect of alkene and catalyst concentration on the catalysis. The kinetic orders of alkene and catalyst can provide important data supporting our proposed mechanism.

### **1.5. Polar Phase Hydroformylation to Hydrocarboxylation Catalysis**

In the early studies of our bimetallic hydroformylation catalyst, graduate student Spencer Train studied a variety of solvents systems for the catalysis.<sup>16</sup> He found that the bimetallic dicationic hydroformylation catalyst was highly sensitive to the solvent system used. The best solvents were polar, but not strongly coordinating. DMF, acetone and acetophenone solvents were found to generate the most active hydroformylation catalyst solutions. MeOH and acetonitrile were found to be very poor solvents, it was believed, due to their too strong coordinating properties. Lower polarity solvents like  $\text{CH}_2\text{Cl}_2$  generated catalyst solutions that were only about 25% as active as that in acetone. The FT-IR of the catalyst in  $\text{CH}_2\text{Cl}_2$ , 1:1  $\text{CH}_2\text{Cl}_2$ /acetone, and pure acetone is shown in Figure 1.13.

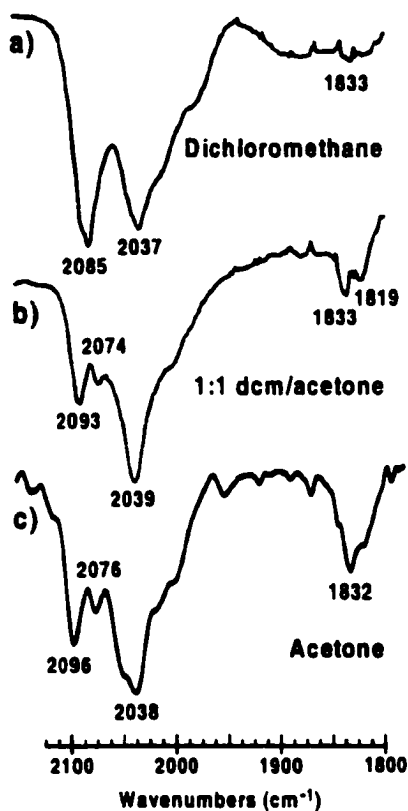


**Figure 1.13.** *In situ* FT-IR spectra of catalyst precursor under hydroformylation conditions (90 psig 1:1 H<sub>2</sub>/CO and 90 °C in the following solvents:(a) CH<sub>2</sub>Cl<sub>2</sub>, (b) 1:1 CH<sub>2</sub>Cl<sub>2</sub>/acetone, and (c) acetone)

The intensity of the bridging CO band seems to correlate directly with the activity of the catalyst solution and the formation of the proposed active catalyst,  $[\text{rac-Rh}_2\text{H}_2(\mu\text{-CO})_2(\text{CO})_2(\text{et,ph-P4})]^{2+}$ , **2r**. The importance of the polar solvent appears to be more than just simple solubility since the catalyst is far more soluble in CH<sub>2</sub>Cl<sub>2</sub> than acetone, but only 25% as active. Prof. Stanley has proposed that the polar solvent may help in minimizing electrostatic repulsion effects when the catalyst rotates from an open-to a closed-mode conformation. This is illustrated in Figure 1.14. The dicationic charge on the open-mode pentacarbonyl **3r** is partially localized on each rhodium center, but will also be



spread out over the surrounding ligand sets. There should be an electrostatic barrier for rotating these similarly charged halves of **4r** or **A** towards each other to form the closed-mode complexes **4r\*** or **B**.

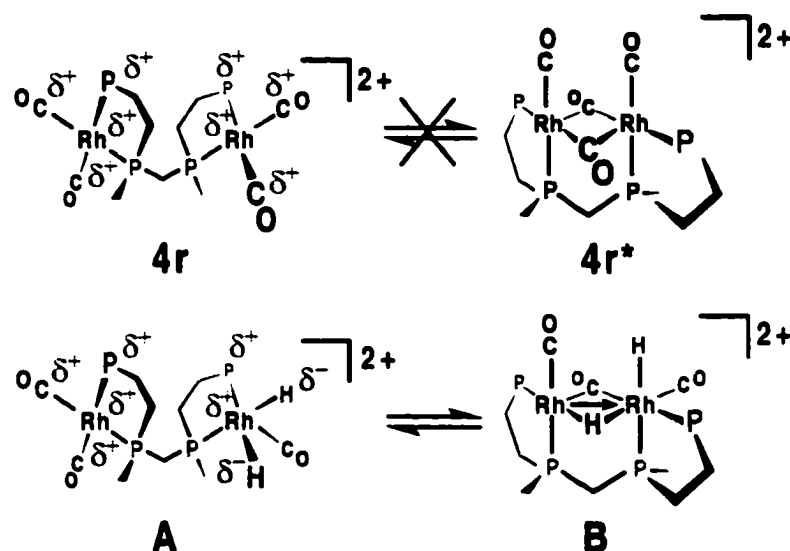


**Figure 1.14.** Illustration of electrostatic effects for conversion of open to closed mode bimetallic structures

We believe that polar solvents help diffuse the cationic charges and lower the electrostatic barrier to rotation from open- to closed-mode structures. Water is one of the most polar solvents and could offer some real advantages in our system. Unfortunately, when we ran the catalyst in water (the precursor norbornadiene complex **1r** is soluble in water) we saw almost no hydroformylation with 1-hexene. Discussions with Dr. Jerry Unruh from Celanese, however, demonstrated that this was completely expected due to the very low solubility of 1-hexene in water. Ruhrchemie performs aqueous phase hydroformylation on propylene using a rhodium catalyst based on the sulfonated triphenylphosphine ligand (TPPS) originally developed by Kuntz at

Rhone Poulenc.<sup>17</sup> They have found that one of the major limitations of this process is the insolubility of higher alkenes in water and the subsequent inability to reach the water-soluble catalyst.

The separation of product from the catalyst solution is one of the major engineering problems associated with any homogeneous process. The Shell Higher Olefin Process (SHOP) represents a classic example of a homogeneous catalyst where this problem was simply solved through the use of a relatively polar diol-based solvent in which the nickel catalyst is soluble, but the oligomerized non-polar alkene product is not. The product, therefore, nicely phase separates out from the catalyst solution and can be easily removed. The previously mentioned Ruhrchemie water-based hydroformylation catalyst that uses the water-soluble TPPS ligand to make a highly water-soluble (and organic insoluble) catalyst that hydroformylates propylene to make the butylaldehyde that phase separates out from the aqueous catalyst solution. The limitation of this process with respect to higher alkenes, however, has prompted considerable research into new variants on these ideas.

Horvath and coworkers,<sup>18</sup> for example, have recently gained quite a bit of attention with the use of catalysts with fluorocarbon-substituted ligands that are soluble in fluorocarbon solvents. At higher temperatures, organic compounds are miscible in fluorocarbon solvents and can access the catalyst. But at lower temperatures the organic products phase separate out. But these fluorous phase catalyst systems face a number of problems and challenges. The fluorocarbon-substituted ligands are challenging to prepare synthetically and

care must be taken to “insulate” the catalyst from the strongly electron-withdrawing fluorocarbon groups. The solubility of the fluorocarbon solvent and catalyst with the organic product can also lead to solvent and catalyst leeching.

The compatibility of our dicationic bimetallic rhodium catalyst with polar solvents lead us to consider attempting to perform polar phase hydroformylation by increasing the polarity of the acetone solvent through the addition of water. Alkenes are soluble enough in this polar solvent mixture to easily reach the catalyst, but the longer chain somewhat less polar aldehyde products could phase separate out. Questions about the stability of our catalyst towards water and the effect of water on hydroformylation could only be answered by trying it out.

The use of a 30% water-acetone mixed solvent system turns out to have a dramatic and highly positive effect on the hydroformylation catalysis. We see an increase in the initial turnover frequency for the hydroformylation of 1-hexene by 49%, about the same aldehyde linear to branched regioselectivity, and a dramatic lowering of the alkene isomerization and hydrogenation side reactions from 12% in pure acetone to under 1% in the water-acetone mixed solvent. A slow leak in the autoclave during these runs proved to be extremely fortuitous by allowing us to accidentally generate the proper reaction conditions to observe the formation of carboxylic acid products, also with high linear to branched regioselectivity.

The observation of carboxylic acids from the hydroformylation of alkenes is unprecedented. As mentioned earlier, Ruhrchemie runs aqueous phase hydroformylation and Prof. Stanley has discussed with Celanese chemists (Ruhrchemie is a subsidiary of Celanese) intimately familiar with this chemistry that they do not produce any carboxylic acids. The reaction of alkenes, CO and water to produce carboxylic acids is known and is called hydrocarboxylation.

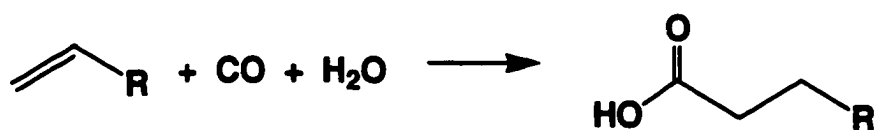


**Figure 1.15.** Hydrocarboxylation catalysis

This is an extremely difficult reaction to perform. The closest related systems are monometallic Pd catalysts, but these usually require the use of strong acids or other modifiers such as  $\text{SnCl}_2$  as co-catalysts. They also typically have slow rates and low product selectivities.<sup>19</sup> Ni and Co complexes are also known to catalyze this reaction, but only under rather high pressures and temperatures ( $> 200$  atm,  $> 200$  °C) and with low product selectivities.<sup>20</sup> A few rhodium-based catalysts are known, but they all use iodide co-catalysts and have low to moderate selectivities.<sup>21</sup> Details on these will be presented later.

A large part of the difficulty in this reaction is in the catalytic activation of water. Virtually every known hydrocarboxylation catalyst uses a modifier such as strong acid or iodide. A question is how our system works since  $\text{H}_2$  is

present. The presence of a leak in the autoclave and initially irreproducible results on the catalysis made additional studies extremely important. We are now pleased to report a major breakthrough in hydrocarboxylation and another example of the importance of our bimetallic rhodium catalyst and tetraphosphine ligand in defining a new area of catalytic research.

## 1.6. References

1. C. Masters, *Homogeneous Transition-Metal Catalysis*, Chapman, Hall, London, 1981.
2. G. W. Parshall, *Homogeneous Catalysis*, Wiley-Interscience, New York, 1980.
3. a) R. B. Jordan, *Reaction Mechanisms of Inorganic and Organometallic Systems*, Oxford University Press, Oxford, 1991; b) B. R. James, *Adv. Organometal. Chem.*, **319**, **1979**, 91; c) J. Halpern, and S. Wong, *J. Chem. Soc., Chem. Comm.*, **1973**, 629, d) P. Meakin, J. P. Jesson, C. A. Tolman, *J. Chem. Soc.*, **1977**, 8055, 99.
4. G. A. Somorjai, *Chemistry in Two Dimensions*, Cornell Univ. Press, Ithaca, N.Y., 1981.
5. R. F. Heck, and D. S. Breslow, *J. Am. Chem. Soc.*, **1961**, **83**, 4023.
6. a) Exxon Chem., (J.A. Hanin), EP 0.343, 819 (1989); b) Exxon Res. Eng., (J.A. Hanin), EP 0.183, 545 (1985).
7. J. D. Unruh, J. R. Christenson. *J. Mol. Catal.*, **1982**, **14**, 19-34.
8. a) B. Cornils and W. A. Herrmann, eds., *Applied Homogeneous Catalysis with Organometallic Compounds*, vol.1., New York, p. 76-80; b) Union Carbide Corp (R. L. Pruett, J. A. Smith), US 3.527.809, **1967**, US 4.148.830, **1969**, DE 2.062.703, **1971**.
9. a) E. L. Muetterties, *Bull. Soc. Chim. Belg.*, **84**, **1975**, 959; b) E. L. Muetterties, *ibid.*, **85**, **1976**, 451, c) E. L. Muetterties, *Angew. Chem. Int. Ed. Engl.* **17**, **1978**, 545, d) E. L. Muetterties, M. J. Krause, *ibid.*, **22**, **1983**, 135.
10. M. Garland, *Organometallics*, **12**, **1993**, 535-543; b) C. Fyhr, M. Garland, *Organometallics*, **12**, **1993**, 1753-1764.

11. a) M. F. Mirbach, *J. Organomet. Chem.*, **1984**, 265, 205; b) W. R. Moser, in *ACS Advances in Chemistry Series*, Vol. 230; ACS: Washington, DC., 1992; c) R. C. Ryan, C.U. Pittman Jr., P. O. O'Connor, *J. Am. Chem. Soc.*, **1977**, 99, 1986; d) C. U Pittman, Jr., G. M. Wilemon, W. D. Wilson, R. C. Ryan, *Angew. Chem. Int. Ed. Engl.*, **1980**, 19, 478; e) G. Süss-Fink, *Angew. Chem.*, **1994**, 106, f) G. Süss-Fink, *Angew. Chem. Int. Ed. Engl.*, **1994**, 33, 67.
12. M. E. Broussard, B. Juma, S. G. Train, W. J. Peng, S. A. Laneman, G. G. Stanley, *Science*, **1993**, 260, 1784.
13. S.A. Laneman, G.G. Stanley, *Adv. Chem.Ser.*, **1992**, 230, 349.
14. G. G. Stanley, in *Catalysis by Di- and Polynuclear Cluster Complexes*, Wiley: New York, 1998.
15. R. C. Matthews, D. K. Howell, W. J. Peng, S. G. Train, W. D. Treleaven, G. G. Stanley, *Angew. Chem., Int. Ed. Engl.* **1996**, 35, 2253.
16. S. G. Train, dissertation for Ph.D. degree at Louisiana State University, 1995.
17. E. Kuntz, *CHEMTECH*, **1987**, 17, 570.
18. I. T. Horvath, G. Kiss, R. A. Cook, J. E. Bond, P. A. Stevens, J. Rabai, and E.J. Mozeleski, *J. Am. Chem. Soc.* **1988**, 120, 3133-3143.
19. a) F. Bertoux, E. Monflier, Y. Castanet, A. Mortreux, *Mol. Catal.* **1999**, 143, 11-22. (b) A. L. Lapidus, S. D. Pirozhkov, *Russ. Chem. Rev.* **1989**, 58, 197-233.
20. a) T. Chenal, I. Cipres, J. Jenck, P. Kalck, Y. Peres, *J. Mol. Catal.*, **1993**, 78, 351. b) L. Garlaschelli, M. Marchionna, M. C. Iapalucci, G. Longoni, *J. Organomet. Chem.* **1989**, 378, 457. d) G. Cavinato, L. Toniolo, D. Botteghi, *J. Mol. Catal.*, **1985**, 32, 211. e) M. Beller et al, *J. Mol. Catal.*, **1995**, 104, 17 and references therein.
21. F. F. Pruchnik, P. Smolenski, E. Galdeka, Z. Galdecki, *New J. Chem.* **1998**, 1395-1398

## CHAPTER 2

### HYDROFORMYLATION KINETIC STUDIES

#### 2.1. Introduction

As stated earlier, there have been numerous studies on polymetallic systems. Many of these studies were on clusters<sup>1</sup> that degrade to a monometallic complex that acts as the active catalyst. The general types of systems studied included homometallic and heterometallic, phosphido-bridged, and ligand-modified clusters.<sup>2</sup> In 1993, Garland<sup>3</sup> reported detailed studies on the hydroformylation catalytic activity of  $\text{Rh}_4(\text{CO})_{12}$ ,  $\text{Rh}_6(\text{CO})_{16}$ ,  $\text{Rh}_2(\text{CO})_4\text{Cl}_2$ ,  $\text{CoRh}(\text{CO})_7$  and  $\text{Co}_2\text{Rh}_2(\text{CO})_{12}$  clusters. Garland clearly demonstrated that all these systems degrade to produce the highly active monometallic catalyst  $\text{HRh}(\text{CO})_3$  under hydroformylation conditions. It should be noted that these cluster systems perform best at high temperatures and pressures<sup>3</sup> where the clusters readily fragment.

Garland understood that it was essential to carry out detailed kinetic studies on catalytic systems in order to gain insight into the true nature of the catalyst and mechanism. One example is the study of  $\text{Rh}_4(\text{CO})_{12}$  in which Garland used infrared spectroscopy to determine the concentrations of the reactants and products. This information was then used to determine reaction rates, kinetic orders, intermediate complexes in the catalysis, to trace the production of the final product (4,4-dimethylpentanal, 44DMP) and the disappearance of the reactants. Garland observed that the original precursor,  $\text{Rh}_4(\text{CO})_{12}$  disappeared, but an intermediate  $(\text{acyl})\text{Rh}(\text{CO})_4$  ( $\text{acyl} =$

(CO)CH<sub>2</sub>CH<sub>2</sub>C(CH<sub>3</sub>)<sub>3</sub>) was being formed and later converted to the final 44DMP product. Garland attributes the presence of the monometallic intermediate to a precatalytic cluster fragmentation sequence.<sup>4</sup> Garland proposed the following reaction sequence for the fragmentation of the starting Rh<sub>4</sub>(CO)<sub>12</sub> cluster to produce the catalytically active HRh(CO)<sub>3</sub> complex (Figure 2.1).

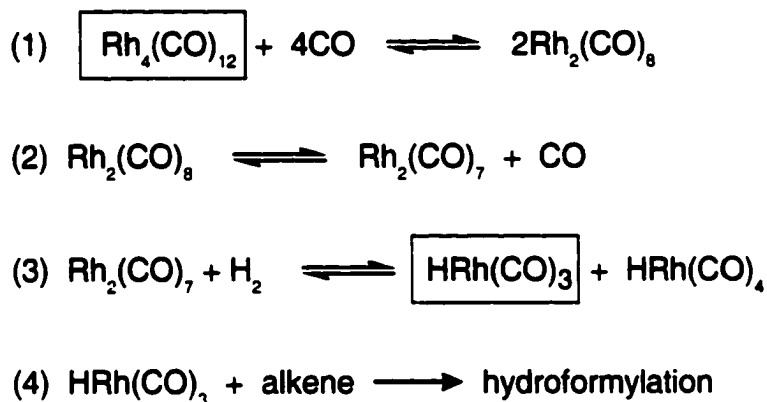


**Figure 2.1.** Garland's precatalytic reaction sequence

The kinetic expression is:  $d[\text{aldehyde}]/dt = k[\text{Rh}_4(\text{CO})_{12}]^{0.25}[\text{CO}]^0[\text{H}_2]^{0.5}[\text{alkene}]^1$ .

The kinetic studies clearly show a 0.25 order dependence on the reaction rate with the starting [Rh<sub>4</sub>(CO)<sub>12</sub>] concentration. This implies that the cluster fragments to produce one active catalyst species while the other three rhodium atoms are involved in inactive metal complexes. The spectroscopic observation of a monometallic rhodium acyl species that is directly related to the eventual aldehyde product formation provides confirming evidence that the active catalyst is the monometallic HRh(CO)<sub>3</sub> catalyst. Garland's careful kinetic studies combined with *in situ* spectroscopic characterization of the catalyst solution is a very nice demonstration of how to figure out how a catalyst system



works. Others in the Stanley group have been working on the *in situ* spectroscopic studies of our catalyst, but no one had performed careful kinetic studies and this formed the core of my first set of studies.

In our case we have a ligand-modified bimetallic catalyst that, unlike the cluster systems, does not degrade to a catalytically active monometallic system. We have proposed that there are two metal centers cooperating to generate a very active and selective catalyst. Kalck<sup>5</sup> has also proposed this type of cooperativity with a thiolato-bridged dirhodium complex that forms an active hydroformylation catalyst. But Davis<sup>6</sup> has shown from mass spectral studies that Kalck's dirhodium complex readily fragments in solution. More recently Claver and van Leeuwen<sup>7</sup> have confirmed the facile fragmentation of Kalck's system under catalytic conditions and that a monometallic Rh catalyst is responsible for the hydroformylation.

It is our intention to gain a clearer understanding of the nature of our bimetallic catalyst system. We would like to obtain further information on the nature of the catalytically active species and more evidence about the bimetallic cooperativity occurring in this catalyst. We believe by performing kinetic studies we can address these concerns. Matthews<sup>8</sup> has previously performed *in situ* IR and NMR studies on  $[\text{Rh}_2\text{H}_2(\mu\text{-CO})_2(\text{CO})_2(\text{et,ph-P4})]^{2+}$ , **2r**. These studies indicated that **2r** was the active catalytic species for our bimetallic system. The studies also provided strong evidence supporting our current proposed bimetallic cooperativity mechanism (section 1.2). These studies combined with our kinetic studies on the orders of the catalyst precursor and alkene (1-

hexene) concentrations will provide important information concerning our bimetallic system. Our goal is to obtain additional evidence to support our theory of bimetallic cooperativity and to provide details on the overall catalytic mechanism.

Previously there were several studies performed by Dr. Spencer Train and Dr. Donna Howell<sup>9,10</sup> to investigate our bimetallic catalyst's performance with different  $\alpha$ -olefins. The results are shown in Table 2.1.

**Table 2.1.** Previous Studies on the Hydroformylation of  $\alpha$ -olefins by 1r showing the "false" odd alkene effect

Olefin	Initial Turnover Rate (TO/hr)	% Alkene Conversion to aldehyde	L/B Aldehyde Ratio	% Alkene Iso <sup>a</sup>	% Alkene Hyd <sup>b</sup>
Ethylene	1930	100	100	0	0
Propylene	1100	100	20.0	0	0
1-Butene	1060	89.9	20.1	5.2	1.0
1-Pentene	580	65.7	23.1	18.5	0.9
1-Hexene	640	85.0	27.5	8.0	3.4
1-Heptene	134	27.1	20.7	36.3	2.8
1-Octene	915	86.7	21.1	5.1	2.1

Note: Experiments were performed at 90°C, 90 psig H<sub>2</sub>/CO in acetone, 1mM catalyst, 1600 equiv of 1-hexene  
<sup>a</sup>iso represents isomerization    <sup>b</sup>hyd represents hydrogenation

When discussing the aldehyde linear to branch regioselectivities (L/B) it should be noted that the ratio can exaggerate the apparent selectivity if the concept of what it stands for is not clearly understood. For example, propylene has a L/B regioselectivity of 20.0 (taken from Table 2.1), which means there is 95.2% linear and there is 4.8% branched. Likewise if we look at 1-hexene, which has a L/B regioselectivity of 27.5 that corresponds to 96.5% linear and

3.5% branched. There is therefore only a 1.25% difference in the linear products made in these two reactions. It is for this very reason that catalytic runs are evaluated by several factors and not just the regioselectivity. To correctly assess a catalytic system's overall efficiency one should take into consideration the initial turnover frequency, conversion of olefin to aldehyde, regioselectivity, isomerization and hydrogenation side reaction

## 2.2. Initial Kinetic Studies and Problems Encountered

Most hydroformylation catalyst have the following general kinetic rate expression ( $k$  = rate constant):

$$\frac{d[\text{aldehyde}]}{dt} = k [\text{alkene}] [\text{H}_2] [\text{CO}]^{-1} [\text{catalyst}]$$

**Figure 2.2.** General hydroformylation kinetic rate expression

We decided to start with determining the alkene and catalyst kinetic orders. In such the initial concentration of one reactant is varied while the other components are kept the same. Measurement and comparison of the initial rates of the reaction with the changes in concentration of the reactant allows the determination of the kinetic order of the reactant. Other group members had previously determined that the change in the hydroformylation rate with the decreasing alkene concentration during a typical hydroformylation run (where the  $\text{H}_2$ , CO and catalyst concentrations stayed approximately the same) did correspond to first order behavior.<sup>9,10</sup> Our interest in possible alkene inhibition effects at higher concentrations, however, prompted the more extensive study that is reported here. 1-hexene was used as our alkene and [*rac*-

$\text{Rh}_2(\text{nbd})_2(\text{et,ph-P4})(\text{BF}_4)_2$ , **1r**, as our catalyst precursor. We used our standard hydroformylation conditions for the runs (90 psig 1:1  $\text{H}_2/\text{CO}$ , 90°C, acetone solvent, 1000 rpm), only varying the amount of 1-hexene added to the reaction to initiate hydroformylation catalysis. The results from an initial series of runs with 1-hexene concentrations ranging from 1.0 to 4.0 M are shown in Table 2.2.

**Table 2.2.** Initial alkene concentration dependency hydroformylation results affected by alkene purity and autoclave leak problems

[alkene]	% iso <sup>a</sup>	L/B <sup>b</sup>	Initial Rate <sup>c</sup>	Factor <sup>d</sup>
1.0 M	8.0	28:1	420	1
1.5 M	15.1	22:1	620	1.5
2.0 M	3.6	33:1	780	1.9
2.5 M	12.6	15:1	1300	3.1
3.0 M	11.2	19:1	1410	3.4
3.5 M	29.0	16:1	1510	3.6
4.0 M	15.8	18:1	2500	5.9

<sup>a</sup>.Iso is an abbreviation for isomerization

<sup>b</sup>.L/B is an abbreviation Linear to branched ratio of aldehyde products

<sup>c</sup> The initial turnover rate that is obtained from the aldehyde production curves

<sup>d</sup>This indicates the relative increase in the initial turnover rate referenced to the 1.0M 1-hexene run

These initial findings indicated that the reaction was 1<sup>st</sup> order in alkene, which was determined by comparison of the initial turnover frequencies relative to the starting alkene concentration. There were, however, some discrepancies at concentrations greater than 2.5 M. Initially, we were unsure why there was a fluctuation in the correspondence of the rates to 1<sup>st</sup> order behavior at higher alkene concentrations. After careful investigation of the aldehyde production curves, we observed that the catalyst continued to hydroformylate 1-hexene even at very high initial concentrations, but that the catalytic reactions only ran

to 65-70% completion (fig. 2.3). We did not observe any alkene-based inhibition that might have indicated the formation of a catalytically inactive bis-acyl species in the catalytic mixture (see section 1.4 and further discussion in section 2.3 of this chapter).

We believe that the discrepancies in the high concentration alkene runs in the high concentration alkene runs were due to impurities in the 1-hexene and a slow leak that was later detected in the system. The 1-hexene that was used to perform these studies had a purity of 97+%. We inquired to the vendor (Sigma-Aldrich) as to what was actually in the 3% impurity and were told that there were stabilizers, binders and possibly some hexane present. We performed a GC-MS analysis of the 1-hexene and found that there was hexane, 2-hexene, and 3-hexene present. Additional information supplied by Dr. Donna Howell and hydroformylation experts at Celanese and Union Carbide on the catalyst deactivating effects of peroxide impurities that are quite common in liquid alkenes, caused us to pay very close attention to how the 1-hexene was purified.

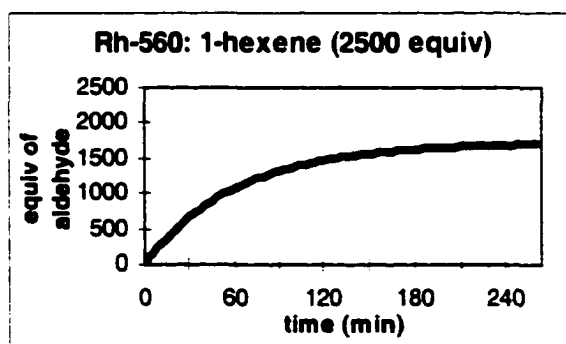


**Figure 2.3.** Aldehyde production curve of run Rh560 showing only 68% conversion of alkene to aldehyde

This study demonstrated two key concepts: 1) impurities can (most likely peroxide-based) drastically effect the initial turnover rate and alkene conversion to aldehyde, and 2) the amount of impurity present in stored 1-hexene can increase over time and thus give variable catalytic results.

### **2.3. Kinetic Study of the Alkene Concentration**

We began by correcting the leak in our autoclave system and then taking special care in removing peroxide impurities by passing the 1-hexene through an alumina slurry under nitrogen before hydroformylation. As we performed a number of hydroformylation runs and experimented with various details on cleaning the alkene, we noticed a few subtleties. First, the olefin must be cleaned immediately before beginning the catalysis run. One unusual feature was that the catalyst would hydroformylate the olefin well in the first hour, but then become significantly slower as the run progressed, i.e. total conversion for the run would be less than 65%.

We eventually realized that the alumina slurry used for removing peroxide could not be used more than once; because it rapidly becomes deactivated presumably from the peroxide impurities or stabilizers present in 1-hexene. The hydroformylation runs shown in Figure 2.4 used the same alumina slurry for successive batches of 1-hexene and demonstrates the reduced effectiveness of the alumina in removing the catalyst deactivating impurities.

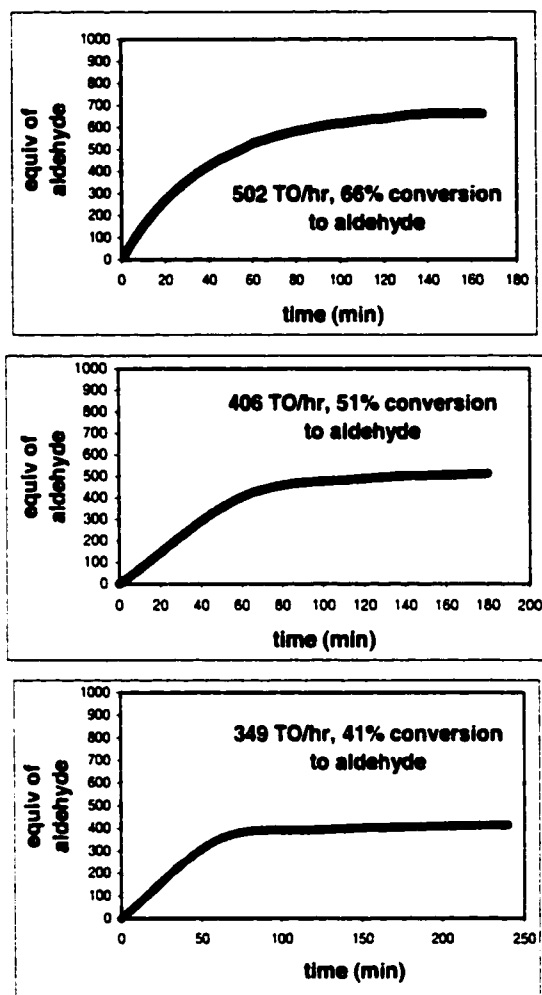


**Figure 2.4.** Illustrations of the impurity distorted hydroformylation runs using the same alumina column to purify the 1-hexene substrate (top to bottom are three consecutive runs showing the detrimental effect on increased alkene impurities on the hydroformylation)

This impurity effect was easily by using fresh alumina for cleaning the 1-hexene immediately prior to each catalyst run. We were able to generate high quality results that are consistent with our initial hypothesis that the alkene is 1<sup>st</sup> order as seen in figure 2.5. The R-value is 0.995 and the straight line indicates that we have a linear dependency.

**Table 2.3.** New alkene concentration dependency results (90 °C, 90 psig 1:1 H<sub>2</sub>/CO, 1M 1-hexene, acetone solvent)

[alkene]	Initial TO/hr <sup>a</sup>	% err <sup>b</sup>	% aldehyde	L/B <sup>c</sup>	% iso <sup>d</sup>	% hyd <sup>e</sup>	Factor <sup>f</sup>
1.0 M	524(21)	4	85.7(8)	28:1	7.8	3.4	1.0
1.5 M	724(25)	3	83.2(10)	22:1	9.6	4.2	1.4
2.0 M	1063(35)	3	85.4(4)	33:1	8.0	3.6	2.0
2.5 M	1356(31)	2	88.9(4)	15:1	5.5	2.5	2.6
3.0 M	1530(24)	1	88.6(5)	17:1	5.7	2.6	2.9
3.5 M	1848(34)	2	87.0(2)	17:1	6.8	3.1	3.5
4.0 M	2063(43)	2	86.0(2)	16:1	8.0	3.7	4.2

<sup>a</sup> average initial turnover rates reported with standard deviations

<sup>b</sup> % error in the average initial TO/hr (Relative Standard Deviation)

<sup>c</sup> L/B is an abbreviation for linear to branched aldehyde regioselectivity ratio

<sup>d</sup> alkene isomerization

<sup>e</sup> alkene hydrogenation

<sup>f</sup> relative initial turnover frequency, normalized to the 1.0 M alkene rate

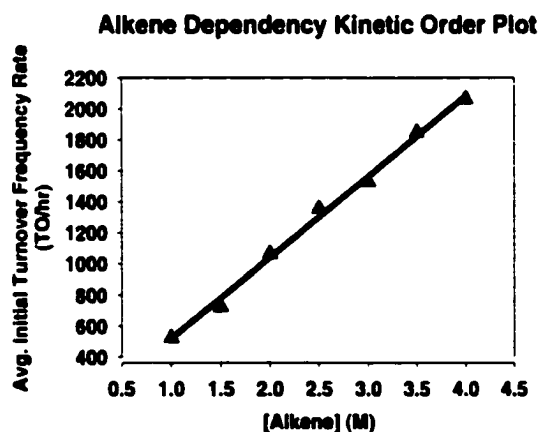


**Figure 2.5.** Alkene dependency kinetic order plot

The purified 1-hexene performed far better and we did not observe any fluctuations in the hydroformylation results. As we increased the concentration of alkene a linear first order increase in the initial turnover rate was observed.



The factor column depicts the relative increase in the initial turnover frequency referenced to the 1.0 M 1-hexene turnover frequency. If the catalysis is first order in alkene, the factor increase in the turnover frequency should correspond to the initial alkene concentration. As indicated by the aldehyde production shown in Fig. 2.6 (derived from gas uptake and verified with GC analysis), there is high conversion of 1-hexene to aldehyde product.

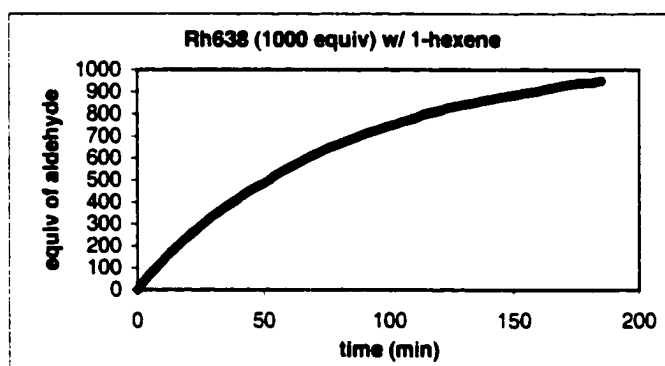


**Figure 2.6.** Aldehyde production for run Rh638

The percent errors were calculated as standard deviation divided by the median (average). The percent errors were very good, all of them were under 5%, which is excellent for catalytic runs such as these. If we compare these results to those reported in *Science*,<sup>11</sup> the 636 turnovers per hour (1.0 mM) reported in the *Science* paper is about 21% better than the 524 turnovers per hour reported in this kinetic study. Our best explanation for this difference is the experimental preparation. When the *Science* paper was written the time needed to heat the autoclaves to 90°C was only about 15 minutes, while the current runs need 45-60 minutes. The longer heating time for the current runs is either due to aging of the heating units or the fact that we are using the “half”

power setting on the heaters to avoid overshooting the target temperature. Our *in situ* spectroscopic studies indicate that the catalyst deactivation steadily occurs under hydroformylation conditions until alkene is added. So our longer heating times prior to alkene addition may well be causing more catalyst deactivation leading to slower initial turnover frequencies.

The linear to branched regioselectivities were similar to what was observed initially (Table 2.2), but we do not understand the decrease in the linear to branched regioselectivity with alkene concentrations of 2.5 M or higher. The other minor variation involved the alkene conversion to aldehyde percentages. As the alkene concentration increases so did the alkene conversion to aldehyde, in part due to lower alkene isomerization side reactions, but at 1.5 M we observed the lowest alkene conversion. The most likely explanation is that all the peroxide impurity may not have been removed from the olefin for this set of reactions. As discussed earlier the purity of the olefin has a strong effect on the alkene conversion to aldehyde. Overall, the alkene dependency kinetic studies allowed us to gain considerably more insight as to how our catalyst performs at different olefin concentrations. The kinetic studies also demonstrated the importance of cleaning the olefin properly.

#### **2.4. Kinetic study of the Dinuclear Dicationic Catalyst**

After performing the kinetic study on 1-hexene, we also wanted to investigate the kinetic order of the catalyst itself. This was done to provide support for our theory of bimetallic cooperativity and further insight into the proposed mechanism. Earlier in section 2.1, the importance of kinetic studies

was discussed and how they can be vital in characterizing and understanding a catalytic system. Garland<sup>3</sup> demonstrated that if special attention is not paid to the kinetics of a catalyst, the incorrect mechanistic pathway may be proposed. Garland illustrated this very point when he chose not to agree with many other researchers that proposed cluster catalysis or catalytic binuclear elimination in Rhodium and mixed Rhodium/Cobalt cluster hydroformylation catalysis. It is our intention to use the kinetic study to determine the order of the dinuclear dicationic catalyst.

The dinuclear dicationic catalyst precursor, *rac*-[Rh<sub>2</sub>(nbd)<sub>2</sub>(et,ph-P4)](BF<sub>4</sub>)<sub>2</sub>, **1r**, was exposed to synthesis gas to generate the active catalyst and then hydroformylated with 1-hexene under our typical reaction conditions. The results are shown in Table 2.4.

**Table 2.4.** Initial catalyst dependency results<sup>a</sup>

[catalyst]	Init. Rate (TO/hr)	Factor <sup>b</sup>
0.5 mM	210	1
1.0 mM	420	2
2.0 mM	820	4

<sup>a</sup>The reaction conditions were 90°C, 90 psig, 1:1 H<sub>2</sub>/CO, 1M 1-hexene, acetone solvent

<sup>b</sup> relative initial turnover frequency, normalized to the 1.0 M alkene rate

These initial studies indicated that that the reaction was 1<sup>st</sup> order in catalyst. It was also noticed, once again, that the hydroformylation runs only ran to 65-70% completion (Fig. 2.7), conversion of alkene to aldehyde. The initial rates, however, did show a first order dependence on catalyst concentration. The low conversion problem is believed to be caused by peroxide impurities in the 1-

hexene, as discussed in sections 2.1 and 2.2. We performed this study again with careful alkene purification prior to each hydroformylation run and the new results are presented in Table 2.5.

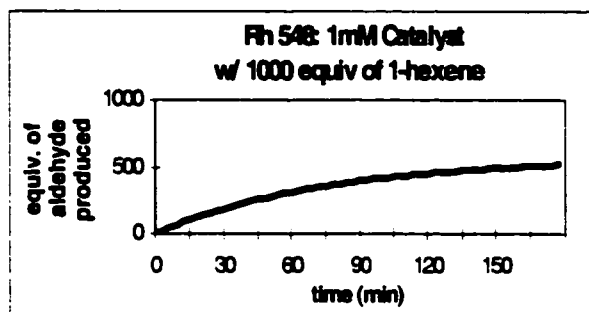


**Figure 2.7.** Hydroformylation run Rh548 showing only 50% conversion of alkene to aldehyde product

**Table 2.5.** New catalyst concentration dependency results (90 °C, 90 psig 1:1 H<sub>2</sub>/CO, 1 M 1-hexene, acetone solvent)

[catalyst]	TO/hr <sup>a</sup>	% err <sup>b</sup>	% aldehyde	L/B <sup>c</sup>	% iso <sup>d</sup>	% hyd <sup>e</sup>	Factor <sup>f</sup>
0.5 mM	250(27)	11	83.2	27:1	9.5	7.3	0.5
1.0 mM	524(21)	4	88.3	28:1	8.1	3.6	1.0
2.0 mM	1050(34)	3	87.1	28.1	10.2	2.7	2.0

<sup>a</sup> average initial turnover rates reported with standard deviations

<sup>b</sup> % error in the TO/hr (Relative Standard Deviation)

<sup>c</sup> L/B is an abbreviation for linear to branched aldehyde regioselectivity ratio

<sup>d</sup> alkene isomerization

<sup>e</sup> alkene hydrogenation

<sup>f</sup> relative initial turnover frequency, normalized to the 1.0 M alkene rate

We confirmed our previous observation that the catalyst was 1<sup>st</sup> order.

This is illustrated in figure 2.8, where the average initial turnover rate increases

linearly and in a first order manner with the increasing catalyst concentration (R-value is 0.999).

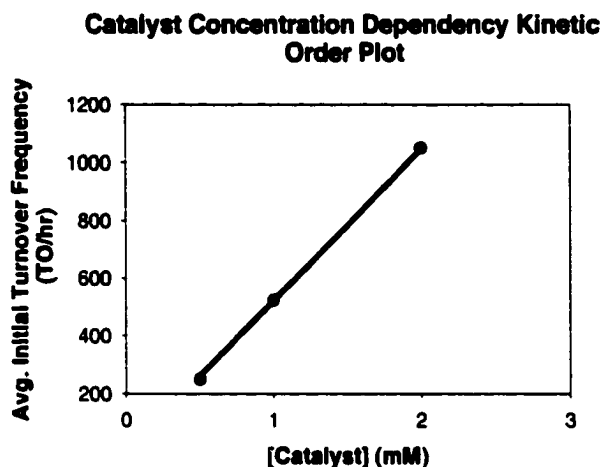


**Figure 2.8.** Catalyst concentration dependency kinetic order plot

We did not observe any catalyst deactivation and noted that the average initial turnover rate (TO/hr) and the conversion to aldehyde both increased. This again demonstrates that the alkene's impurity did affect the initial turnover rate and alkene conversion to aldehyde for both the alkene and catalyst dependency studies. It should also be noted that at 1 M 1-hexene and 1 mM catalyst the regioselectivity is virtually the same for both the alkene and the catalyst dependency kinetic studies. This represents a good internal check on the reproducibility of our catalytic runs and techniques. The aldehyde production curve (Fig. 2.9) indicated an increase in the completion percentages to the expected level.

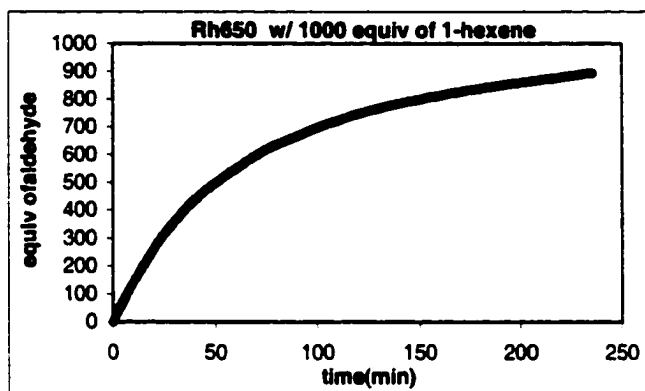


**Figure 2.9.** Aldehyde production for run Rh650

## 2.5. Bis-acyl Species

Previously, there were cursory kinetic studies performed on the dicationic bimetallic catalyst. One observation was the inhibition of the hydroformylation catalysis at high concentration (~2-3 M) of 1-hexene (substrate). This observation could be consistent with the proposed bimetallic mechanism. Upon examination of the mechanism (Figure 1.10 and 1.12) we see the  $rac\text{-}[\text{Rh}_2\text{H}_2(\mu\text{-CO})_2(\text{CO})_2(\text{et,ph-P4})]^{2+}$  species has two hydrides, one on each metal center. Normally one rhodium metal center reacts with one 1-hexene (substrate) and CO to produce the acyl ligand. The other rhodium metal center is then used in the intramolecular hydride transfer that eliminates the final aldehyde product. But, if there is a high enough concentration of the alkene (1-hexene) present it might be able to add to both rhodium metal centers to ultimately produce the bis-acyl species shown in Fig. 2.10.

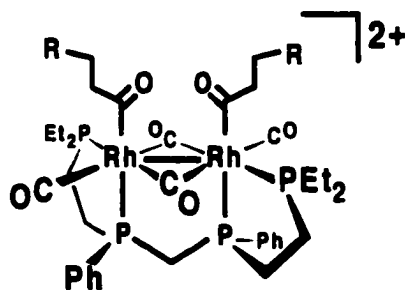


**Figure 2.10. Bis-acyl species**

This species should not be able to perform the intramolecular hydride transfer needed to produce the final aldehyde product. The proposed bis-acyl complex, however, could do a bimolecular reductive elimination of a diketone product (Figure 1.12). This is a very unusual process and we have not seen any evidence for this type of reaction in any of our runs.

After performing the kinetic study of the 1-hexene and the dinuclear dicationic catalyst, we did not observe any inhibition that would suggest the production of the bis-acyl species. We believe that the previous studies that showed an inhibition at higher alkene concentrations may have suffered from catalyst deactivation by peroxide impurities present in the 1-hexene. We also made several attempts to crystallize out the bis-acyl or other species that might be present by placing 2.5-4.0 M solutions from the alkene dependency study in the glove box refrigerator but were unable to form any crystals.

## 2.6. Summary

To recap the results, we found that the order of the catalyst precursor and the alkene is each one. Garland's studies of the  $\text{Rh}_4(\text{CO})_{12}$

hydroformylation catalyst system revealed an order of 0.25 for the catalyst. This meant that only one Rh out of the four originally present in the  $\text{Rh}_4(\text{CO})_{12}$  cluster formed an active catalyst. This, combined with *in situ* spectroscopic studies, clearly pointed to cluster fragmentation and the formation of a monometallic catalyst. The first order kinetic behavior of the bimetallic catalyst precursor strongly supports a bimetallic active catalyst. Fragmentation to produce two active monometallic catalysts would have given a second order rate dependency. We cannot absolutely rule out fragmentation to produce one catalytically active monometallic complex and another catalytically inert monometallic complex. But this is similar to Garland's  $\text{Rh}_4(\text{CO})_{12}$  fragmentation and unless it is very carefully balanced, one would expect sub-first order kinetics in this case.

We also learned vital information concerning 1-hexene, namely that if it is not cleaned properly it has a very detrimental effects on the catalytic run. We believe, but did not identify, that peroxide impurities in the alkene are responsible for this catalyst deactivation.

## 2.7. References

1. a) A. D. Harley, G. J. Guskey, G. L. Geoffroy, *Organometallics*, **2**, 1983, 53. b) C. Mahe, H. Patin, J.-Y. Le Marouille, A. Benoit, *Organometallics*, **2**, 1983, 1051. c) A. Ceriotti, L. Garlaschelli, G. Longoni, M.C. Malatesta, D. Strumolo, A. Fumagalli, S. Martinengo, *J. Mol. Catal.*, **24**, 1984, 309. d) S. Zue, Y. Luo, H. Fu, Y. Yin, *Ranlio Huazue Zuebao*, **14**, 1986, 354; *Chem. Abstr.*, **107**, 1987, 9264. e) T. Hayashi, Z. H. Gu, T. Sakakura, M. Tanaka, *J. Organomet. Chem.*, **352**, 1988, 373. f) W. Dai, H. Guo, R. Jiang, Q. Zhou, W. Wei, *Shiyong Huagong*, **17**, 1988, 707; *Chem. Abstr.*, **110**, 1989, 233.576. g) J. Evans, G. Jingxing, H. Leach, A.C. Street, *J. Organomet. Chem.*, **372**, 1989, 61. h) A. R. El'man, V. I. Kurkunin, E. V. Slivinskii, S. M. Lotev, *Netfekhimiya*, **30**, 1990, 46; *Chem Abstr.*, **112**, 1990, 197.383.



2. D. T. Brown, I. Eguchi, B. T. Heaton, J. A. Iggo, R. Whyman, *J. Chem. Soc., Dalton Trans.*, **1991**, 667.
3. a) M. Garland, *Organometallics*, **12**, **1993**, 535-543. b) C. Fyhr, M. Garland, *Organometallics*, **12**, **1993**, 1753-1764.
4. G. Parshall, *Homogeneous Catalysis*; Wiley: New York, **1980**; p. 17
5. a) P. Kalck, J.M. Frances, P. M. Pfister, T. G. Southern, *J. Chem. Soc. Chem. Commun.*, **1983**, 510. b) P. Escaffre, A. Thorez, P. Kalck, B. Benson, R. Perron, Y. Colleuille, *J. Organomet. Chem.*, **C17**, **1986**, 302. c) A. Dedieu, P. Escaffre, J. M. Frances, P. Kalck, A. Thorez, *New. J. Chem.*, **10**, **1986**, 631. d) P. Kalck, Y. Peres, R. Queau, J. Molinier, P. Escaffre, E. Leandro de Oliveira, B. Peyrille, *J. Orgomet. Chem.*, **C16**, **1992**, 426.
6. R. Davis, J.W. Epton and T.G. Southern, *J. Mol. Catal.*, **77**, **1992**, 159-163.
7. M. Dieguez, C. Claver, A. M. Masdeu-Bulto, A. Ruiz, P. W. N. M. van Leewen, and G. C. Schomaker, *Organometallics*, **18**, **1999**, 2107-2115.
8. R. C. Matthews, dissertation for Ph.D. degree at Louisiana State University, 1999.
9. S. G. Train, dissertation for Ph.D. degree at Louisiana State University, 1995.
10. D. K. Howell, dissertation for Ph.D. degree at Louisiana State University, 1999.
11. M. E. Broussard, B. Juma, S. G. Train, W. J. Peng, S. A. Laneman, and G. G. Stanley, *Science*, **260**, **1993**, 1784-1788.

## CHAPTER 3 HYDROCARBOXYLATION

### 3.1. Introduction to Polar Phase Hydroformylation

After the completion of our kinetic study, we decided that we would revisit the idea of trying to use a very polar solvent for our hydroformylation catalyst. Several years ago, we were experimenting with very polar solvent phases with our hydroformylation catalyst to try and obtain phase separation of the organic aldehyde products. This idea originated from the Shell higher olefin process (SHOP)<sup>1</sup> that is based on homogeneous nickel catalysts that were discovered by Keim.<sup>2</sup>

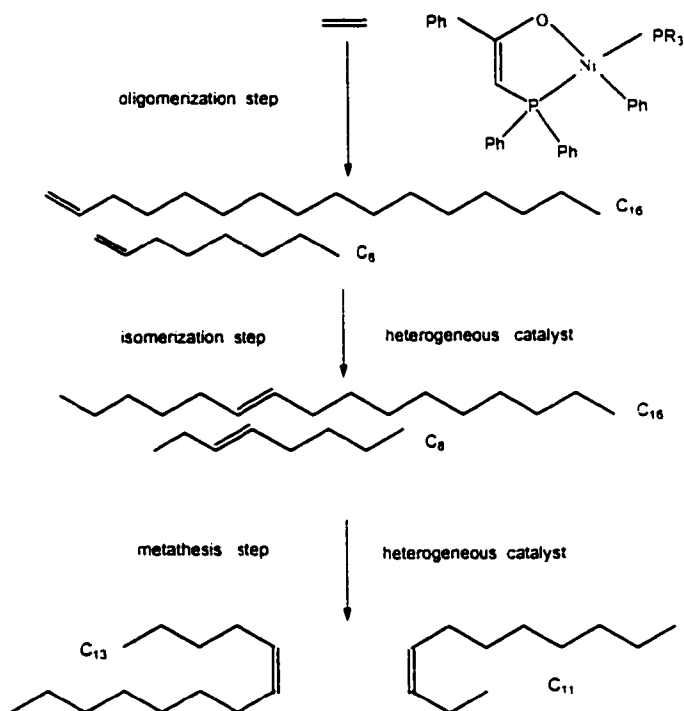


**Figure 3.1.** The Shell higher olefin process (SHOP)

The nickel catalysts oligomerize ethylene to produce various  $\alpha$ -olefins of different chain lengths (i.e.,  $\text{C}_6$ - $\text{C}_{20}$ ). The oligomerization step is carried out

using a very polar solvent like an alkanediol (e.g. 1,4-butanediol). This polar solvent will dissolve the nickel catalyst, but the non-polar  $\alpha$ -olefin products phase separate out from the catalyst solution. The chain lengths that are C<sub>10</sub>-C<sub>14</sub> are the desired products, because they can be hydroformylated to produce C<sub>11</sub>-C<sub>15</sub> alcohols that are used in detergent products. The process also takes the undesired products (long C<sub>16</sub>-C<sub>20</sub> and short C<sub>6</sub>-C<sub>9</sub>  $\alpha$ -olefin chains) and manipulates them by metathesis and isomerization to produce the desired product distribution.

The idea to use a liquid-liquid biphasic process, in which a reagent or catalyst is designed to reside in one of the liquid phases and the product forms the other liquid phase, could be the enabling approach for the commercial application of many selective homogenous catalytic chemical reactions.<sup>3</sup> Currently there are several commercial systems that use liquid-liquid biphasic processes. One is the Ruhrchemie/Rhône Poulenc,<sup>4</sup> water soluble rhodium hydroformylation catalyst, HRh(CO)(TPPTS)<sub>3</sub> (TPPTS = trismeta-sulfonated triphenylphosphine), to produce aldehyde products. They react HRh(CO)(TPPTS)<sub>3</sub> with propene and H<sub>2</sub>/CO in water to form aldehyde product that is not water-soluble and forms a separate organic liquid phase, while the catalyst stays in the aqueous phase. The aldehyde is decanted and fractionally distilled into the linear and branched aldehydes (n-butanal and iso-butanal). It should be noted that this system does require that excess TPPTS ligand be maintained in order to slow the decomposition of the catalyst, just as with the Rh/PPh<sub>3</sub> catalyst.

In the area of liquid-liquid biphasic chemistry there is a relatively new concept called the fluorous biphasic concept developed by Horvath.<sup>3</sup> Horvath developed this concept in an attempt to find a new approach for selectively oxidizing methane to methanol using molecular oxygen. He used perfluoroalkanes, perfluorodialkyl ethers, and perfluorotrialkyl amines to make the catalyst more "fluorous" and thereby more soluble in the fluorous solvent phase. The organic product would phase separate from the fluorous solvent allowing facile separation. The catalyst can be made fluorous by attaching fluorocarbon moieties to the ligands in appropriate size and number. Horvath found that the most effective groups were linear or branched perfluoroalkyl chains with high carbon numbers that contain heteroatoms, which he called fluorous ponytails. Fluorine is very well known for its electron withdrawing properties, and the fluorous ponytails had to be attached properly or they could significantly change the electronic properties of the catalyst. Horvath then demonstrated that catalysts and reagents could be made fluorous-soluble and, thus, enhance the separation of the organic products from the fluorous phase. He also found that some systems would become a single phase if the temperature was increased, but then separate out at lower temperatures.

Horvath also added fluorous ponytails to the phosphine ligands of a rhodium catalyst<sup>5</sup> and demonstrated that the catalyst could hydroformylate low and high molecular weight olefins and provides very easy separation of the catalyst phase and the product phase. Overall, Horvath showed the ability to completely separate a catalyst or reagent from the products under mild

conditions could expand the application of liquid phase catalyst. It was our intention to try and design our system so that it would allow us to separate out our aldehyde products from the catalyst solution through the use of a very polar mixed acetone-water solvent system.

### 3.2. Initial Polar Phase Hydroformylation Catalytic Runs

We used a mixed solvent phase consisting of water and acetone with 25-50% water compositions. The hydroformylation runs were performed under our normal catalytic conditions (90 psi, 1:1 H<sub>2</sub>/CO, 90°C, 1000 equivalents 1-hexene, 1 mM catalyst). Below are three representative production curves of the 25%, 30%, 50% water solvent systems.

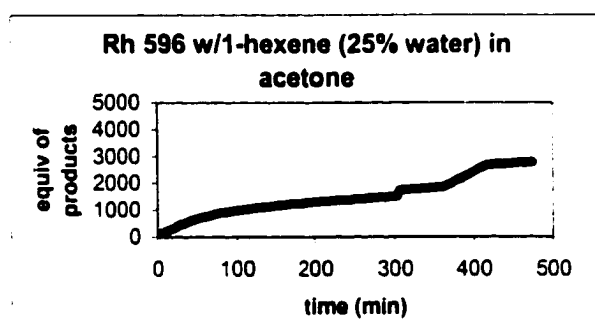


**Figure 3.2.** Production curve for run Rh596 based on gas uptake

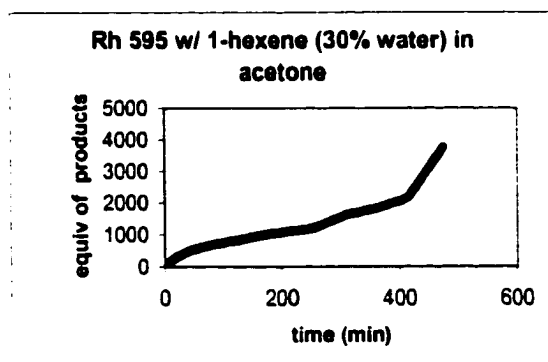


**Figure 3.3.** Production curve for run Rh595 based on gas uptake

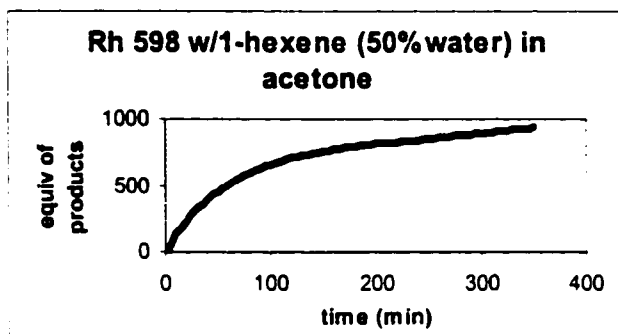


**Figure 3.4.** Production curve for run Rh598 based on gas uptake

When we first saw the aldehyde production curves we had mixed emotions. The catalyst appeared to have converted most of the alkene to aldehyde, but we then realized that we had a variable leak in the autoclave system. The tail ends of each of the above runs tend to keep rising and do not level off as in a normal run. In the 25% and 30% runs (Figures 3.2 and 3.3) there are two "bumps"; the first bump is from taking a sample from the autoclave that causes a small loss of  $H_2/CO$  gas. The production curves are based on the  $H_2/CO$  gas consumption from the gas reservoir of the autoclave system. During sampling, the inlet valve is closed and a stainless steel cannula is placed through a rubber septum over the sampling valve; and a 1-2 mL sample is taken from the autoclave. Since the autoclave is under 90 psig of  $H_2/CO$  gas, there is a small portion of gas lost when the sampling occurs. This lost gas causes an artificial jump in the uptake curve. We could correct for this, but we rarely do since it is usually a small factor. In these particular runs we did not consume as much  $H_2/CO$ , therefore; the sampling jump is more pronounced.

Each run produced phase separated samples, a dark reddish brown organic layer on top and a light rusty orange aqueous layer. The dark color of the organic phase indicated that the majority of the catalyst partitioned into the organic layer. The GC-MS analysis of the organic layer showed that we had produced the expected aldehyde products with 20:1 linear to branched regioselectivity. Surprisingly there appeared to be very low alkene isomerization and hydrogenation side reactions (< 1%) and the initial turnover frequency appeared to be considerably higher than that observed in pure acetone. But, we were amazed to observe the formation of large amounts of linear heptanoic acid in some of the runs, along with a small amount of the branched carboxylic acid (Figure 3.5). The formation of carboxylic acids under mild hydroformylation reaction conditions is virtually without precedent.

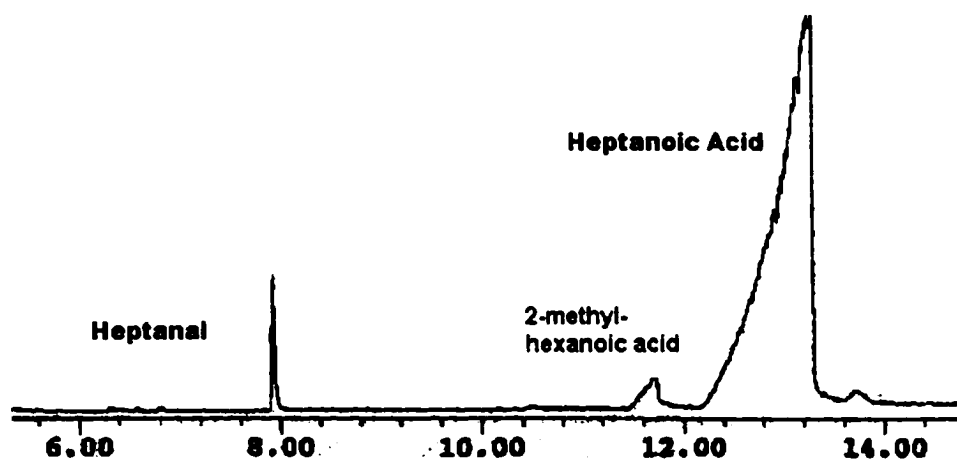


**Figure 3.5.** Representative GC/MS analysis of Rh595 (30%)

The reactant/product analysis for run Rh598 shown in Figure 3.6 indicates that the 1-hexene is rapidly hydroformylated to aldehyde. There then appears to be a second catalytic reaction that converts aldehyde and water to

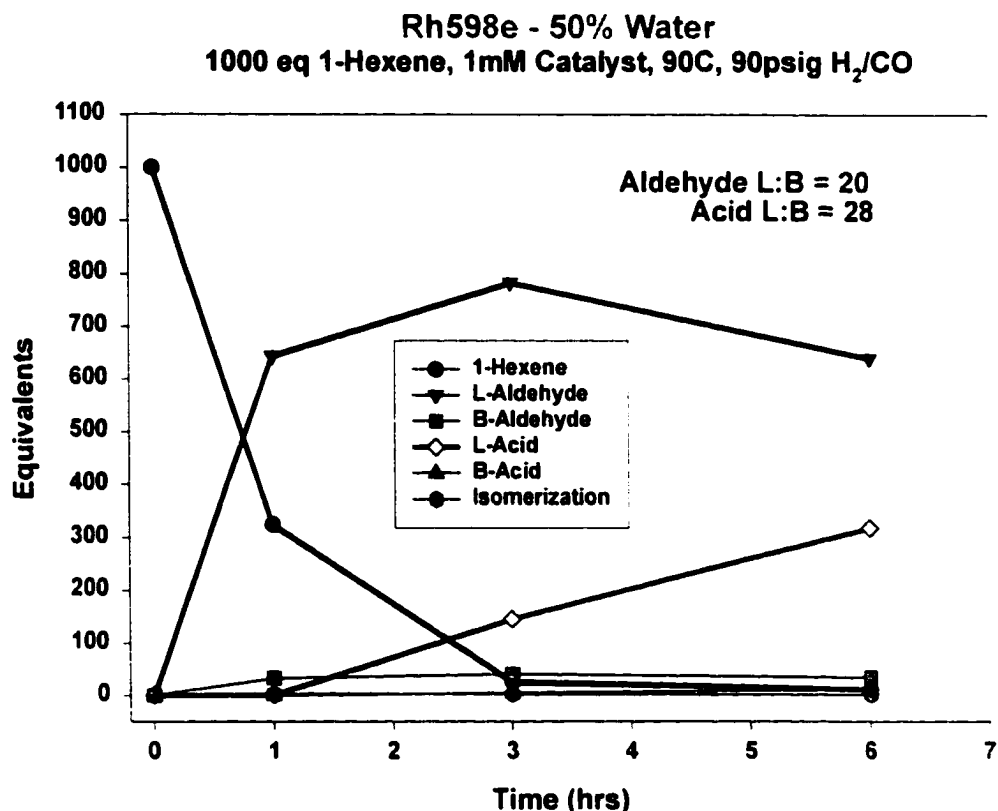


**Figure 3.6.** Production and consumption plot for run Rh589e

form carboxylic acid and H<sub>2</sub>. Depending on the amount of water present (25-50%) and the variable nature of the leak in the autoclave, we observed the full range of aldehyde to carboxylic acid conversions that ranged from trace amounts to almost 100%. The best results for producing carboxylic acid seemed to be for 25-30% water, with 50% water runs typically giving lower amounts of carboxylic acid product. Run Rh598, for example, with 50% water gave about 66% aldehyde and 33% carboxylic acid. The linear to branched carboxylic acid ratios were extremely high and varied from about 25-50:1. In almost all runs we have observed very low alkene isomerization and hydrogenation side reactions, in marked contrast to hydroformylation runs in



pure acetone. Reactant and product analyses for run Rh-598e were corrected to 1000 equivalents of starting 1-hexene. The data at 3 hrs was estimated based on complete consumption of alkene at this point (from other similar runs) and a linear extrapolation of the carboxylic acid production.

Careful analysis of the gas uptake data from run Rh598 allowed us to estimate the rate of the leak present from the data between 180 and 360 minutes when no further hydroformylation was occurring. This corresponds to a constant leak of 10 psig per hour, which can be translated to a correction of approximately 50 turnovers/hr. Using this correction we arrive at a more accurate estimate of the initial turnover frequency of 730 TO/hr, which is 40% faster than similar runs in pure acetone (e.g., 524 TO/hr), representing a considerable increase in the reaction rate.

We initially chose only to sample the phase separated organic layer for simplicity, not knowing that this would affect our results. We noticed in certain runs that considerable amounts of the carboxylic acid being produced was "disappearing." This is illustrated in Figure 3.7. NMR analysis of the aqueous phase, which we weren't analyzing at this point in the project, showed that the "disappearing" carboxylic acid was dissolving into it. This behavior prompted us to modify our analytical procedure to do a "total" analysis of both the organic and aqueous solutions whenever phase separation occurred. This was done by adding enough acetone to the solution to generate a single phase from which GC samples and analyses were performed.

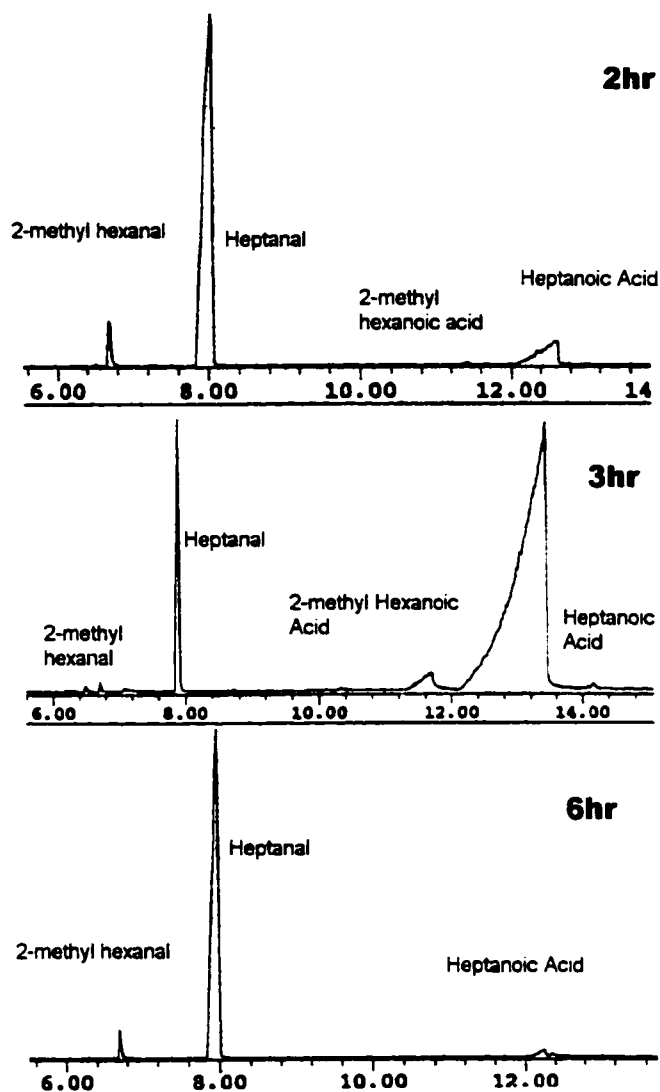


**Figure 3.7.** GC/MS traces of run Rh594 (25% water) showing the loss of acid from the organic phase

### 3.3. Background on Hydrocarboxylation Catalysis

Hydrocarboxylation catalysis is used by a variety of authors to designate several similar reactions shown in Figure 3.8 to produce carboxylic acid or ester products. We will use hydrocarboxylation to specifically refer to the most

difficult of these processes, namely the catalytic reaction of alkenes (typically  $\alpha$ -olefins), CO and water to produce carboxylic acids.

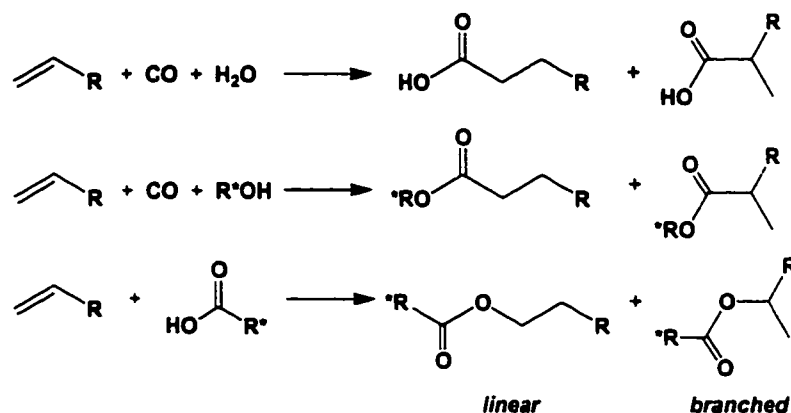


**Figure 3.8.** Different types of hydrocarboxylation reactions

Hydrocarboxylation catalysis has attracted considerable interest<sup>6</sup> since its discovery by Reppe in 1953<sup>7</sup>. Cobalt and nickel catalysts<sup>6</sup> will perform this reaction at high temperatures and pressures (200-300 °C, 200-300 atm CO). Under this forcing conditions very poor chemo- and regioselectivity is seen for all but the simplest alkene and alkyne substrates. Reppe's  $\text{Ni(CO)}_4$ -based catalyst system was commercially used for many years to produce acrylic and propionic acids from acetylene and ethylene. Heck<sup>8</sup> proposed the generally accepted mechanism for this catalytic reaction (Figure 3.9) in analogy with the nickel-catalyzed carbonylation of allyl and alkyl halides. A key feature of this proposed mechanism is the need to typically add a strong acid (HX) to the solution to generate the starting  $\text{HNiX(CO)}_2$  catalyst from  $\text{Ni(CO)}_4$ . Once this Ni-H species is generated, alkene can coordinate and do a migratory insertion to produce the Ni-alkyl. CO can coordinate and do another migratory insertion to produce the Ni-acyl complex. At this point one has two possible routes to

forming the final carboxylic acid. One can have a reductive elimination of an acyl halide (center part of the proposed mechanism in Figure 3.9) that then reacts with water to form the carboxylic acid and the strong acid HX.

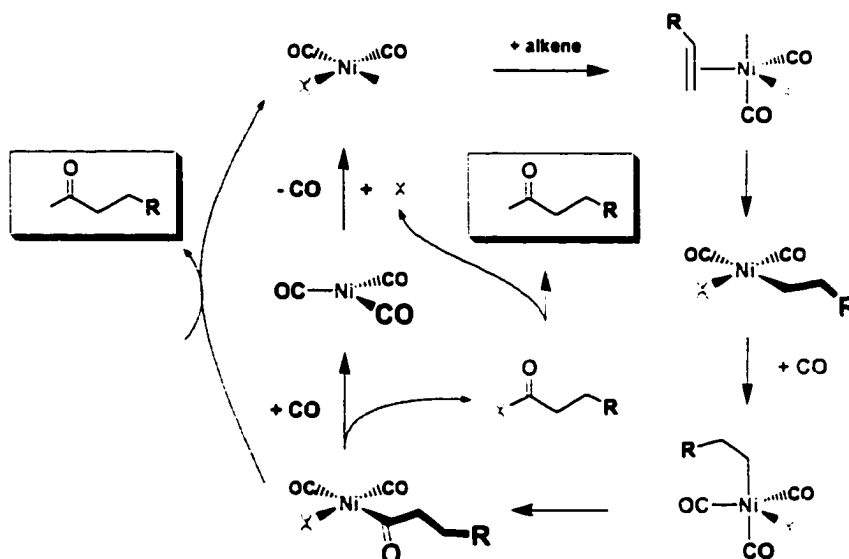


**Figure 3.9.** Heck's proposed mechanism for the Ni-catalyzed hydrocarboxylation of alkenes

The other proposed reaction step involves the direct reaction of water with the Ni-acyl complex to kick off the carboxylic acid product and regenerate the  $\text{HNiX(CO)}_2$  catalyst. This is shown on the left hand side of Figure 3.9. At the time Heck proposed these steps, there was little known about this type of catalysis. In the 1970's, however, researchers at Monsanto discovered and studied the mechanism of the rhodium- and iridium-catalyzed carbonylation of methanol to produce acetic acid – commonly known as the Monsanto Acetic Acid Process.<sup>9</sup> They also found that these systems could catalyze hydrocarboxylation under somewhat more moderate reaction conditions relative to Ni and Co-catalyzed reactions (150-220 °C, 30 atm CO), but still with

generally poor regioselectivity (50-70% linear carboxylic acids). Forster's<sup>10</sup> mechanistic work on the acetic acid process clearly showed that the presence of a strong acid, specifically HI, was critically important for the activity of the catalyst. They proposed the novel doubly catalyzed system shown in Figure 3.10. HI reacts with  $\text{CH}_3\text{OH}$  to produce water and  $\text{CH}_3\text{I}$ . The reactive  $\text{CH}_3\text{I}$  can now do an oxidative addition to the metal center to make the  $\text{CH}_3\text{-Rh(III)-I}$  complex. A CO migratory insertion produces the Rh-acyl complex. A CO migratory insertion produces the Rh-acyl complex.

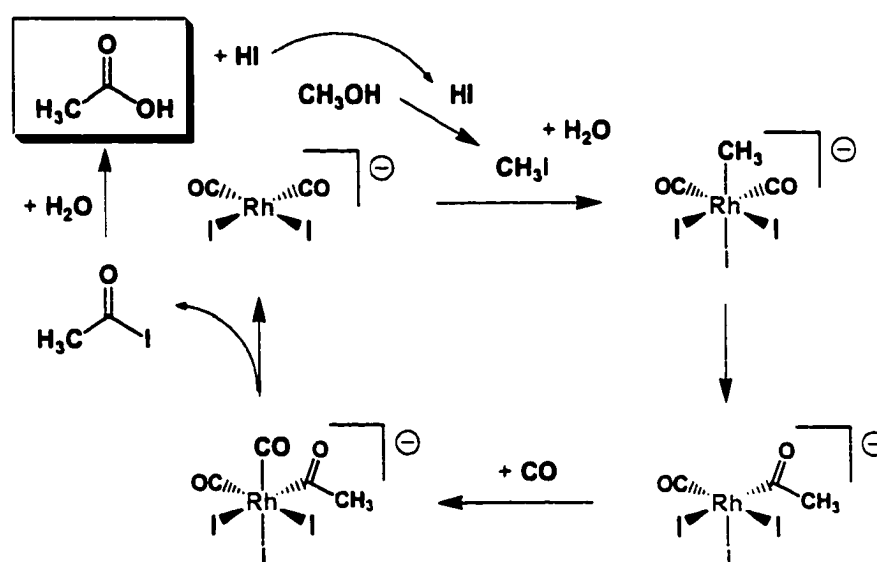


**Figure 3.10.** Proposed mechanism for Monsanto acetic acid process

Careful mechanistic studies have demonstrated that the next step is the reductive elimination of acyl-iodide, which regenerates the starting  $\text{Rh(I)}$  catalyst.<sup>11</sup> The acyl iodide can react with water (formed from the initial attack of  $\text{HI}$  on methanol) to form acetic acid and regenerate  $\text{HI}$ , which can react with another methanol to produce  $\text{CH}_3\text{I}$  and  $\text{H}_2\text{O}$ . So one has a  $\text{Rh}$ -catalyzed carbonylation of  $\text{CH}_3\text{I}$  and an  $\text{HI}$ -catalyzed activation of methanol to produce

methyl iodide. Note that the carboxylic acid is formed from reaction of the acyl iodide and water, not the direct activation of water on the metal catalyst. The presence of a strong acid to activate the initial substrate is also very important.

The key role of the HI acid in the Monsanto Acetic Acid process caused Heck to propose another alternative reaction step to that discussed for the Ni-catalyzed hydrocarboxylation reaction. He suggested that the strong acid was adding directly to the alkene to generate a more reactive alkyl halide that can react with the catalyst without the need for a metal-hydride species. This then eventually eliminates an acyl halide, directly analogous to the Monsanto Acetic Acid mechanism. The reaction of acid with alkene is shown in Figure 3.11, along with the subsequent steps that produce the acyl-iodide, which can then react with water to produce carboxylic acid and regenerate the HX acid (not shown in Figure 3.11).

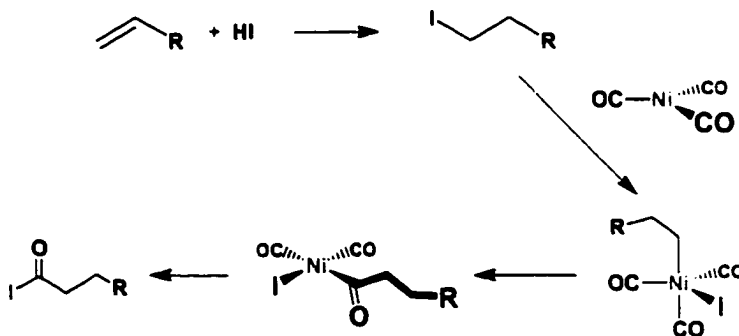


**Figure 3.11.** Alternate Heck proposal for the activation of alkenes by HI to perform hydrocarboxylation catalysis

Forster and coworkers<sup>10</sup> at Monsanto have studied Rh- and Ir-catalyzed hydrocarboxylation catalytic reactions and concluded that both work by reaction of HI with the metal to generate a M(III)-hydride that then can react with the alkene. They also propose that there is a reductive elimination of acyl iodide

that reacts with water to produce the carboxylic acid and regenerate HI. This is shown in Figure 3.12. They also found that if too much HI was present it would deactivate the catalyst by reacting with the  $[\text{HRhI}_3(\text{CO})_2]^-$  complex to eliminate  $\text{H}_2$  and produce catalytically inactive  $\text{Rh(III)-iodide}$  complexes.

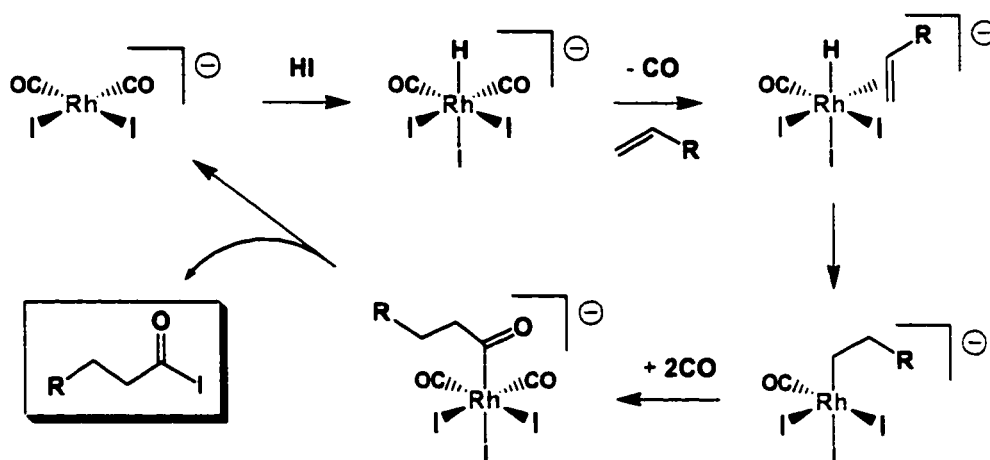


**Figure 3.12.** Monsanto mechanism for  $[\text{RhI}_2(\text{CO})_2]^-$  catalyzed hydrocarboxylation

Zoeller<sup>12</sup> from Eastman Chemical recently patented a phosphine modified  $\text{Rh-iodide}$  catalyst system for the hydrocarboxylation of alkenes. He claimed that this improved system operates at lower pressures, gives higher rates of reaction, and higher linear to branched carboxylic acid ratios relative to other hydrocarboxylation catalysts. The two best systems reported in his patent are both based on a rhodium-iodide catalyst with either  $\text{PPh}_3$  or  $\text{Ph}_2\text{P}(\text{CH}_2)_4\text{PPh}_2$  ligands. The  $\text{PPh}_3$ -modified catalyst gave a higher L:B ratio of 6.7 for the hydrocarboxylation of 1-pentene, but a slower rate of 56 TO/hr at 190 °C and 27.2 atm  $\text{CO}$ . The  $\text{Ph}_2\text{P}(\text{CH}_2)_4\text{PPh}_2$  ligand gave a lower L:B regioselectivity of 4.6 for 1-pentene, but a faster rate of 135 TO/hr under the same reaction

conditions. The lower L:B regioselectivity, but faster rate for the less sterically hindered  $\text{Ph}_2\text{P}(\text{CH}_2)_4\text{PPh}_2$  ligand-based catalyst is what one might expect for a catalyst that has a more open and less sterically hindered binding site for the alkene substrate. They used propionic acid as a solvent for the catalysis.

Pruchnik<sup>13</sup> and coworkers have reported the only rhodium-based catalyst system that does some hydrocarboxylation catalysis under hydroformylation-like conditions. They used the cationic monodentate phosphine ligand,  $\text{mtpa}^+\text{I}^-$  (shown below in Figure 3.13), to make the water-soluble rhodium catalyst precursors  $[\text{RhI}(\text{CO})(\text{mtpa}^+\text{I}^-)_2]$  and  $[\text{RhI}(\text{CO})(\text{mtpa}^+\text{I}^-)_3]$ . These act as hydroformylation catalysts for 1-hexene (~60 atm 1:1  $\text{H}_2/\text{CO}$ , 80 °C, 3000 equivalents of 1-hexene) to give the product distribution shown in Table 3.1.

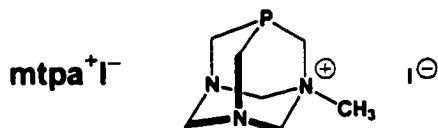


**Figure 3.13.** Structure of  $\text{mtpa}^+\text{I}^-$

**Table 3.1.** Catalytic results from Pruchnik's  $[\text{RhI}(\text{CO})(\text{mtpa}^+\text{I}^-)_2]$  precursor for the hydroformylation of 1-hexene at 60 atm 1:1  $\text{H}_2/\text{CO}$  and 80 °C

Catalyst	Avg. TOF (hr <sup>-1</sup> )	Ald. <sup>a</sup> L:B	% conversion	Aldehyde:Acid ratio	Acid L:B	% iso <sup>b</sup>
$[\text{RhI}(\text{CO})(\text{mtpa}^+\text{I}^-)_2]$	117	1.1	70	--	--	16
+ 6 equiv. ligand	150	1.6	91	2.3	1.1	--

<sup>a</sup>ald stands for aldehyde

<sup>b</sup>iso stands for alkene isomerization

When Pruchnik uses six equivalents of excess  $\text{mtpa}^+\text{I}^-$  ligand he observes the formation of about 27% carboxylic acids with low L:B regioselectivity. We



believe that the presence of iodide is transforming his catalyst into a more Monsanto-like iodide-promoted (strong acid) catalyst cycle. Indeed, his catalyst may be operating much like Zoeller's Eastman Chemical phosphine-modified Rh-iodide hydrocarboxylation catalyst. By operating at a much lower temperature (80 °C vs. Zoeller's 190 °C) and with the presence of H<sub>2</sub> gas, Pruchnik also generates a hydroformylation catalyst and gets competing catalytic reactions occurring.

These are the only examples of Rh-catalyzed hydrocarboxylation that we could find in the literature. There are, however, quite a few Pd-based catalytic results for this reaction. The palladium catalysts are of the general type PdCl<sub>2</sub>(PAr<sub>3</sub>)<sub>2</sub> and require the addition of modifiers such as strong acid (HX, X<sup>-</sup>, = Cl<sup>-</sup>, Br<sup>-</sup>, I<sup>-</sup>, CF<sub>3</sub>CO<sub>2</sub><sup>-</sup>, PF<sub>6</sub><sup>-</sup>, BF<sub>4</sub><sup>-</sup>, *p*-toluenesulfonate, etc.), SnCl<sub>2</sub>, CuCl<sub>2</sub>, or a combination of SnCl<sub>2</sub> or CuCl<sub>2</sub> and acid.<sup>14</sup> Typical CO pressures are 40-70 atm with reaction temperatures of 90-120 °C. Initial turnover frequencies and L:B carboxylic acid regioselectivities are typically quite low (<10 TO/hr, 1:1 L:B selectivity) for 1-alkenes like butene or higher. Alkene isomerization side reactions can be quite prominent (Figure 3.14).

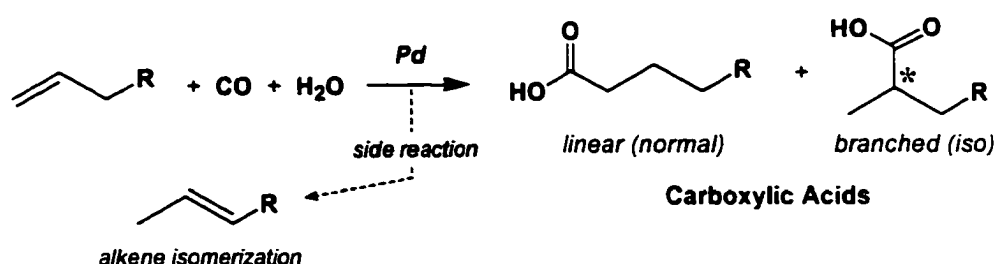


**Figure 3.14.** Pd-catalyzed hydrocarboxylation catalysis

The fastest Pd hydrocarboxylation catalyst for small  $\alpha$ -olefins like propylene has been reported by Sheldon<sup>15</sup> and coworkers and is based on the sulfonated triphenylphosphine ligand, tppts. They reported a remarkable TOF of 2800 hr<sup>-1</sup> for propylene at 130 °C, 50 atm CO, 0.067 mmol PdCl<sub>2</sub>, 0.67 mmol tppts, 0.2 mol propylene, 142 mL H<sub>2</sub>O, and 30 mmol *p*-toluenesulfonic acid. The L:B regioselectivity, however, was quite low at 1.4. The situation completely changes with longer alkenes like 1-octene, where extensive isomerization is observed, an average TOF of only 32 hr<sup>-1</sup>, and a low L:B regioselectivity of 1.4. Part of this is undoubtedly due to the low solubility of 1-octene in the aqueous solvent.

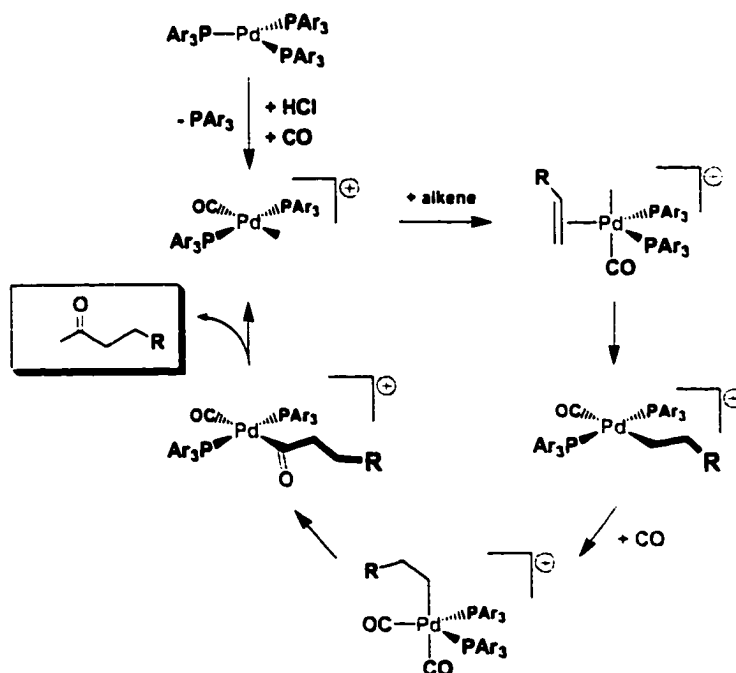


**Figure 3.15.** Proposed Pd-catalyzed hydrocarboxylation mechanism

Sheldon's proposed mechanism for the Pd catalyst system is shown in Figure 3.15. The loss of a  $\text{PAr}_3$  ligand is followed by an oxidative addition of the

strong acid and coordination of CO to form  $\text{HPd}(\text{PAr}_3)_2\text{CO}$ . Next, the addition of alkene to form  $\text{HPd}(\text{PAr}_3)_2\text{CO}(\text{alkene})$  and a migratory insertion on the alkene into the Pd-H bond to form the alkyl species. This is followed by CO addition and a migratory insertion of the CO into the Pd-alkyl bond to produce the acyl ligand. This species undergoes hydrolysis to produce the carboxylic acid and the  $\text{HPd}(\text{PAr}_3)_2\text{CO}$  to begin the catalytic cycle again.

There are several problems, however, with this proposed mechanism. First is that the regioselectivity for linear acid should be much higher if  $\text{HPd}(\text{CO})(\text{PAr}_3)_2$  is the actual catalyst. The analogous  $\text{HRh}(\text{CO})(\text{PPh}_3)_2$  hydroformylation catalyst, for example, gives anywhere from 8:1 to 20:1 L:B regioselectivity for  $\alpha$ -olefins, depending on the amount of excess phosphine ligand used. The tppts-based aqueous-phase Rh catalyst run by Rhurchemie, for example, gives 18:1 L:B regioselectivity for propylene. The rather low L:B regioselectivity implies that the actual catalyst is probably the mono-phosphine coordinated complex  $\text{HPd}(\text{CO})_2(\text{PAr}_3)$  that has considerably lower steric effects to direct the alkene for a migratory insertion reaction with the Pd-H to produce the linear alkyl intermediate.

The second problem is the proposed hydrolysis of the Pd-acyl to eliminate the carboxylic acid product and regenerate the Pd-H starting catalyst. As shown in Figure 3.16 the polarization of the Pd-acyl bond should place a partial negative charge on the formally anionic acyl ligand. This is unlikely to interact with the partially negatively charged oxygen of the incoming water molecule to eliminate the carboxylic acid. Indeed, the water seems more likely to bind to

the cationic Pd center and transfer a proton to the acyl ligand to eliminate an aldehyde from the Pd. The excess strong acid present also might be expected to rapidly protonate off any acyl ligands formed.

Prof. Stanley believes that another type of reaction may be occurring here. Protonation of the oxygen atom of the acyl could produce a dicationic Pd-carbene that should be highly reactive towards even weak nucleophiles like water. This could easily lead to the observed carboxylic acid. To our knowledge no one has proposed this type of carbene mechanism, but we think it represents a viable alternative to explain the Pd chemistry.

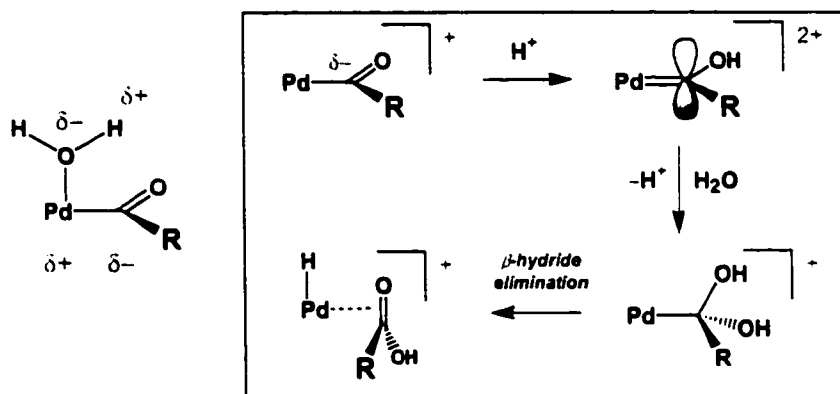


**Figure 3.16.** Polarizations of Pd-acyl and water and an alternate carbene mechanism

### 3.4. Polar Phase Hydroformylation to Hydrocarboxylation - New Studies

The initial polar phase hydroformylation studies with the acetone-water solvent system provided some major surprises. First was that we observed considerably faster and more chemoselective hydroformylation than in pure acetone. Second, and far more importantly, we observed a completely unexpected new catalytic reaction that produced carboxylic acids and  $H_2$  (based

on the stoichiometry of the reaction, not directly observed) from the reaction of aldehyde and water. Although Rh-catalyzed hydrocarboxylation is known, our work is unprecedented in that we have no modifiers (like iodide) or strong acid present to co-catalyze this reaction. We are also seeing extremely high linear regioselectivities – far higher than anyone has ever seen – under very mild reaction conditions.

There were a number of problems present, however, in our initial catalytic studies that we needed to address. Foremost was the intermittent leak in the autoclave that was producing variable catalytic results. Then there was the question about the nature of the hydrocarboxylation catalysis. We have  $H_2$  present, which is not formally required in a hydrocarboxylation reaction. The initial data, however, indicated that we had a two-stage catalytic reaction: first the hydroformylation of alkene to produce aldehyde for which  $H_2$  was needed; followed by the reaction of aldehyde and water with catalyst to produce carboxylic acid and  $H_2$ . There was the somewhat remote possibility that we were directly activating the alkene and water to perform true hydrocarboxylation and this needed to be tested. It was also clear that we had to analyze the entire product solution and procedures for doing so needed to be developed and tested. Finally, the amount of water needed for optimum catalysis had to be studied.

#### **3.4.1. Original Hydrocarboxylation Experiment**

The first thing done was to track down the leak and repair it. This was done and a catalytic run performed to test if we could do hydrocarboxylation

with only alkene, CO and H<sub>2</sub>O (no H<sub>2</sub>). Only a very small amount (< 5% conversion) of aldehyde was produced after 6 hours (Figure 3.18). This may indicate that we are doing a small amount of water-gas shift catalysis (H<sub>2</sub>O + CO  $\rightleftharpoons$  H<sub>2</sub> + CO<sub>2</sub>) to produce some H<sub>2</sub> that can be used for hydroformylation. Pruchnik's [RhI(CO)(mtpa<sup>+</sup>I<sup>-</sup>)<sub>2</sub>] catalyst, discussed earlier, was reported to be a relatively active water-gas shift catalyst (140 TO/hr at 80 °C and ~80 bar CO)<sup>13</sup>, so it isn't too surprising that our rhodium catalyst can do this as well. But this is clearly a minor and very slow side reaction.

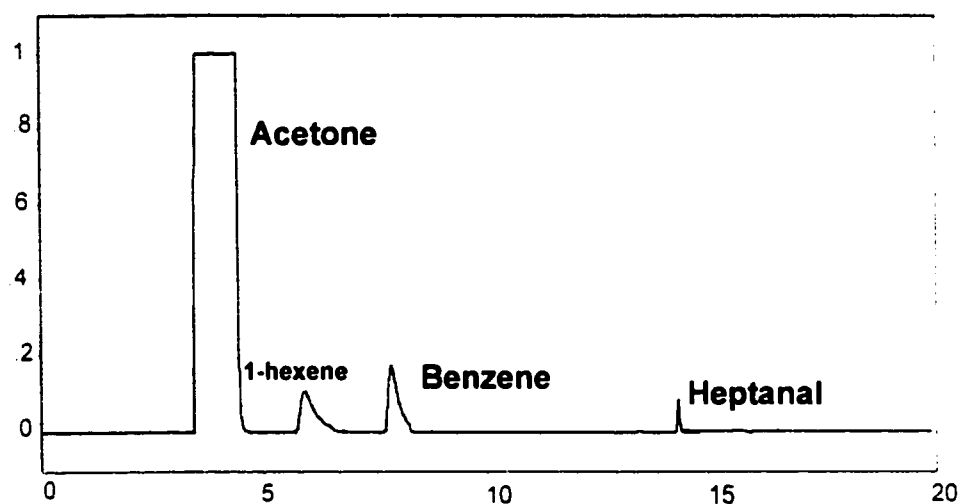


**Figure 3.17.** GC trace of run Rh618

We then prepared a 30% water – 70% acetone solvent run to check the hydroformylation and hydrocarboxylation of 1-hexene under our standard conditions (90 °C, 90 psig H<sub>2</sub>/CO). Fast, regio- and chemoselective hydroformylation was observed (780 TO/hr, 27:1 L:B aldehyde regioselectivity, and little to no alkene isomerization or hydrogenation) – BUT no hydrocarboxylation catalysis (Figure 3.18)!

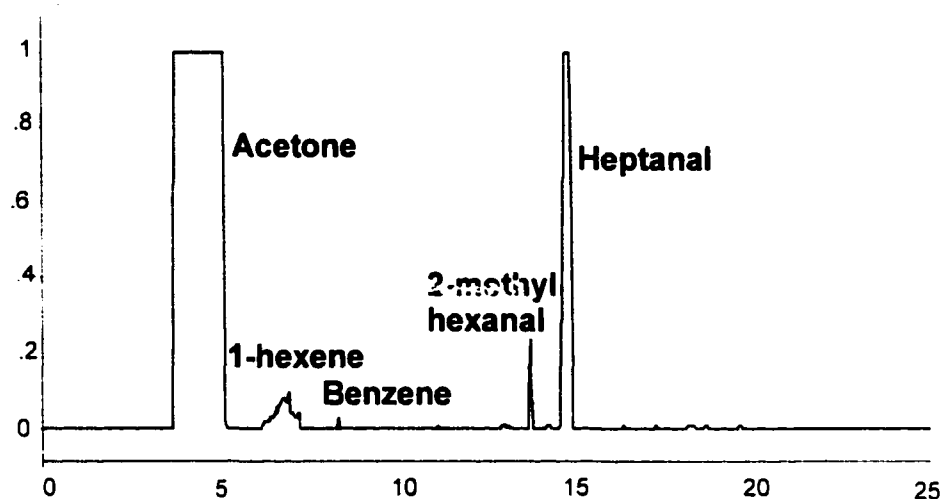


**Figure 3.18.** GC trace of run Rh632 (30% water)

Quite a few catalytic runs were performed to confirm this with different water concentrations, but we only observed hydroformylation. There seems to be little change in the hydroformylation catalysis with differing amounts of water used. Table 3.2 lists the results from several experiments.

**Table 3.2.** Data analysis from GC/MS of hydroformylation of 1-hexene systems using different % water in acetone

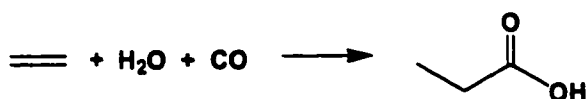
% Water used	Aldehyde l/b ratio	Initial Turnover Rate (TO/hr)	Isomerization & Hydrogenation
25%	26:1	743	1%
30%	27:1	780	1%
50%	19:1	509	1%

### 3.4.2. Hydrogenation of Heptanoic Acid

The failure to produce carboxylic acids in these runs was extremely troubling. After considerable thought Prof. Stanley and I came down to the conclusion that somehow the leak that was present in the original runs was

generating reaction conditions that allowed the aldehyde-water shift catalysis to occur. Our hypothesis was that with the leak fixed and a 1:1 H<sub>2</sub>/CO atmosphere present any H<sub>2</sub> produced from the reaction of aldehyde and water to produce carboxylic acid would build up an excess of H<sub>2</sub>. This might cause the back hydrogenation of the carboxylic acid to aldehyde and water.

The thermodynamics of the overall hydrocarboxylation reaction and the reaction of aldehyde and water to produce carboxylic acid and hydrogen is shown in Figure 3.19. Both are spontaneous at 90 °C, although the reaction of aldehyde with water to produce carboxylic acid and H<sub>2</sub> only has a  $\Delta G_{\text{rxn}}$  (363K) = – 6.8 Kcal/mol. The reverse reaction, i.e., hydrogenation of carboxylic acid to aldehyde and water is non-spontaneous by +6.8 Kcal/mol, but might be able to occur if enough excess H<sub>2</sub> pressure built up.



$$\Delta H_{\text{rxn}} = -166.9 \text{ KJ/mol } (-39.9 \text{ Kcal/mol})$$

$$\Delta S_{\text{rxn}} = -296 \text{ J/mol K}$$

$$\Delta G_{\text{rxn}} (363 \text{ K, } 90 \text{ C}) = -59.3 \text{ KJ/mol } (-14.2 \text{ Kcal/mol})$$



$$\Delta H_{\text{rxn}} = -9.6 \text{ KJ/mol } (-2.3 \text{ Kcal/mol})$$

$$\Delta S_{\text{rxn}} = +51.9 \text{ J/mol K}$$

$$\Delta G_{\text{rxn}} (363 \text{ K, } 90 \text{ C}) = -28.4 \text{ KJ/mol } (-6.8 \text{ Kcal/mol})$$

**Figure 3.19.** Thermodynamics for hydrocarboxylation catalysis and reaction of aldehyde with water to produce carboxylic acid and H<sub>2</sub>



We attempted the hydrogenation of heptanoic acid using our bimetallic catalyst under a variety of reaction conditions (90 and 150 psig  $H_2$ ) and with different concentrations of the carboxylic acid. Only traces ( $\ll 1\%$ ) of aldehyde were observed (Figure 3.20). This demonstrated that the back hydrogenation of the carboxylic acid was not occurring and that some other effect was important in catalyzing the production of the carboxylic acid and  $H_2$  from water and aldehyde.

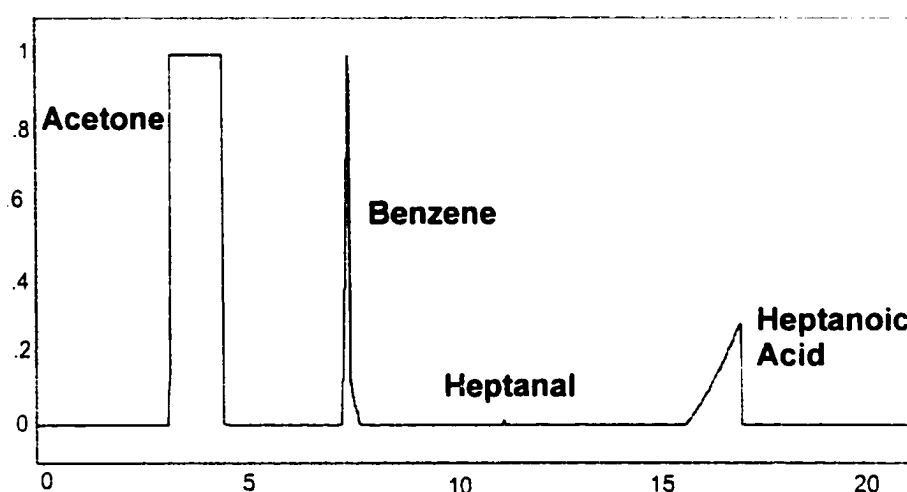


**Figure 3.20.** GC trace of run Rh687 where the hydrogenation of heptanoic acid to heptanal and  $H_2O$  was attempted

### 3.4.3. Modified Hydrocarboxylation

The next hypothesis was that while hydrogen and CO were needed for the initial hydroformylation to produce aldehyde, hydrogen was a strong *inhibitor* for the second catalytic reaction of aldehyde and water to produce carboxylic acid and  $H_2$ . The accidental leak may have purged out enough  $H_2$  to allow the formation of the carboxylic acid. Careful examination of the product distribution with time from the initial catalytic runs also showed that carboxylic

acid didn't seem to be produced until there was a fair bit of aldehyde present. We calculated that the approximate time needed to convert about 33% of the starting 1-hexene to aldehyde under our reaction conditions was 10 minutes.

The idea was to run the catalytic reaction with 1:1 H<sub>2</sub>/CO for 10 minutes and then switch the reaction gas to pure CO. The ongoing hydroformylation catalysis would rapidly deplete the H<sub>2</sub> gas in the autoclave and create severely H<sub>2</sub>-deficient conditions. This might then allow the catalytic reaction of aldehyde and water to produce carboxylic acid and H<sub>2</sub>. The H<sub>2</sub> produced would immediately be consumed by the hydroformylation of the remaining alkene to produce more aldehyde that would, in turn, feed the catalytic reaction making carboxylic acid and H<sub>2</sub>.

We tried this and observed the production of heptanoic acid in good yield and with essentially complete linear regioselectivity (no branched acid was observed in the GC shown in Figure 3.21). The aldehyde L/B regioselectivity was 28:1 with 75% conversion to highly linear carboxylic acid (3:1 acid to aldehyde ratio). Very low amounts of alkene hydrogenation and isomerization were, once again, observed. We believe that complete conversion to carboxylic acid did not occur due to the buildup of excess H<sub>2</sub> once all the alkene was consumed.

The next experiment was to study the effect of reaction initial reaction time with H<sub>2</sub>/CO before switching over to pure CO. We already knew that using 1:1 H<sub>2</sub>/CO did not produce carboxylic acid as shown once the leak in the autoclave

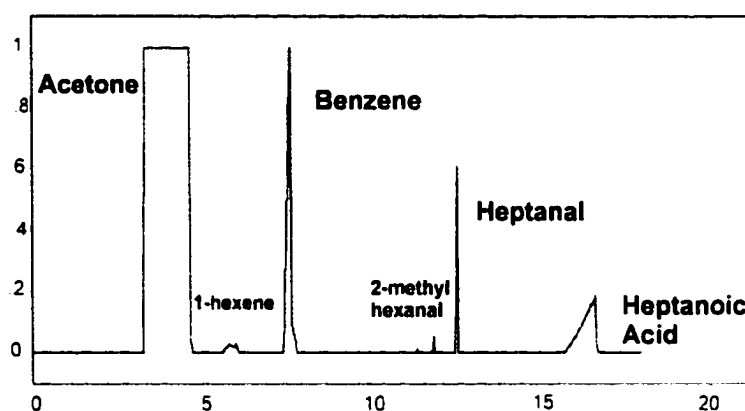


**Figure 3.21.** GC final product analysis of catalytic run Rh690 with 30% water and 10min of H<sub>2</sub>/CO - then switching over to pure CO

system had been repaired. We decided to study this by changing the amount of time for the initial exposure of H<sub>2</sub>/CO gas to the reaction. These runs were carried out 90 °C, 90 psig H<sub>2</sub>/CO, 1000 equivalents of 1-hexene, and 30% water/acetone and for the specified time increment (0, 5, or 15 minutes) the H<sub>2</sub>/CO was exposed to the system and then pure CO was introduced for the remainder of the catalytic run. The results are shown in Table 3.3.

**Table 3.3.** Results of H<sub>2</sub>/CO reaction time experiments for modified hydrocarboxylation

H <sub>2</sub> /CO rxn <sup>a</sup> time	Initial Turnover (TO/hr)	L/B aldehyde ratio	Acid:Aldehyde Ratio	Isomer (%)
0	--	--	--	--
5	1776	15:1	--	1%
10	4788	21:1	3:1	1%
15	1432	39:1	--	1%

<sup>a</sup> rxn stands for reaction

The zero time H<sub>2</sub>/CO run involved pre-soaking the catalyst precursor solution under H<sub>2</sub>/CO while the autoclave was heating up to 90°C. Once the

temperature stabilized we switched the supply gas to pure CO and added the 1-hexene to the catalyst solution with only the initial amount of H<sub>2</sub>/CO gas present. At time zero H<sub>2</sub>/CO we did not observe any catalytic activity. At 5 and 15 minutes, we only observed the production of aldehydes. Ten minutes is where we observed the production of aldehydes and carboxylic acids. We concluded that our reaction was very sensitive to the initial catalysis time under H<sub>2</sub>/CO before switching to pure CO. The initial reaction with H<sub>2</sub>/CO appears to be essential for producing enough aldehyde product that can then be converted to carboxylic acid and H<sub>2</sub>, but it appears that some starting 1-hexene needs to be present to reduce the amount of H<sub>2</sub> present in order to initiate the aldehyde-water shift catalysis.

We also noticed that when we did produce carboxylic acid it was usually by the first hour and no further production was seen after that. So we reran this experiment (Figure 3.22) with more frequent samples during the first several hours in order to more carefully track the reactant and product distributions.

During the first 10 minutes of the catalysis we have 80-90% conversion of 1-hexene to aldehyde product. Only a very small amount of carboxylic acid product (< 6%) is seen at this early stage in the catalysis. The overall mass balance of the reaction is not perfect since the sum of alkene, aldehyde, acid and minor side products (alkene isomerization and hydrogenation) at the 10 minute mark does not add up to 100%. This indicates that our GC calibrations and correction factors for these reactants and product species need to be redone to more accurately account for their absolute amounts present. It is likely that we

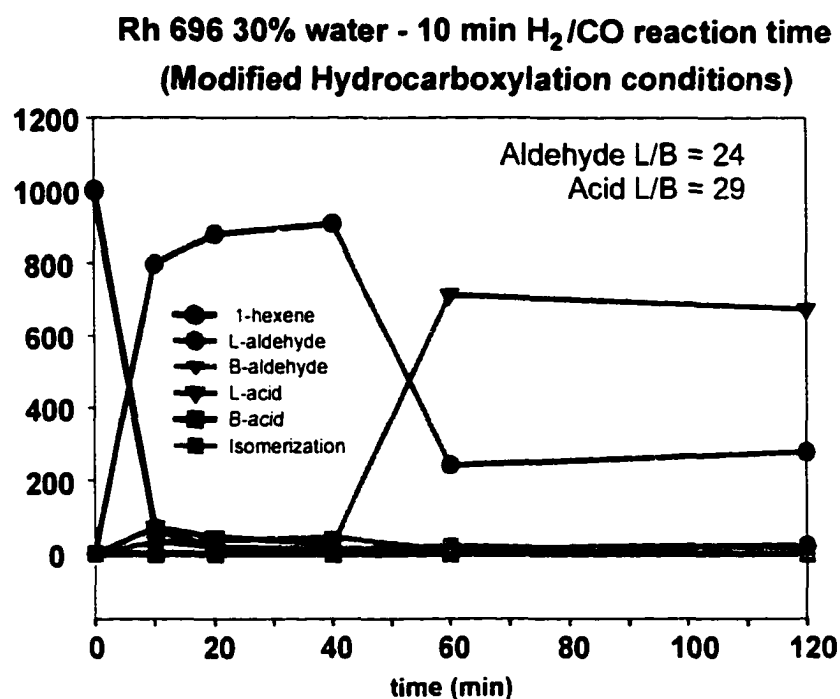


**Figure 3.22.** Reactant loss and product production plot of run Rh696 from GC analysis of autoclave samples

are overestimating the amount of 1-hexene consumed at the 10 minute mark and that our aldehyde GC analysis is probably the more correct indicator of the progress of the reaction at this point. Acetone solvent sometimes interferes with the 1-hexene peak in the GC making that the more problematic analysis.

The production of 800 equivalents of aldehyde at the 10-minute mark corresponds to an initial turnover frequency of almost 4800 TO/hr. This is far faster and more selective than any other hydroformylation catalyst known under these mild conditions. At the 10-minute point the supply gas to the autoclave is replaced with CO. This leads to rapid H<sub>2</sub> depletion in the autoclave and dramatic drop-off in the hydroformylation rate. Between 10 minutes and 40 minutes the remaining 1-hexene is more slowly converted to aldehyde product via consumption of the remaining H<sub>2</sub> in the autoclave. The H<sub>2</sub>-poor conditions

in the autoclave at the 40-minute mark initiates the second catalytic process – namely the conversion of aldehyde and water to produce carboxylic acid and  $H_2$  gas. This, too, is quite rapid with about 650 equivalents of aldehyde being converted to carboxylic acid over the course of about 20 minutes. This corresponds to an initial TOF of approximately 2000 TO/hr. This is 10-100 times faster than any other hydrocarboxylation catalyst previously observed. The almost complete linear carboxylic acid regioselectivity is no doubt a result of the high amount of linear aldehyde product produced from the initial hydroformylation catalysis.

There is a slight decrease in the amount of carboxylic acid in the 120-minute analysis, but it goes back up at the next analysis point (not shown in Figure 3.22). We, therefore, believe that the amount of carboxylic acid is essentially unchanged after the 60-minute mark and the small decrease at the 120-minute mark is most likely an artifact – but additional studies will be done by the next student on this project to verify this. The lack of further conversion of aldehyde to carboxylic acid after 60 minutes is most likely due to the build up of  $H_2$  gas in the autoclave that stops the aldehyde-water shift catalysis. There is no more 1-hexene present at this point to consume the  $H_2$  gas via hydroformylation to produce more aldehyde. Presumably we could purge out the  $H_2$  gas and convert the rest of the aldehyde to carboxylic acid. Future workers on this project will study this very point.

Following this experiment we also altered the water concentration. We had previously done 25 and 50%, so we decided to test 20 and 40%. When

water was present we clearly had faster hydroformylation with low alkene isomerization and hydrogenation side reactions. But we were uncertain as to the optimum concentration of water for the conversion of aldehyde to carboxylic acid and  $H_2$ . The GC analysis of both the 20% and the 40% water catalytic run show little or no production of carboxylic acid (Figures 3.23 and 3.24).

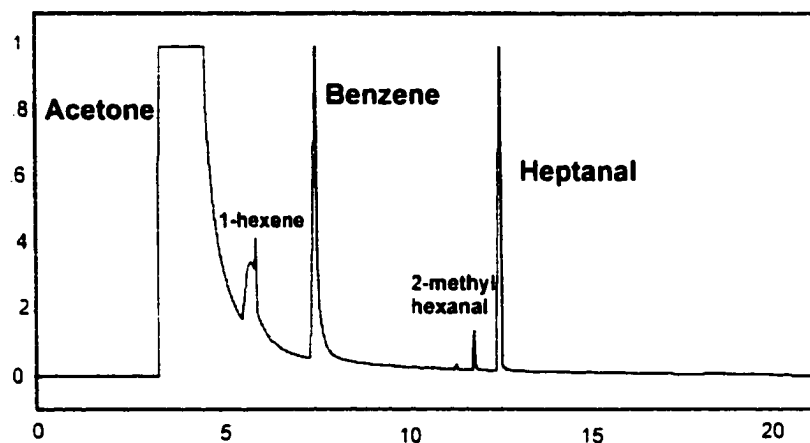


**Figure 3.23.** GC analysis of run Rh701 with 20% water and 10min  $H_2/CO$

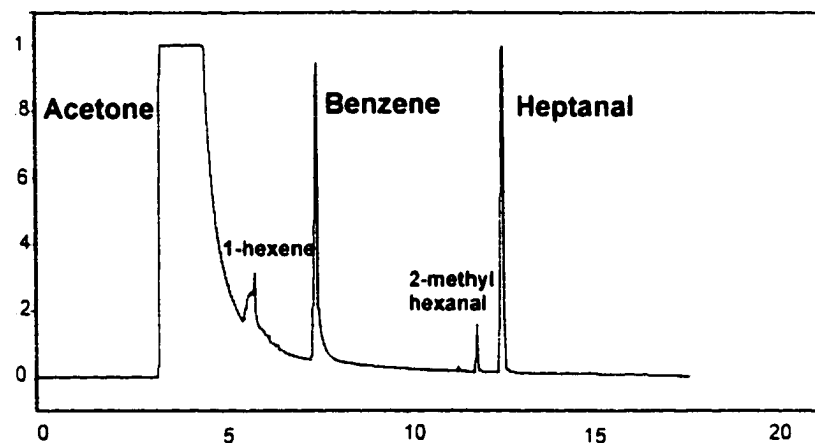


**Figure 3.24.** GC analysis of run Rh700 with 40% water and 10min of  $H_2/CO$

### 3.5. Polar Phase Bimetallic Hydroformylation Mechanistic Consideration

The addition of water to our hydroformylation catalyst dramatically improves the rate (a 40% increase), maintains the high L/B aldehyde

regioselectivity, and lowers the alkene isomerization and hydrogenation side reactions from around 12% in acetone to less than 1%. We certainly did not expect such a large improvement in our already excellent bimetallic hydroformylation catalytic results. While we do not fully understand all the factors that lead to these favorable changes, our spectroscopic studies on the catalyst and information from the Ruhrchemie-Rhone Poulenc aqueous phase monometallic hydroformylation process provide a basis for making some interesting proposals.

The *in situ* NMR studies on our bimetallic catalyst currently indicate that there is a relatively facile fragmentation pathway that leads to the formation of catalytically inactive monometallic and bimetallic double-P4 ligand rhodium complexes. This is shown below in Figure 3.26. Unlike monometallic rhodium hydroformylation catalysts that fragment the phosphine ligand, usually via the susceptible P-Ph bonds, to generate catalytically inactive phosphido-bridged dimers and clusters, we have not observed any phosphine ligand degradation reactions. Instead, the electronic effects present in the symmetrical dihydride catalyst,  $[\text{rac-Rh}_2\text{H}_2(\mu\text{-CO})_2(\text{CO})_2(\text{et,ph-P4})]^{2+}$ , **2r**, cause a labilization of the four coordination sites that are approximately *trans* to the Rh-Rh bond. We will refer to these locations as the axial coordination sites.

The lability of these axial coordination sites is great for the dissociation of the axial carbonyl ligands that is necessary for opening up a coordination site for the alkene to coordinate to in order to initiate the hydroformylation. But dissociation of one of the chelating phosphine ligands, which also occupies this



labile site, leads to fragmentation of the bimetallic unit to generate the  $\eta^4$ -et,ph-P4 coordinated monometallic complex  $[\text{rac-RhH}_2(\eta^4\text{-et,ph-P4})]^+$ , or the double tetraphosphine coordinated bimetallic complex,  $[\text{rac,rac-Rh}_2\text{H}_2(\mu\text{-CO})_2(\text{et,ph-P4})_2]^{2+}$  (Figure 3.25). Neither of these complexes are catalysts.

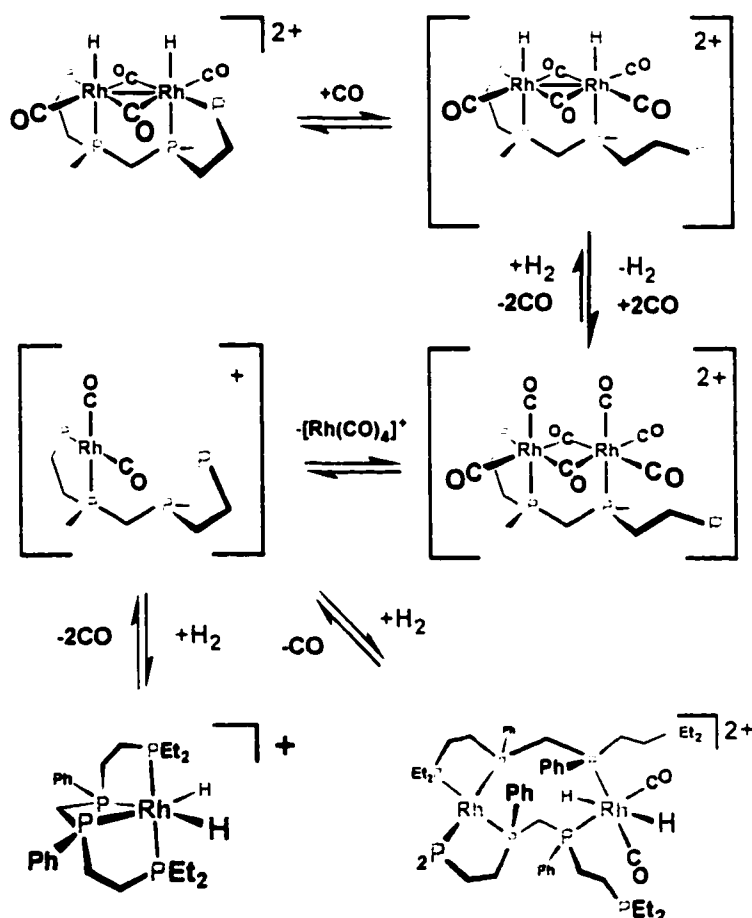


**Figure 3.25.** Proposed fragmentation mechanism to produce catalytically inactive mono- and bimetallic rhodium complexes

We know that soaking our catalyst under 90 psig  $\text{H}_2/\text{CO}$  at 90 °C overnight leads to a catalytically inactive solution. This is a common simple stability test for hydroformylation catalysts and almost always leads to deactivation of the catalyst. The lower activity seen for our current catalytic

runs in acetone relative to the original set of runs performed for the 1993 *Science* paper indicates that we may be seeing partial catalyst fragmentation/deactivation effect. The catalyst solution is presoaked at 45 psig  $\text{H}_2/\text{CO}$  while the autoclave temperature ramps up to 90 °C at the beginning of a catalytic run. Once the temperature stabilizes at 90 °C, we use 90 psig of  $\text{H}_2/\text{CO}$  gas pressure to force the alkene substrate from the small external reservoir into the autoclave in order to initiate the hydroformylation catalysis. The pre-soak ramp up time back in 1992 for the autoclaves was only about 15 minutes, while it now takes 40-60 minutes for the autoclaves to stabilize at 90°C. We believe that the longer presoaking time for the current runs is causing additional catalyst deactivation relative to the 1992-era runs. Once the alkene is added, however, there appears to be little or no change in the catalyst activity during a typical run.

One of the beneficial effects of adding water to the solvent system may be to inhibit the dissociation of the external phosphine ligand that we believe leads to catalyst fragmentation reactions. The reason for this is not well understood, but it is known to play an important role in the aqueous phase Ruhrchemie tppts-based rhodium hydroformylation system.  $\text{PPh}_3$  ligands are known to rapidly come on and off the  $\text{HRh}(\text{CO})(\text{PAr}_3)_2$  catalyst system. This is one reason why excess phosphine ligand needs to be added to the catalyst in order to maintain a good concentration of the selective bis-phosphine catalyst (Figure 3.26). The  $\text{Rh-PPh}_3$  catalyst system, which is run in organic solvents,

requires a very large excess ( $> 0.4 \text{ M PPh}_3$ ,  $\sim 1\text{mM Rh catalyst}$ ) of phosphine ligand.

But the Ruhrchemie sulfonated-tppts aqueous phase rhodium catalyst requires a considerably lower amount of excess phosphine ligand in order to maintain a given concentration of selective bis-phosphine rhodium catalyst. Electronically and sterically, both ligands are nearly identical in their rhodium binding properties. Ruhrchemie believes that the tppts ligand dissociates far less readily in aqueous solvent. This may be due to the poor coordinating properties of the water that would replace a dissociated tppts ligand. It may also be due to a hydrogen-bonded solvent shell and hydrogen bonding to the sulfonate groups on the tppts ligands.

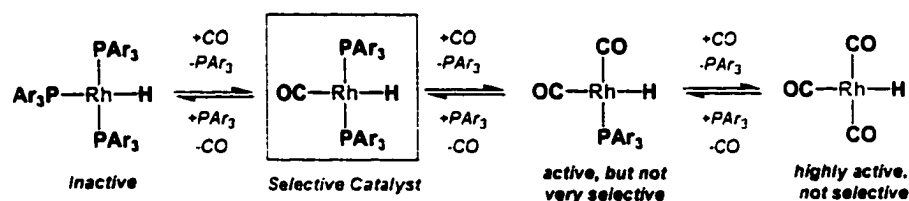


**Figure 3.26.** Phosphine ligand dissociation equilibria for monometallic rhodium hydroformylation catalysts

We believe that the same type of effect occurring in our catalyst with the water inhibiting the terminal phosphine dissociation and limiting catalyst fragmentation. This would increase the amount of active catalyst present and nicely explain the 40% increase in the initial turnover frequency in water-acetone solvent. *In situ* spectroscopic studies should be able to confirm this, and these are planned for the future and will be performed by students in the Stanley group.

Another factor where the more polar water could be assisting the catalysis is in facilitating the rotation from an open-mode conformation to a closed-mode structure. We believe that polar solvents help diffuse the cationic charges on the two halves of the bimetallic complex and lower the electrostatic barrier to rotation from open- to a closed-mode structure (Figure 3.27). Water is one of the most polar solvents and should help this key transformation and increase the amount of catalyst in the Rh-Rh bonded state.

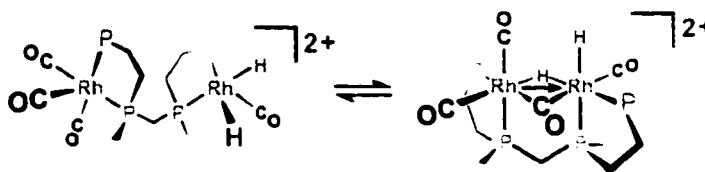


**Figure 3.27.** Rotation of open-mode hydride catalyst complex to the closed-mode conformation

The alkene hydrogenation and isomerization side reactions may well be catalyzed by the open-mode dihydride catalyst species shown above in Figure 3.28. If the presence of water favors the formation of closed-mode Rh-Rh bonded structures like **2r** and this results in lower side reactions, the source of the alkene isomerization and hydrogenation side reactions should be related to a decrease in other complexes present in the catalyst solution. Since both of the fragmentation side products discussed earlier are saturated 18e<sup>-</sup> species and would not be expected to do much of anything, an unsaturated open-mode hydride complex like that shown above seems like a likely species for catalyzing these side reactions. Once again, future *in situ* spectroscopic studies on water/acetone catalyst solutions should shed light on this issue.

### 3.6. Bimetallic Hydrocarboxylation Mechanism Discussion

As surprised as we were to observe the dramatic improvement in bimetallic hydroformylation when water was added to the acetone solvent, this barely compared to our amazement at the formation of large amounts of carboxylic acid with high linear regioselectivity. As discussed earlier, the formation of carboxylic acids from alkene, CO, and water is a very difficult catalytic reaction and ranks as a "Holy Grail"-class problem for carbonylation catalysis. Virtually every other catalyst we found in the literature required the use of some sort of modifier or co-catalyst – usually iodide or strong acid. The best current catalyst for hydrocarboxylation in terms of a combination of rate and L:B regioselectivity for the carboxylic acid products formed from higher 1-alkenes is probably Zoeller's  $\text{PPh}_3$ -modified Rh-iodide system. His  $\text{PPh}_3$ -modified catalyst has a rate of 56 TO/hr at 190 °C and 27.2 atm (400 psig) CO and a L:B carboxylic acid ratio of 6.7 for the hydrocarboxylation of 1-pentene. A Hastelloy autoclave must be used due to serious corrosion problems introduced by the formation of HI in this reaction.

In marked contrast our bimetallic catalyst has an estimated initial turnover frequency for the conversion of aldehyde to carboxylic acid of about 1950 TO/hr – or if you want to consider the overall conversion of alkene to acid, the TOF is about  $700 \text{ hr}^{-1}$  at 90 °C and 90 psig. Our catalyst is not using any modifiers or co-catalysts, so we do not have any corrosion problems with our standard stainless steel autoclave. Perhaps most impressively, we are getting what appears to be essentially complete selectivity to linear carboxylic acid. One

minor problem is that we have not achieved complete aldehyde to acid conversion, but we believe that this can be solved by proper flow-reactor engineering to control the amount of H<sub>2</sub> gas present (see discussion below). Thus, our bimetallic catalyst represents by far the best system for performing this important and extremely difficult reaction.

The evidence collected so far strongly implies that we have a novel two-stage coupled catalytic process (see Figure 3.28). First is hydroformylation catalysis to convert a certain fraction of the starting alkene to aldehyde for which a H<sub>2</sub>/CO gas mixture is needed. It seems to be quite important to both build up the concentration of aldehyde and reduce the concentration of alkene to a certain critical level. One then needs to drop back on the amount of H<sub>2</sub> gas present to start the second stage catalytic conversion of aldehyde and water to produce carboxylic acid and H<sub>2</sub>, which we will refer to as the aldehyde-water shift reaction. Excess hydrogen appears to strongly inhibit the aldehyde-water shift reaction, but we believe that some H<sub>2</sub> is needed to maintain the proper catalytic species in solution.

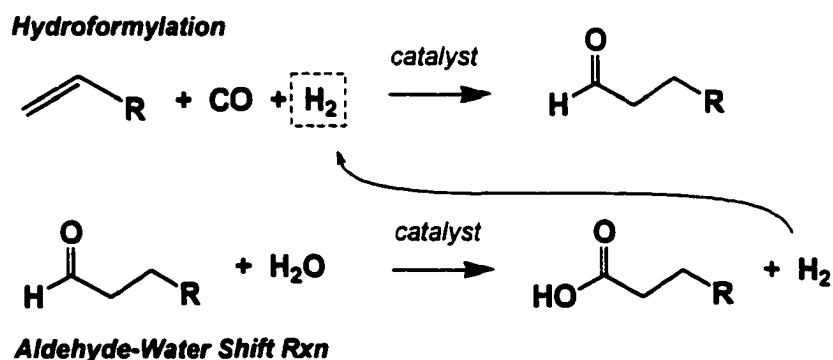


**Figure 3.28.** The two catalytic reactions occurring to transform alkene, water, and CO into carboxylic acid

The extreme sensitivity of the aldehyde-water shift reaction to the amount of alkene and aldehyde present is indicated by the observation of carboxylic acid products when one runs with 1000 equivalents (1 M 1-hexene, 1 mM catalyst) for 10 minutes with H<sub>2</sub>/CO before switching over to pure CO. Runs with 5 or 15 minutes of H<sub>2</sub>/CO before switching over to CO only give hydroformylation. This can be explained by the better coordinating ability of alkene relative to the aldehyde. If there is too much alkene present when the shift to pure CO occurs, its stronger metal coordinating ability can block out the smaller concentration of aldehyde from coordinating to the catalyst. If there is too little alkene left (as in the 15 minute H<sub>2</sub>/CO run), there is not enough present to consume the H<sub>2</sub> produced from the aldehyde-water shift reaction. This leads to a build-up of excess H<sub>2</sub> that appears to stop the aldehyde-water shift reaction dead in its tracks. This also explains the lack of carboxylic acid formation when we tried the catalysis with 2000 equivalents of 1-hexene. The H<sub>2</sub>/CO run time needs to be carefully adjusted in order to give the proper aldehyde/alkene ratio when one shifts to pure CO. The faster rate of hydroformylation with higher concentrations of alkene makes this target trickier to hit.

The strong inhibition of the aldehyde-water shift reaction by H<sub>2</sub> implies that the bimetallic catalyst hydride complex  $[rac-Rh_2H_2(\mu-CO)_2(CO)_2(et,ph-P4)]^{2+}$ , **2r**, is probably not the catalyst for this reaction. This leaves one of the isomeric bimetallic carbonyl-only complexes shown in Figure 3.29 as the likely catalyst. We have not had a chance to test **4r**, the open-mode dirhodium tetracarbonyl

complex, with an aldehyde/alkene/H<sub>2</sub>O mixture to see if it will work as a catalyst for the production of carboxylic acid (the right amount of alkene is probably needed to act as a hydroformylation scavenger for the H<sub>2</sub> produced in the aldehyde-water shift reaction).

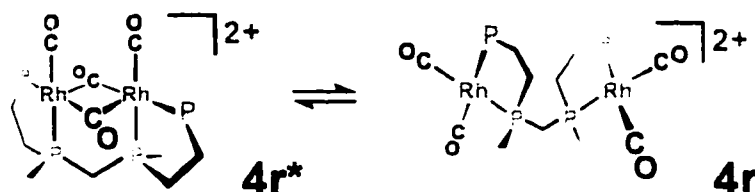


**Figure 3.29.** Possible catalysts for the aldehyde-water shift reaction

The closed-mode bimetallic isomeric complex **4r\*** is part of our proposed bimetallic hydroformylation cycle (Figure 1.10) and we have some tentative *in situ* spectroscopic data supporting its presence. **4r\*** seems to be only formed from **4r** in the presence of H<sub>2</sub>, since the rotation of **4r** from an open to close-mode conformation appears to be sterically and electrostatically difficult (see discussion in introduction). Hydrogen seems to dramatically lower the barrier for the formation of bridged-carbonyl bimetallic complexes (both hydride-containing and CO-only).

We currently favor the closed-mode CO-bridged bimetallic complex **4r\*** as the catalyst for the aldehyde-water shift reaction. We believe that the CO-bridged dirhodium complex  $[rac-Rh_2(\mu-CO)_2(CO)_2(et,ph-P4)]^{2+}$ , **4r\***, plays a critically important in the catalytic activation of the aldehyde and water. Placing two d<sup>8</sup> metal centers adjacent to one another in a bimetallic complex like this will lead to what we believe will be enhanced reactivity towards the coordination



and activation of the aldehyde. This enhanced reactivity is based on Gray's proposal that weak symmetry induced M-M bonding interactions can be formed in some  $d^8$  Rh and Ir complexes (i.e.,  $[\text{Rh}(\text{CNR})_4]^+$ ).<sup>16</sup>

A simple MO diagram illustrating the interactions of the filled  $d_z^2$  HOMO and  $p_z$  based LUMO for two interacting  $d^8$  metal centers are shown in Figure 3.30. The close proximity of the metals causes their two filled  $d_z^2$  orbitals to

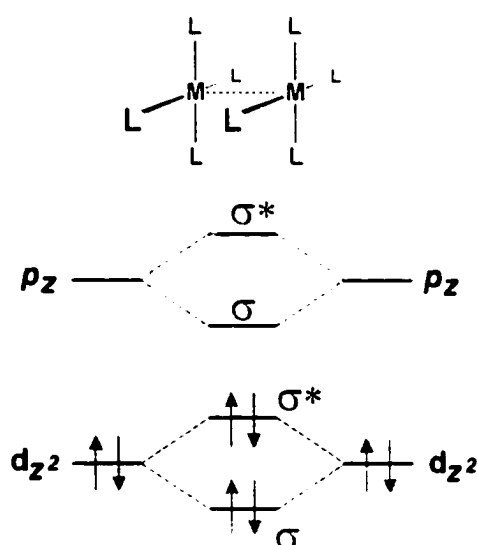


**Figure 3.30.** MO diagram proposed by Gray

split apart forming a new pair of  $\sigma$  and  $\sigma^*$  MO's. Similarly the interaction of the two empty metal  $p_z$  orbitals generates another set of  $\sigma$  and  $\sigma^*$  MO's. We are most interested in the filled HOMO and empty LUMO. The raising and lowering of these orbitals is in exactly the right direction for promoting a weak interaction between the LUMO and the aldehyde  $\pi$ -system. The higher energy of the HOMO, on the other hand, may act as a donor to the aldehyde  $\sigma^*$  orbital, helping to weaken the C=O bond and assisting the nucleophilic attack by the

water. Both of these interactions will be favored by the presence of a second closely interacting metal center. The presence of bridging CO's will change this simple orbital picture, but we think that the net orbital effect will be similar.

Based on this we have proposed a mechanism for aldehyde-water shift reaction catalysis. (Figure 3.31) The aldehyde reacts with  $4r^*$  to form I. The

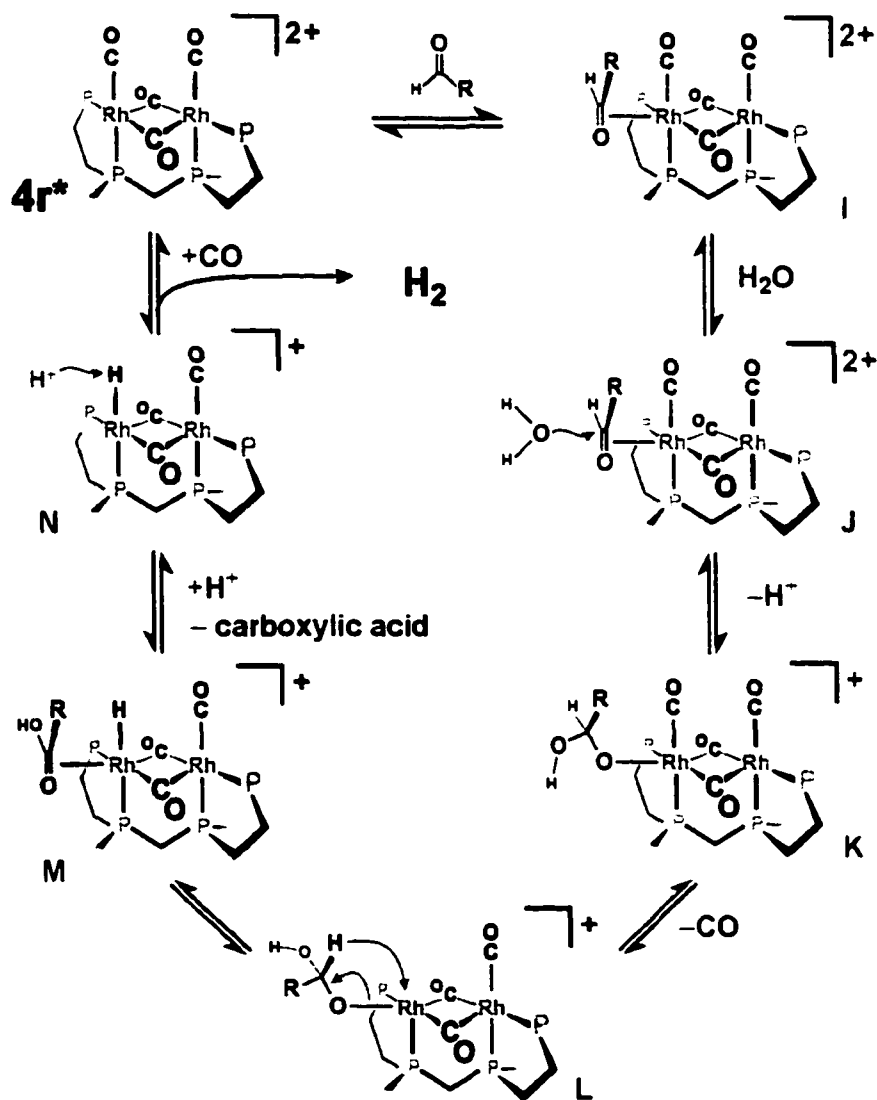


**Figure 3.31.** Proposed mechanism for aldehyde/water shift catalysis

cationic charge on the metal activates the coordinated aldehyde for reaction with water to form J. Loss of a proton produces the alkoxide-bound

monocationic species, **K**. Loss of CO opens a coordination site, **L**, allowing a  $\beta$ -hydride elimination to form the carboxylic acid and the metal-hydride complex, **M**. Dissociation of carboxylic acid and protonation of the hydride by free acid ( $\text{H}^+$ ) produces **N**. Hydrogen gas is protonated off and addition of CO regenerates the starting catalyst. The hydride in complex **N** that is protonated by the free acid is more basic relative to than the hydrides of **2r**. The hydride in **N** is more basic thus, since the Rhodium atom that it is coordinated to is formally neutral it is easier to protonated it off as hydrogen gas.

Precedence for the aldehyde-water shift reaction and our mechanism comes from unpublished work of Tyler<sup>17</sup> and coworkers from University of Oregon. They have demonstrated that their cationic  $[\text{Cp}'_2\text{Mo}(\text{OH})(\text{H}_2\text{O})]^+$  ( $\text{Cp}' = \text{Me-Cp}$ ) complex can slowly catalyze the reaction of aldehyde and water to produce carboxylic acid and  $\text{H}_2$ . Their proposed mechanism is shown in Figure 3.32 (plain Cp is used in the figure for clarity).

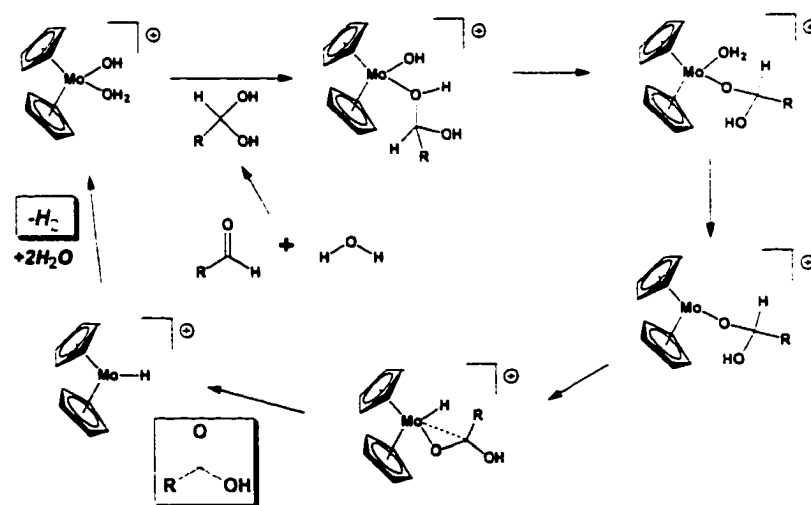


**Figure 3.32.** Proposed mechanism for Tyler's  $[\text{Cp}'_2\text{Mo}(\text{OH})(\text{H}_2\text{O})]^+$ -catalyzed aldehyde-water shift reaction

They propose an aldehyde-water pre-equilibrium step that produces a gem-diol. This displaces the labile coordinated water on the Mo. They favor a gem-diol because they have done quite a bit of work on the reaction of alcohols with this complex and have a slight bias for an initial alcohol-type reaction. But there is little difference here with our mechanism where we first coordinate the aldehyde to the cationic metal center, which should activate the aldehyde even more for reaction with water. A proton transfer from the coordinated gem-diol to the Mo-OH generates an alkoxide and a labile water. Dissociation of the water opens a coordination site that permits a  $\beta$ -hydride elimination to produce the carboxylic acid and the Mo-hydride. Tyler and his group have already shown that this  $[\text{Cp}'_2\text{Mo-H}]^+$  complex reacts with water to produce  $\text{H}_2$  and regenerate the starting  $[\text{Cp}'_2\text{Mo}(\text{OH})(\text{H}_2\text{O})]^+$  complex.

They have little evidence for this mechanism and have not published it as yet. Their mechanism therefore is just as speculative as ours. But we derive some comfort from the fact that they have proposed a similar reaction sequence. There are two big differences between their system and ours. Tyler's catalyst is far slower (only several turnovers per hour) and does not do hydroformylation catalysis. We believe that the combination of bimetallic cooperativity via the  $d^8-d^8$  orbital interactions, the dicationic charge on the bimetallic complex, and electron-withdrawing carbonyl ligands all work together to dramatically enhance the reactivity of our catalyst relative to theirs. Electrophilic activation of the aldehyde almost certainly plays an important role in this catalytic reaction.

Presently we are still in the introductory stage of this work. The examination of our results indicates that we can produce carboxylic acid using our bimetallic hydroformylation catalyst. We feel that we must use the modified hydrocarboxylation conditions until an optimized one can be found. There will have to be further studies to determine exactly what complex is the key catalyst for the production of carboxylic acid. We would like to be able to convert 100% of the aldehyde into carboxylic acid product. We believe this will be possible once the catalytic conditions are optimized.

### 3.7. References

1. R. H. Crabtree, *The Organometallic Chemistry of Transition Metals*, 2<sup>nd</sup> ed., John Wiley & Sons, New York, 1994, Chap. 11.
2. a) W. Keim, et al., *Organometallics*, 2, **1983**, 594; b) K. Hirose, and W. Keim, *J. Mol. Catal.*, 73, **1992**, 271.
3. I. T. Horvath, *Acc. Chem. Res.*, 31, **1988**, 641-650.
4. B. Cornils and W. A. Herrmann, eds., *Applied Homogenous Catalysis with Organometallic Compounds*, vol. 1, p. 80-81.
5. I. T. Horvath, J. Rabai, *Science*, 266, **1994**, 72-75; I. T. Horvath, J. Rabai, US Patent 5,463,082, **1995**.
6. J. Falbe, ed., *New Syntheses with CO*, Springer, Berlin-Heidelberg and New York, 1980, hydrocarboxylation chapter.
7. a) W. Reppe, *Justus Liebigs Ann. Chem.*, 582, **1953**, 1; b) W. Reppe and H. Kröper, *Ibid.*, 582, **1953**, 38.
8. R. F. Heck, *J. Am. Chem. Soc.*, 85, **1963**, 2013.
9. J. H. Craddock, A. Hershmann, F. E. Paulik, and J. F. Roth, US Patent 3,579, 552, **1981**.
10. D. Forester, A. Hershman, and D. E. Morris, *Catal. Rev. -Sci. Eng.*, 23, **1981**, 89-105.
11. D. Forester, *J. Am. Chem. Soc.*, 85, **1976**, 846.
12. J. R. Zoeller, US Patent 5,977,4077, **1999**.

13. F. P. Pruchnik, P. Smolenski, E. Galdecka, Z. S. Galdecki, *New J. Chem.*, **22**, **1998**, 110-114.
14. a) A. L. Lapidus, and S. D. Pirozhkov, *Russ. Chem. Rev.*, **58**, **1989**, 117-233; b) G. k-I Magomedov, L. V. Morozov, A. V. Medvedeva, et al., USSR Patent. 721 409; *Byul Izobret.*, **10**, **1980**, 94.
15. G. Verspui, J. Feken, G. Papadogianakis, R. A. Sheldon, *J. Mol. Catal. A*, **146**, **1999**, 299-307.
16. K. R. Mann, J. G. II Gordon, H. B. Gray, *J. Am. Chem. Soc.* **1975**, **97**, 3553-3555.
17. Private communication between Prof. Stanley and Prof. Tyler (U. Oregon).

## **CHAPTER 4**

### **CONCLUSION/ FUTURE STUDIES**

#### **4.1. Hydroformylation Kinetic Studies**

We accomplished our initial goal of determining the kinetic orders of the alkene (olefin) and dinuclear dicationic catalyst and demonstrated that they are consistent with our proposed bimetallic mechanism. The rate was first order for both components. Garland's work on  $\text{HRh}(\text{CO})_3$ -catalyzed hydroformylation clearly emphasized the importance of performing detailed kinetic studies. The orders of the  $\text{H}_2$  and  $\text{CO}$  in this reaction need to be determined in order to complete the kinetic study. Knowledge of the kinetic orders provides us with data to support our theory of bimetallic cooperativity and help refine our proposed bimetallic hydroformylation mechanism.

#### **4.2. Aldehyde/Water Shift Reaction Catalysis**

We initially began this study to investigate if our catalyst could hydroformylate in a very polar solvent system and, if so, would the products phase separate. Our findings indicated that the addition of water produced much cleaner and faster hydroformylation along with the production of highly linear carboxylic acid, which was completely unexpected. This led us to question how our system was producing carboxylic acid and whether we could control it.

The reaction studies indicate that the bimetallic dicationic catalyst first hydroformylates  $\alpha$ -olefins into aldehyde products. Then a second catalytic reaction involving an aldehyde/water shift reaction occurs under the proper

conditions to convert aldehyde and water into carboxylic acid and  $H_2$ . This second reaction is inhibited by too much hydrogen, so it is important to reduce the hydrogen gas present in order to get this reaction to occur. An extremely fortunate leak in our autoclave during the initial studies accidentally purged enough hydrogen gas from the reactor to allow the aldehyde-water shift catalysis to occur. The aldehyde-water shift catalysis was activated by replacing the  $H_2/CO$  gas, initially used to start the hydroformylation, by pure CO after 10 minutes of hydroformylation catalysis (1mM catalyst concentration, 30% water to 70% acetone solvent, and 1000 equivalents of 1-hexene). We have found that the aldehyde/water shift reaction is very delicately balanced and that when these conditions are altered it can drastically change the final results (discussion below).

Initially, it was our intention to find a set of optimum conditions to perform this reaction so that we could convert as much aldehyde product as possible to carboxylic acid product. We have begun to perform these experiments and have observed, for example, that when the alkene concentration is increased (2000 equivalents, 10 minutes  $H_2/CO$ ) it slows down the aldehyde/water shift catalysis reaction. The run time under  $H_2/CO$  before switching to pure CO is clearly critical, and the optimum time has not yet been found for this alkene starting concentration. It is our belief that the reaction is best performed using a flow reactor system, where the amount of  $H_2$  and alkene present can more easily be adjusted.



Spectroscopic and kinetic studies also need to be performed on this reaction. In section 3.5 there was a discussion on reasons for the increased initial turnover frequency and low side reactions when water is added to the acetone. It is believed that spectroscopic studies will address these issues and whether **4r\*** is favored as the catalyst (see Figure 3.32) for the aldehyde/water shift catalysis reaction. Spectroscopic studies should help us understand by which mechanistic pathway our aldehyde/water catalysis reaction is proceeding. We believe there should be some correlations with our bimetallic hydroformylation mechanism. It is believed that both the bimetallic hydroformylation and the aldehyde/water incorporate bimetallic cooperativity. Kinetic studies also need to be performed and will complement the spectroscopic studies and give us a clearer understanding of this aldehyde/water shift catalysis reaction. The reactant loss and product production determination plot (Figure 3.22) also indicates there is a strong interrelationship between the alkene and aldehyde concentrations in order to initiate the aldehyde/water shift reaction.

Finally, we would like to do comparison tests with Sheldon's Palladium hydrocarboxylation system (Figure 3.15). We believe this would be an excellent way to compare our catalyst to another active system. The Stanley group has previously done this with our bimetallic dicationic hydroformylation catalyst system and the Union Carbide Rh-PPh<sub>3</sub> catalyst system. In addition to this experiment we would also like to set up a reaction with our carbonyl catalyst precursor, **3r**, under modified conditions (30% water – 70% acetone, 1000

equivalents of olefin, 90 psig CO) with differing ratios of alkene and aldehyde. We would like to investigate the following in this reaction: 1) Can the simple dicationic carbonyl  $[rac-Rh_2(CO)_4(et,ph-P4)]^{2+}$ , **4r**, catalyze the aldehyde/water shift reaction? Or is some  $H_2$  initially needed to generate the closed mode isomeric complex  $[rac-Rh_2(\mu-CO)_2(CO)_2(et,ph-P4)]^{2+}$ , **4r\***? 2) What is the proper ratio of alkene to aldehyde need in order to observe high conversion to carboxylic acid and  $H_2$ ? Does too much alkene inhibit the aldehyde/water shift reaction? Does too little alkene allow excess  $H_2$  build up that stops the reaction? 3) Can we simulate a more flow-reactor-type situation where we can observe the aldehyde/water shift reaction directly by flushing away the  $H_2$  produced? All of these should lead to a considerably improved understanding of the unusual catalytic reaction.

The aldehyde/water shift reaction catalysis is definitely in its early stages and there is much for us to learn about this system. We believe that the uniqueness of the system represents an exciting new catalyst system and potentially another dramatic demonstration of the effectiveness of bimetallic cooperativity in homogeneous catalysis.

## CHAPTER 5

### EXPERIMENTAL

#### 5.1. General Synthesis

All general synthetic procedures were performed under inert atmosphere ( $N_2$ ) using Schlenk line techniques and/or glove boxes. Several synthesis procedures required the use of both. Several solvents were purchased from Sigma Aldrich that had been packed under nitrogen: toluene, hexane, diethyl ether, tetrahydrofuran (THF), dichloromethane (DCM), methanol, ethanol, tetraglyme and benzene. All solvents were used as received. Acetone and pentane were degassed by bubbling with nitrogen. The water used for hydrocarboxylation experiments was also degassed by bubbling with nitrogen. The following chemicals were purchased and used as received:  $Rh(CO)_2(acac)$  (PGP Industries), phenylphosphine and diethylzinc (Strem Chemicals), 1-hexene, phosphorous trichloride, vinylmagnesium bromide,  $HBF_4 \cdot OEt_2$ , dimethylformamide (DMF), heptaldehyde, bicyclo[2.2.1]hepta-2,5-diene or 2,5 norbornadiene (nbd), sodium cyanide (NaCN) and nickel thiocyanate ( $Ni(SCN)_2$ ) (Sigma Aldrich). 1-hexene was purchased packed under nitrogen, but we also passed it through a fresh Alumina column prior to each use. The gases were purchased from BOC Gases and used as received. The gases were either high purity or ultra-high purity.

##### 5.1.1. Synthesis of methylenebis(phenylphosphine), or bridge<sup>1</sup>

In a 1 liter Schlenk flask, 20.0 g (0.175 moles) of phenylphosphine was mixed with 7.70 g (0.091 moles) of dichloromethane in 209 mL of DMF. The

solution was cooled to 0°C in an icebath. 27.0 mL (0.414 moles) of a 56% solution of KOH was added drop-wise to the reaction mixture. The solution will become increasing bright yellow after each addition of KOH and will eventually stay bright yellow. The solution was allowed to stir for approximately 4 hours after all the KOH was added and the solution color will become white. To quench the reaction, 138 mL of water was added to the reaction mixture. The product was then extracted with 60 mL of pentane (3 washes). The pentane was evaporated from the extractions, and byproducts (salts) were removed at 90°C under vacuum. 9.0 g (43% yield) of bridge was produced.  $^{31}\text{P}\{^1\text{H}\}$  NMR ( $\text{d}_6$ -benzene,  $\delta$  in ppm,  $\text{H}_3\text{PO}_4$  reference): -56.3 and -57.6 (s) (racemic and meso diastereomers).

It was found that the yields could be increased when the batch size was doubled. The yields would usually increase to 65% or better. Also if less pentane is used when performing the extraction the yield will also increase.

#### **5.1.2. Synthesis of diethylchlorophosphine ( $\text{Et}_2\text{PCI}$ )<sup>2</sup>**

A solution of 46.0 g (0.361 moles) of diethylzinc in 50 mL of tetraglyme was prepared. A solution of 50.0 g (0.364 moles) of phosphorus trichloride in 50.0 mL of tetraglyme was also prepared. Both solutions were cooled to 0 °C in an ice bath. The diethylzinc solution was added drop-wise to the phosphorus trichloride solution. The product was separated from the mixture by trap-to-trap distillation. 20.6 g (45.3 % yield) of  $\text{Et}_2\text{PCI}$  was obtained.  $^{31}\text{P}\{^1\text{H}\}$  NMR (d-chloroform,  $\delta$  in ppm,  $\text{H}_3\text{PO}_4$  reference): at 120 ppm,  $^1\text{H}$  NMR (d-chloroform,  $\delta$  in ppm, TMS reference): 6H (m) at 1.05 ppm, 4H (m) at 1.7 ppm.

This reaction can be very problematic. Difficulties occur maximizing the amount of  $\text{Et}_2\text{PCI}$  produced and when collecting (trap-to-trap distillation) the final product. To increase the yield of the final product, we added an excess of diethylzinc (approximately 20%). In every trial we were able to obtain pure diethylchlorophosphine. The second problem posed more difficulty than expected. We originally used THF instead of tetraglyme, but THF azetropes with diethylchlorophosphine and can be difficult to separate. Tetraglyme was then used and because of its high boiling point, it did not azetrope with the diethylchlorophosphine. The only shortcoming of tetraglyme was that it was viscous enough that it would often be difficult to distill the diethylchlorophosphine from it. To rectify this we heated the solution in a warm water bath to assist in the collection of the  $\text{Et}_2\text{PCI}$ . These improvements usually increase isolated yields to 70% or better.

### **5.1.3. Synthesis of diethylvinylphosphine<sup>2</sup>**

In a 1 liter Schlenk flask, 247 mL (0.25 moles) of 1.0 M Vinylmagnesiumbromide solution (in THF) and 217 mL of tetraglyme were placed. The THF solvent is then removed by trap-to trap distillation. Hunt<sup>3</sup> developed this solvent displacement procedure in order to allow the easier isolation of the  $\text{Et}_2\text{P}(\text{CH}=\text{CH}_2)$  product that azeotropes with THF. The Grignard tetraglyme solution is then cooled in a 0 °C ice bath. 30.0 g (0.24 moles) of  $\text{Et}_2\text{PCI}$  were slowly added to the solution and stirred for approximately a half hour. A second trap-to-trap vacuum distillation (gentle heating with a warm water bath) isolates the product. 15.0 g (60% yield) of diethylvinylphosphine was

collected.  $^{31}\text{P}\{^1\text{H}\}$  NMR (d-chloroform,  $\delta$  in ppm,  $\text{H}_3\text{PO}_4$  reference):  $-20$  ppm,  $^1\text{H}$  NMR (d-chloroform,  $\delta$  in ppm, TMS reference): multiplet  $0.7\text{--}1.5$  ppm (ethyl group, and  $-\text{CH}_2$ ), multiplet at  $5.3\text{--}6.2$  ppm (vinyl group).

The main improvement was to increase the batch size of  $\text{Et}_2\text{PCI}$  added and to heat the final reaction mixture (tetraglyme and diethylvinylphosphine) in a warm bath to assist in the final distillation to isolate product.

#### 5.1.4. Synthesis of et,ph-P4 ligand<sup>4</sup>

In a 250 mL flask, 10.0 g (0.043 moles) of bridge were mixed with 10.1 g (0.087 moles) of diethylvinylphosphine. The mixture was stirred for at least three hours under Xenon lamp irradiation. The product is a 1:1 *racemic:meso* mixture of ligand. 20.0 g (100% yield) of ligand was obtained.  $^{31}\text{P}\{^1\text{H}\}$  NMR ( $\text{d}_6$ -benzene,  $\delta$  in ppm,  $\text{H}_3\text{PO}_4$  reference): diastereotopic internal phosphorous atoms,  $-26.3$  (1 P, dd,  $J_{\text{P-P}} = 10.4$  and  $12.2$  Hz) and  $-25.5$  (1 P, dd,  $J_{\text{P-P}} = 10.2$  and  $12.1$  Hz); external phosphorus atoms,  $-18.37$  (1 P, dd,  $J_{\text{P-P}} = 10.3$  and  $12.5$  Hz) and  $-18.31$  (1 P, dd,  $J_{\text{P-P}} = 10.4$  and  $12.3$  Hz).  $^1\text{H}$  NMR ( $\text{d}_6$ -benzene, TMS reference):  $0.74\text{--}0.85$  (m,  $\text{P-CH}_2\text{-CH}_3$ ),  $1.02\text{--}1.14$  (m,  $\text{P-CH}_2\text{-CH}_3$ ),  $1.19\text{--}1.33$ ,  $1.33\text{--}1.46$  (m,  $\text{P-CH}_2\text{-CH}_2\text{-P}$ ),  $1.72\text{--}1.89$  (m,  $\text{P-CH}_2\text{-P}$ ),  $6.98\text{--}7.10$  and  $7.41\text{--}7.47$  (m, Ph).

There were two improvements that I made in this procedure. The addition of an excess of diethylvinylphosphine combined with allowing the mixture to be irradiate by the Xenon lamp overnight. We noticed that side products were often produced with shorter irradiation times and stoichiometric

amounts of diethylvinylphosphine, these turn out to be intermediates in the reaction and unreacted bridge. When we add more diethylvinylphosphine and allow the solution to irradiate overnight, no appearance of any intermediates or unreacted bridge is observed. The excess diethylvinylphosphine is easily removed by vacuum evaporation at room temperature leaving pure et,ph-P4 ligand.

#### **5.1.5. Synthesis of $\text{Rh}(\text{nbd})(\text{acac})^2$**

In a 250 mL Schlenk flask 3.0 g (0.011 moles) of  $\text{Rh}(\text{CO})_2(\text{acac})$  was mixed with 85 mL of nbd. The flask was attached to a reflux condenser and exposed to nitrogen. Two needles were placed in the top of the reflux condenser to expel the carbon monoxide gas produced by the norbornadiene substitution reaction. The mixture was heated using a heating mantle apparatus to approximately 80 °C, with continuous stirring for 4 hours. The solution turned from dark green to bright yellow. The solution was cooled, filtered, and the unreacted nbd was removed by vacuum. The resulting product was a yellow powder that was recrystallized from THF. 2.8 g (82% yield) of yellow crystals of  $\text{Rh}(\text{nbd})(\text{acac})$ .

#### **5.1.6. $[\text{Rh}(\text{nbd})_2]\text{BF}_4^2$**

In a 50 mL flask, 2.01 g (0.007 moles) of  $\text{Rh}(\text{nbd})(\text{acac})$  was dissolved in 30 mL of THF in the glovebox. The solution was cooled to -20 °C. 2.37 g of  $\text{HBF}_4 \cdot \text{OEt}_2$  (in THF) was placed in a 50 mL flask and added drop-wise to the  $\text{Rh}(\text{nbd})(\text{acac})$  solution and shaken vigorously. The solution turned from yellow

to dark red. 3.0 g (0.033 moles) of nbd was placed in a 50 mL flask and added drop-wise while vigorously shaking the reaction mixture. An orange-red precipitate formed. The solution was filtered immediately. The orange-red powder was washed with diethyl ether. This changes the color of the powder to dark red. The powder was allowed to dry overnight under vacuum. Final product was a red powder, 90-95% yield.  $^1\text{H}$  NMR ( $\text{CD}_2\text{Cl}_2$ ): 1.7 (br s, bridging  $\text{CH}_2$  of nbd), 4.3 (br s, bridgehead  $\text{CH}$  of nbd), 5.3 and 5.6 (br m, and br s, olefinic  $\text{CH}$  of nbd).

#### 5.1.7. Nickel Separation of *meso* and *racemic* diastereomers of et,ph-P4<sup>4</sup>

Part I (performed completely in the glovebox): In a 1 L Schlenk flask, 22.2 g (0.127 moles) of  $\text{Ni}(\text{SCN})_2$  and 250 mL of ethanol was stirred. In a 250 mL flask 30.0 g (0.065 moles) of ligand and 125 mL of ethanol was slowly added to the mixture. The mixture was stirred overnight. The maximum stir time should not exceed 15 hours. We originally stirred the solution for 24 – 48 hours, but were generating numerous side products.<sup>2</sup> The stir time was reduced to 24 hours but little improvement in the yield was seen. Decreasing the stir time to 12-16 hours, however, increased overall yield by 15 – 20%.

Part II: The mixture from part I was filtered and washed with ethanol. The *meso* nickel complex was the precipitate that is collected in the frit, while the soluble *racemic* nickel complex ( $\text{Ni}_2(\text{SCN})_4(\text{et,ph-P4})$ ), which is dark red. The ethanol was completely evaporated, and the flasks were taken into the box to scrape and recover the  $\text{Ni}_2(\text{SCN})_4(\text{et,ph-P4})$ . 13.3 g (32% yield) of  $\text{Ni}_2(\text{SCN})_4(\text{et,ph-P4})$  was isolated.



Part III: In a 500 mL Schlenk flask, 13.26g (0.016 moles) of racemic nickel complex,  $\text{Ni}_2(\text{NCS})_4(\text{et,ph-P4})$ , was suspended in 250 mL of hexane and stirred. In a 250 mL Schlenk flask, 12.0g (0.25 moles) of NaCN was completely dissolved in 34 mL of water. Then, 34 mL of methanol was added to the cyanide water mixture. The NaCN solution was quickly added to the racemic nickel complex mixture. The solution was allowed to stir for 2-3 minutes. The solution color was orange-red. The organic layer was collected and washed three times with water. The organic layer was placed back into the glovebox and filtered through an alumina slurry using a chromatography column with a stopcock. The excess hexane was then removed under vacuum. 4.89 g (40% yield) of racemic et,ph-P4 was collected. The final product was a clear viscous liquid.

#### 5.1.8. Synthesis of $[\text{rac-Rh}_2(\text{nbd})_2(\text{et,ph-P4})](\text{BF}_4)_2$ <sup>2</sup>

In the glove box, 4.03g (0.011 moles) of  $[\text{Rh}(\text{nbd})_2]\text{BF}_4$  was dissolved in 10 mL of DCM in a 50 mL Erlenmeyer flask. In another 50 mL Erlenmeyer flask, 2.5g (0.005 moles) of *rac*-et,ph-P4 was dissolved in 10 mL of DCM and added dropwise to the  $[\text{Rh}(\text{nbd})_2]\text{BF}_4$  mixture with vigorous shaking. This solution was then added dropwise, with vigorous shaking to 150 mL of diethyl ether in a 250 mL Erlenmeyer flask. The vigorous shaking must be performed along with the addition to avoid oiling of the product. The solution containing an orange precipitate was filtered immediately. The precipitate was dissolved in acetone and placed in the freezer for recrystallization. The final product was orange-red crystals. The yield was ~90%. <sup>31</sup>P NMR ( $\text{CD}_2\text{Cl}_2$ ): 47.5 (dm,  $J_{\text{P-Rh}}$

= 156 Hz, internal phosphorus atoms) and 58.0 (dd,  $J_{P-P} = 23$  Hz and  $J_{P-Rh} = 150$  Hz, external phosphorus atoms).  $^1H$  NMR ( $d\text{-CD}_2\text{Cl}_2$ ): 0.8 – 1.4 (m,  $PCH_2CH_3$ ), 1.5 – 2.1 (m,  $PCH_2CH_3$  and m,  $PCH_2CH_2P$  and s,  $CH_2$  of nbd), 2.9 (t,  $PCH_2P$ ), 3.6 – 4.2 (br d, bridge head  $CH$  of nbd), 4.8 and 5.3 (br s, olefinic  $CH$  of nbd).

## 5.2. Hydroformylation and Hydrocarboxylation Experiments

Hydroformylation and hydrocarboxylation experiments were performed in stainless steel autoclaves from Parr. The reaction process was observed by the gas uptake in a reservoir that was connected to a two-stage regulator, which delivered gas at a constant pressure. All the information was recorded onto the Parr 4850 controller during the catalytic run and transferred to a PC for data workup.

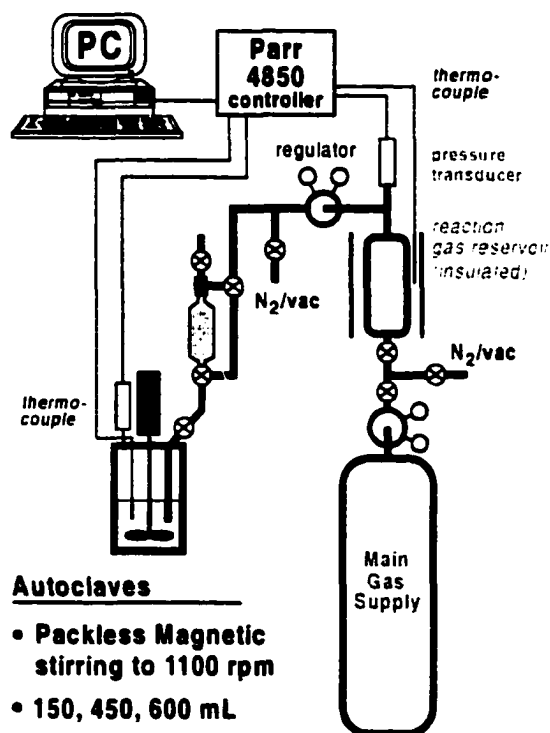


**Figure 5.1.** Diagram of the autoclave setup

Hydroformylation run conditions were 90 psig  $\text{H}_2/\text{CO}$ , 90 °C, 1 mM (92 mg,  $8.9 \times 10^{-5}$  moles) catalyst concentration, 80 mL of acetone and 1000 equivalents of 1-hexene (7.4 g,  $8.9 \times 10^{-2}$  moles, 11.0 mL). Hydrocarboxylation run conditions were the same except that the solvent concentrations were altered to contain 25% (20 mL), 30% (24 mL) or 50% (40 mL) water by volume. After the leak in the system was corrected the kinetic studies were repeated and the normal hydroformylation conditions were used.

The hydrocarboxylation experiments used different conditions: 1 mM (92 mg,  $8.9 \times 10^{-5}$  moles) of catalyst, 1000 equivalents of 1-hexene (7.4 g,  $8.9 \times 10^{-2}$  moles, 11.0 mL), 30% water (24 mL), 56 mL of acetone, 90 psig  $\text{H}_2/\text{CO}$ , and 90 °C to generate the active catalyst. Once the autoclaves ramped to 90 °C the olefin was added and the experiment run for approximately 10 minutes. The inlet valve was then closed and the reservoir was purged of  $\text{H}_2/\text{CO}$  and was replaced by CO. The inlet valve was then reopened and the reaction was completed. There were other experiments similar to this one, where we changed the olefin concentration to 2000 equivalents instead of 1000, the time increment of 10 minutes to 5 and 15 minutes, and the percentage of water to 20% (16 mL) and 40% (32 mL).

We also did an experiment where we used heptanoic acid as the substrate instead of olefin (1-hexene). In this experiment we used normal amounts of catalyst, acetone, 90 psig  $\text{H}_2/\text{CO}$  at 90 °C, the autoclave was allowed to ramp to 90 °C and then the active catalyst was generated for

approximately 10 minutes. The inlet valve was closed and the reservoir was purged of  $\text{H}_2/\text{CO}$  and was replaced by  $\text{H}_2$ . The inlet valve was reopened and the reaction was monitored.

### **5.3 Gas Chromatography Analysis**

Samples were taken from the hydroformylation and hydrocarboxylation experiments and analyzed by gas chromatography. These samples were tested using a Hewlett Packard 5890 Series II Gas Chromatograph equipped with a DB-1 capillary column for calculation of branched to linear ratios, final conversion, hydrogenation and isomerization amounts. Initial hydrocarboxylation experiments were performed on Hewlett Packard 5890 Series II Gas Chromatograph/ Mass Spectrometer equipped with a DB-5 capillary column. Once identification procedures were completed the remaining experiments were performed on the first instrument described. All products were identified by comparing retention times to that of standards or separated aldehyde and carboxylic acid products from the hydroformylation and hydrocarboxylation experiments. Data was collected using National Instruments Virtual Bench and Microsoft Excel, then displayed in GRAMS 32 version 5 by Galactic Software.

**Table 5.1. Order of retention times<sup>a</sup>**

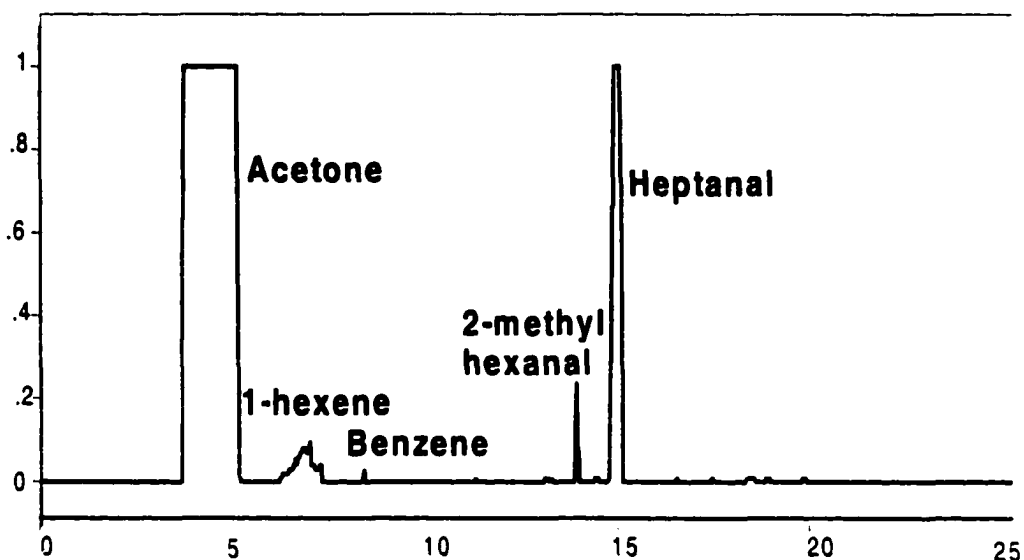
Name of Component	Retention Time (min)
Acetone	3.50
1-Hexene	5.86
Hexane	6.00
Trans-2-Hexene	6.36
Trans-3-Hexene	6.51
Cis-2-Hexene	6.81
Benzene	8.00
Trans-2-Hexanal	12-13
Heptanal	14.30
Trans-2-Hexanoic Acid	16
Heptanoic Acid	17

<sup>a</sup> The initial temperature was 40°C with a hold time 5 minutes. The ramp rate was 15°C/min. The final temperature was 150°C and a hold time of 5 minutes. The column pressure was 36 – 40 psi.

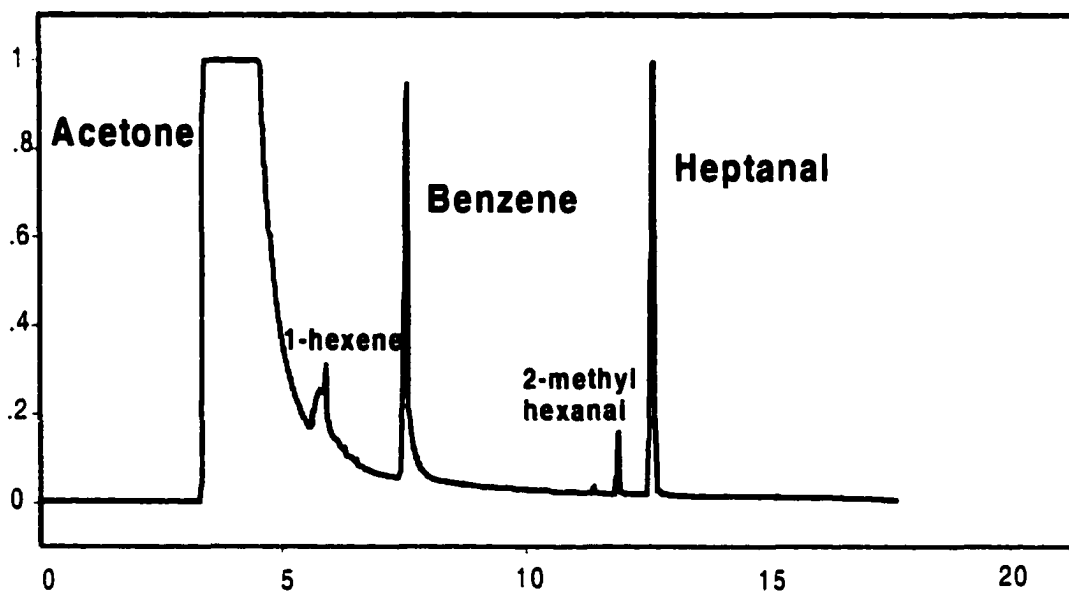
#### **5.4. References**

1. Laneman, S. A., Fronczek, F. R., Stanley, G. G., *Inorg. Chem.*, **28**, 1989, 1872.
2. Albuquerque, P. R., dissertation for Ph.D. degree at Louisiana State University, 1997.
3. Hunt, Jr., C., dissertation for Ph.D. degree at Louisiana State University, 2000.
4. Albuquerque, P. R., Juma, B., Bridges, N. N., Laneman, S. A., Fronczek, F. R., Stanley, G. G., manuscript in preparation.

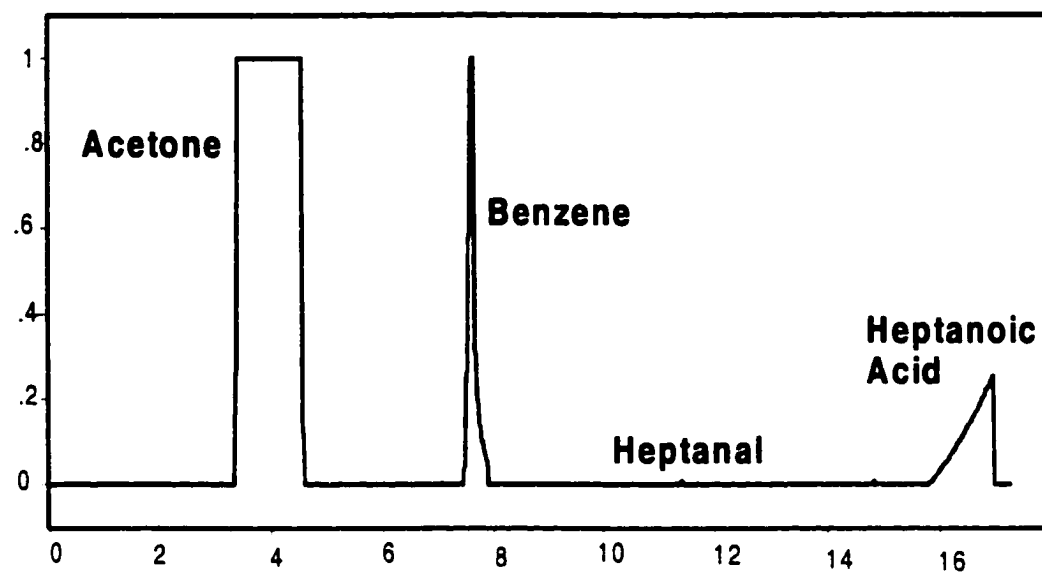
## APPENDIX A GAS CHROMATOGRAMS



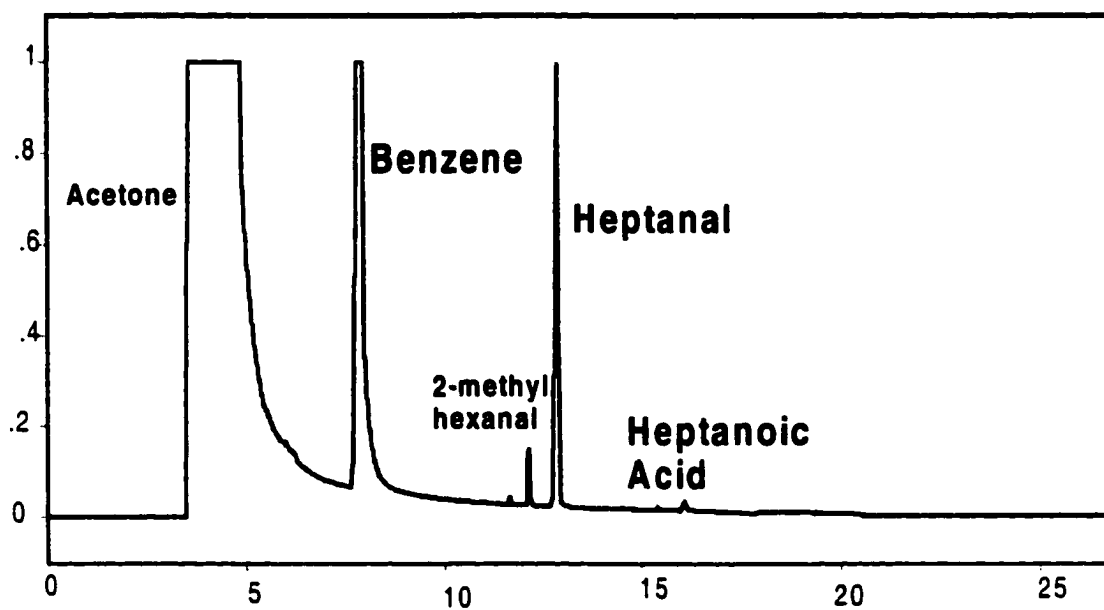
**A.1. GC analysis of Run Rh632**  
(1000 equiv 1-hexene in acetone, 90 psig  $H_2/CO$  and 90°C)



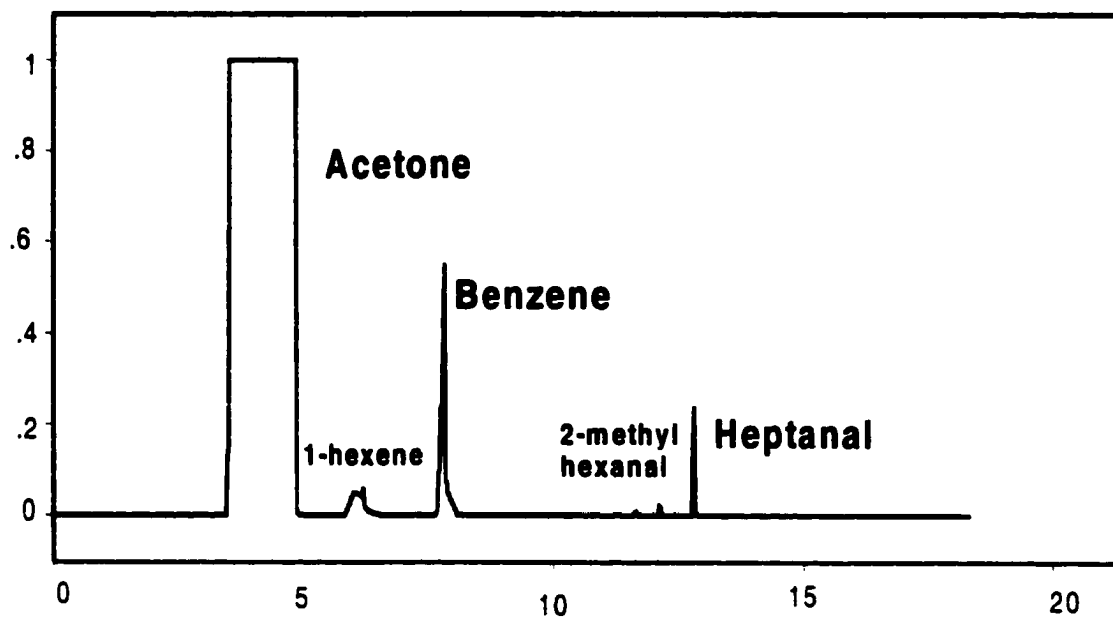
**A.2. GC analysis of Run Rh689**  
(30% water, 1000 equiv of 1-hexene, 90 psig  $H_2/CO$  and 90°C)



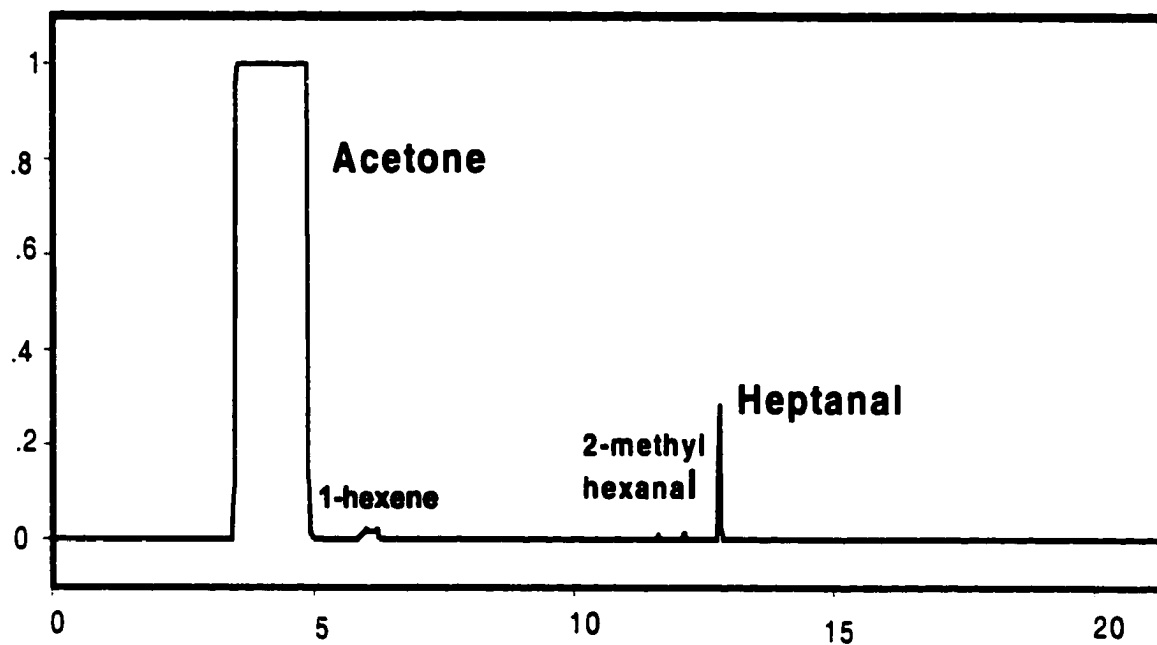
**A.3. GC analysis of Run Rh688**  
 (Hydrogenation of Heptanoic Acid, 1000 equiv of Heptanoic acid, 90 psig  $H_2/CO$  and 90°C)



**A.4. GC analysis of Run Rh696**  
 (10 min w/  $H_2/CO$  and then pure CO at 90 psig, 30% water, and 90°C)



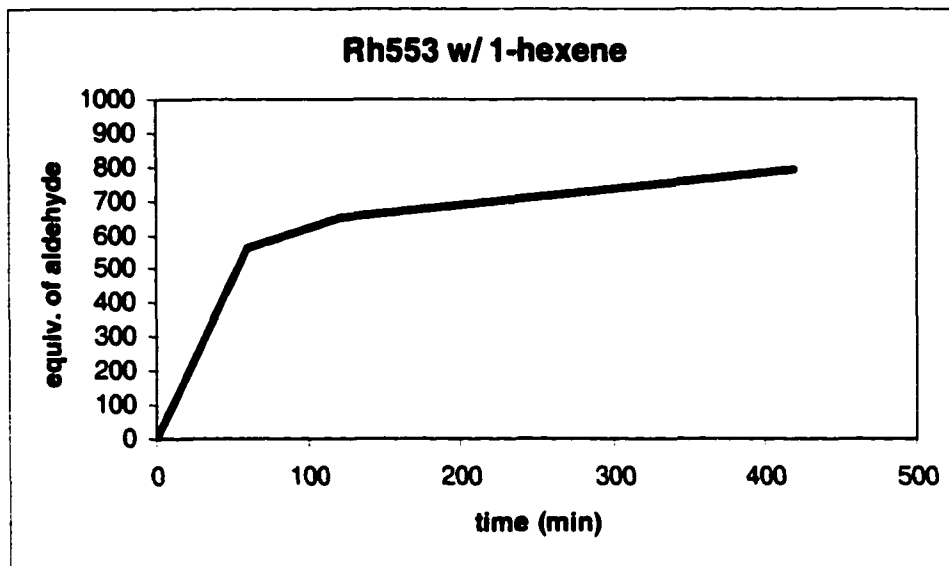
**A.5. GC analysis of Run Rh699**  
 (10 min w/  $H_2/CO$  and then pure  $CO$  at 90 psig, 20% water, and 90°C)



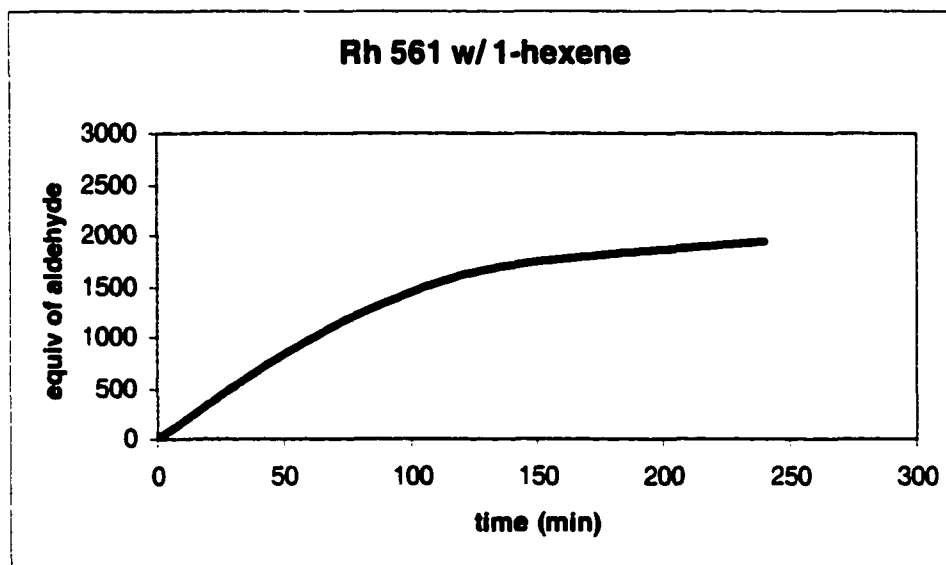
**A.6. GC analysis of Run Rh700**  
 (10 min w/  $H_2/CO$  and then pure  $CO$  at 90 psig, 40% water, and 90°C)



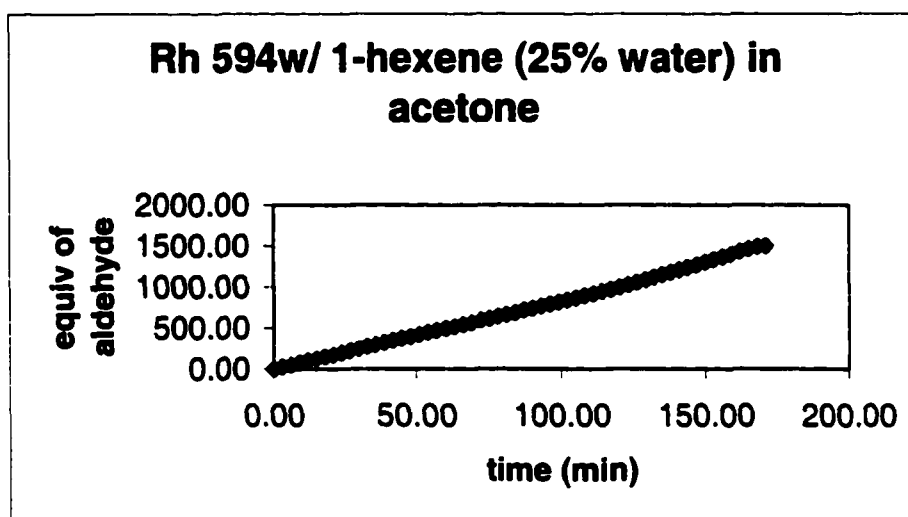
## APPENDIX B ALDEHYDE PRODUCTION CURVES



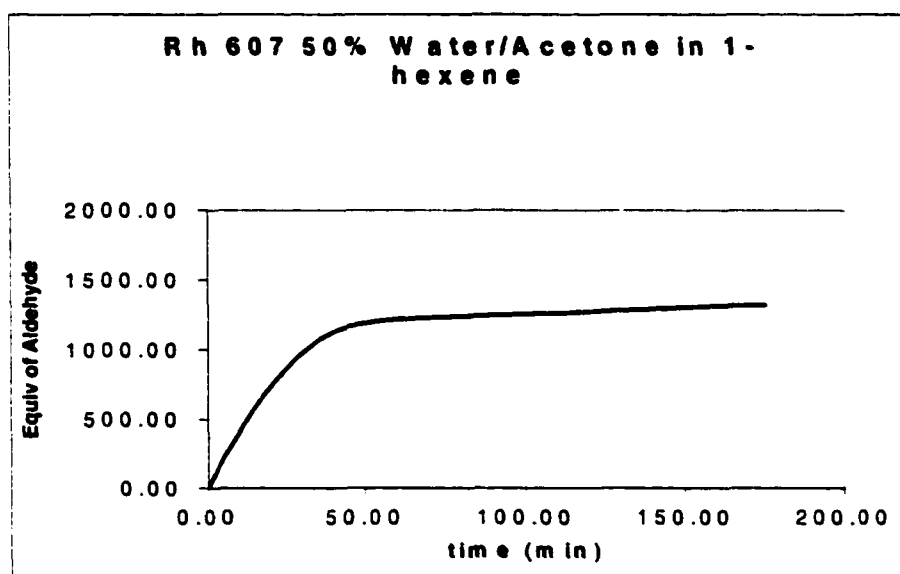
**B.1. Aldehyde production curve of Run Rh553  
(1000 equiv 1-hexene in acetone, 90 psig  $H_2/CO$ , and 90°C)**



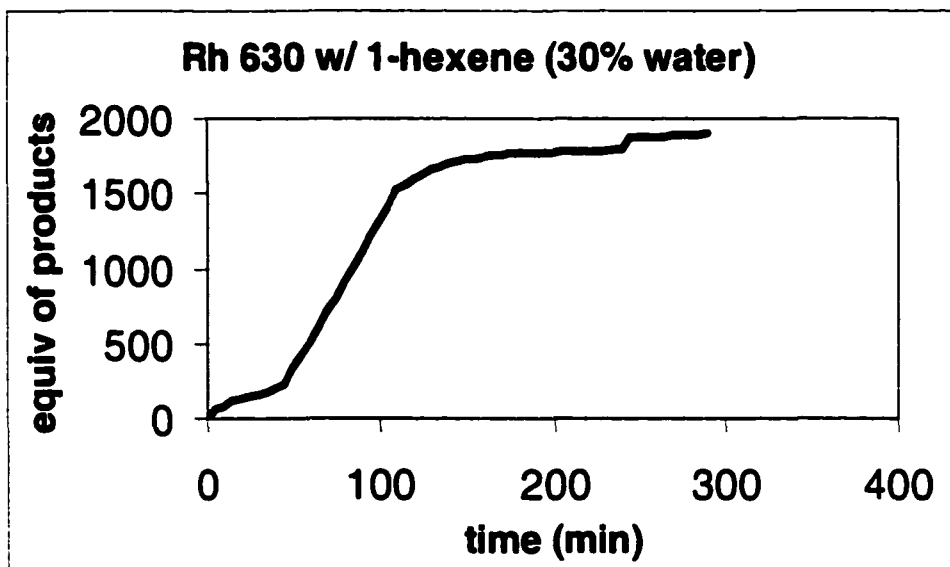
**B.2. Aldehyde production curve of Run Rh561  
(2500 equiv 1-hexene in acetone, 90 psig  $H_2/CO$ , and 90°C)**



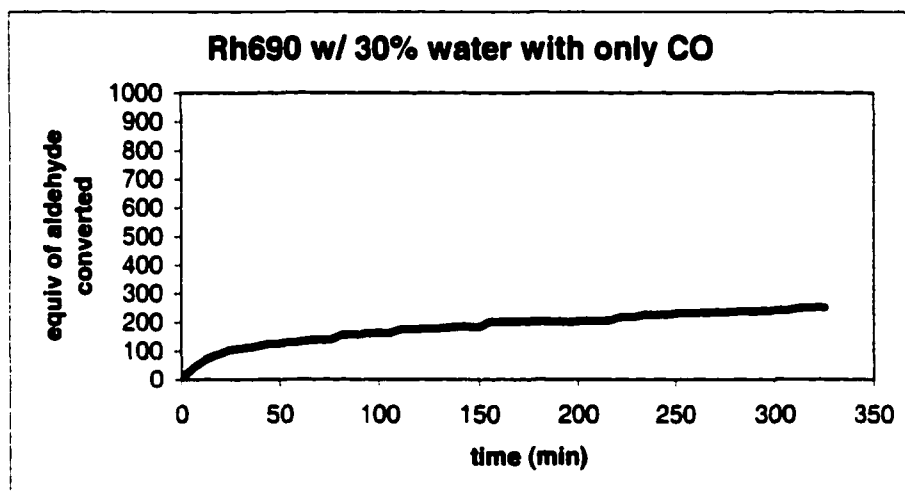
**B.3. Production curve of Run Rh594  
(25% water, 1000 equiv 1-hexene in acetone, 90 psig H<sub>2</sub>/CO, and 90°C)**



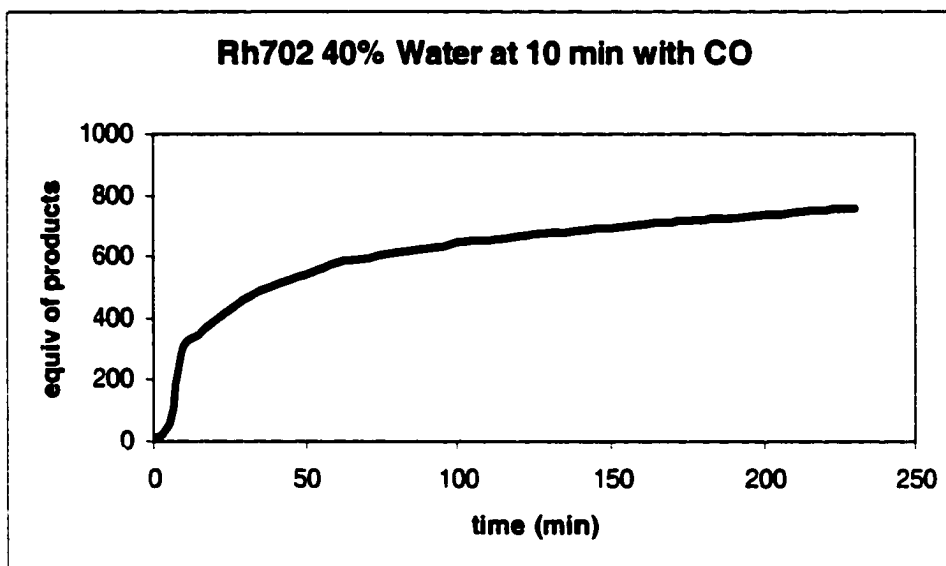
**B.4. Production curve of Run Rh607  
(50% water, 1000 equiv 1-hexene in acetone, 90 psig H<sub>2</sub>/CO, and 90°C)**



**B.5. Production curve of Run Rh630  
(30% water, 1000 equiv 1-hexene in acetone, 90 psig H<sub>2</sub>/CO, and 90°C)**



**B.6. Production curve of Run Rh690 (30% water, 1000 equiv 1-hexene in  
acetone, 90 psig CO, and 90°C)**



**B.7. Production curve of Run Rh702**  
**(40% water, 1000 equiv 1-hexene in acetone, 10 min of H<sub>2</sub>/CO then pure**  
**CO at 90 psig, and 90°C)**

## **VITA**

Novella Nicole Bridges was born on August 9, 1972, in Detroit, Michigan. Her parents are Willie and Carrie Bridges. She is the youngest of five children. Novella graduated from Lutheran High School East in Harper Woods, Michigan, with honors in June of 1990. Then she graduated with honors from Jackson State University in Jackson, Mississippi, in May of 1994. She entered the doctoral program in the Chemistry Department at Louisiana State University in 1995. She will be graduated in May of 2001 with the degree of Doctor of Philosophy.

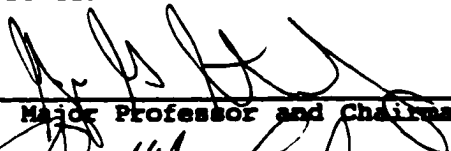
DOCTORAL EXAMINATION AND DISSERTATION REPORT

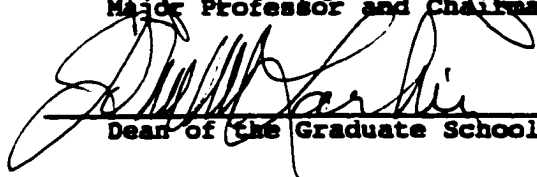
**Candidate:** Novella Nicole Bridges

**Major Field:** Chemistry

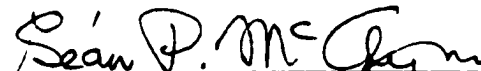
**Title of Dissertation:** Kinetic and Mechanistic Studies of a Bimetallic Hydroformylation Catalyst

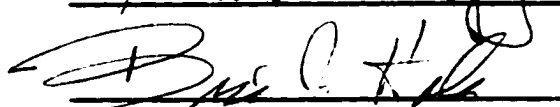
**Approved:**

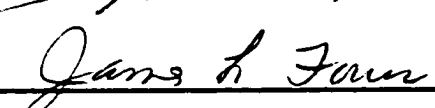
  
Major Professor and Chairman

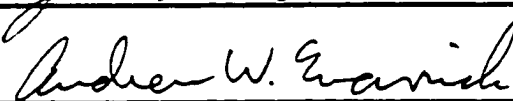
  
Dean of the Graduate School

**EXAMINING COMMITTEE:**

  
Sean P. McGovern

  
Bruce C. H. H.

  
James L. Fourn

  
Andrew W. G. G.

**Date of Examination:**

December 14, 2000